LEAF-SHAPE MUTANTS AND HOMEOBOX GENES IN *ANTIRRHINUM MAJUS*

Mario Roccaro

Doctor of Philosophy
(PhD)

University of Edinburgh
1997

Acknowledgements

There a number of people that I have met along the period spent at The University of Edinburgh whom I would like to thank. First of all, thanks to Dr. Andrew Hudson, my supervisor. He has introduced me to the world of plant molecular biology, wisely, patiently and humorously.

Of course, I will never forget the atmosphere of the lab and the people who have worked there. To begin with I would like to thank Ian for always being helpful in numerous occasions. Thanks to Gavin for help in the sequencing of part of the *SNAP2* cDNA clone, many thanks to Arnold for the numerous coffee and cigarette breaks, to Isma for never going to the cinema, Alicia for nice conversations about the meaning of life, Amanda for the music, all the researchers of Prof. A. Trewavas and Dr. S. Smith labs for the advice and solutions interchanged, to all the people that work at the Rutherford building, to Roger and Billy for caring about the plants, to John L. for keeping up the image of Italians, and to anyone else whom I have met along this period. Special thanks go to Dr. H. Sommer for giving me the time to finish this project.

I would like to dedicate this thesis to three people whom I love deeply: Antonio e Lucia my parents, and Monica.

"Our lives were frail, full of agonies of embarrassment and regret, of misunderstood communication and strong with the intense feeling of wonder at the torrent of ideas released by books, music, art, other people; it was a time of finding shelter among the mightily capitalled abstractions of Love, Life, Time, Age, Youth, Imagination."

Janet Frame
An Angel At My Table

TABLE CONTENTS **PAGES**

Abbreviations

%	percentage
A	adenine
AMPS	ammonium persulphate
bar	unit of pressure
bp	base pair
BSA	Bovine Serum Albumin
C	cytosine
cm	centimetre
CTAB	cityltrimethylammonium bromide
DEPC	Diethyl-pyrocarbonate
dH_2O	distilled water
DNA	deoxyribonucleic acid
dNTP	any deoxyribonucleotide triphosphate
DTT	dithiothreitol
E. coli	*Escherichia coli*
EDTA	disodium ethylenediaminetetraacetic acid
EtBr	ethidium bromide
EtOH	ethanol
G	guanine
g	gram/s
g	gravity
hr	hour/s
IPTG	isopropyl β-D-thiogalactoside
K-Ac	Potassium acetate
kb	kilo base
l	litre/s
M	molarity
mF	milliFaraday
µg	microgram/s
mg	milligram/s
µl	microlitre/s
ml	millilitre/s

mM	millimolarity
mV	milliVolt/s
mW	milliWatt/s
Na-Ac	Sodium acetate
ng	nanogramme/s
nm	nanometre
OD	optical density
P	phosphate element
PEG	polyethylene glycol
psi	unit of pressure per square inch
rpm	revolution per minute
S	sulphur element
sec	second/s
SEM	Scanning Electron Microscopy
T	thymine
TEMED	N,N,N',N-tetramethylethylenediamine
TM	Trade Mark
U	unit of enzyme activity
UV	ultra-violet light
V	Volt/s
v	volume
VIS	visible light
w	weight
XGal	5-bromo-4-chloro-3-indolyl β-D-galactopyranose
°C	degree/s Centigrade

ABSTRACT

Plants are composed of homologous repeating structures produced continuously by the apical meristem. Cells of the apical meristem show few morphological differences, but may have vastly different fates depending on their position. For instance, group of cells in the flanking parts of the apical meristem will form leaves, while those in the central zone of the meristem will remain in an undifferentiated state of growth. This suggests that patterns exist in the meristem. However, meristems are small and not suited to biochemical and surgical analysis. As a result, relatively little is known of the mechanisms which determine patterns and cell fate in the apical meristem, and in the leaves produced by them.

To investigate the genetic control of leaf development two alternative approaches were used. The first approach was to identify transposon induced leaf-shape mutations in an attempt to isolate and characterise the affected genes by transposon tagging. The second approach was to isolate by homology genes which show patterns of expression within the meristem and have the potential to control developmental fate.

Fourteen different leaf shape mutants were identified by screening populations of *Antirrhinum* plants carrying active transposons. The mutants were characterised genetically and morphologically. Only one (*Graminifolia*) showed the genetic instability of transposon-induced mutations. Southern hybridisation was used to identify a transposon copy that appeared to be responsible for the mutation. Unfortunately, it was not possible to determine whether sequences flanking the transposon contain part of the *Gráminifolia* gene.

Moreover three new homeobox genes, *SNAP1*, *SNAP2* and *SNAP3* were isolated by sequence homology. The gene product of *SNAP1* shows a high degree of homology with the product of the homeobox gene *KNOTTED1* of maize, whereas in *SNAP2* and *SNAP3* products, the homology is restricted to characteristic highly conserved regions of the KNOTTED1 protein. Using in situ hybridisation the mRNA expression patterns of these three hox-genes have been determinated. Interestingly, all three *Antirrhinum* homeobox genes have the same pattern of expression localised in the peripheral zone of the shoot apical meristem, at the site of initiation of new lateral primordia, and along the provascular tissue. This represents a new domain of expression for homeobox genes of the *KN1* gene family. Since the three *SNAP* genes show the same spatial and temporal expression, they might work in concert in the specification of those processes that lead to the development of the vascular tissue.

CHAPTER 1

Introduction

Introduction

1.1: Aim of the project

The morphology and anatomy of the aerial parts of plants (shoot apex, leaves, bracts, flowers and stem) have been extensively documented (e.g. Esau, 1977). Nevertheless, substantial questions about the developmental control of the aerial parts, especially that of leaves, remain unanswered. The small size of plant meristems makes them difficult to investigate biochemically. In addition, the wound responses shown by plant tissues, which include localised cell death and proliferation of dedifferentiated cells, have limited the success of surgical approaches to the investigation of plant morphogenesis.

However, in the last seven years, significant advances have been made in the study of plant morphogenesis in both *Antirrhinum majus* and *Arabidopsis thaliana* using the techniques of molecular genetics (Carpenter and Coen, 1990; Sommer *et al.*, 1990; Bowman *et al.*, 1991; Coen, 1991; Coen and Meyerowitz, 1991; Schwarz-Sommer *et al.*, 1992; Bradley *et al.*, 1993). In particular, a number of genes that specify the identity of meristems and floral organs were identified by mutation and isolated, making it possible to study the roles of these genes and their interactions using molecular and genetical approaches.

One of the first visual characteristics of an organ is its shape, and this can be attributed to spatial variations in the rate, duration and orientation of cell division and cell expansion. However, the morphogenetic factors which control and coordinate these processes have not yet been clearly defined.

The aim of this project was to isolate and characterise genes involved in leaf morphogenesis. To achieve this aim two alternative approaches were used.

The first was to identify transposon-induced leaf-shape mutants. Analysis of these mutants was expected to suggest the functions of the affected genes in leaf morphogenesis, and allow their isolation and characterisation by transposon tagging.

The second approach was to isolate and characterise genes that show patterns of expression within the meristem and have the potential to control developmental fate. Several homeobox genes which have this capacity and affect the morphogenesis of the

leaf had previously been cloned from maize (Vollbrecht *et al.*, 1991; Becraft and Freeling, 1994).

1.2: The leaf as a model system to study plant morphogenesis

Leaves represent only one of the aerial parts of the plant. A question can therefore be asked: does the leaf provide a developmental model which can be applied to the remainder of the plant? In this context, it is necessary to consider the relationship between leaves and other parts of the plant.

Leaves, bracts and floral appendages have a number of common characteristics. Firstly, they are determinate structures, that is their development has a defined beginning and end. This is in contrast to the shoot apical meristem (SAM) and inflorescence meristem (IM) which have the capacity to grow indefinitely. Secondly, lateral organs show bilateral symmetry, whereas the SAM does not. In other words they tend to be dorso-ventral. This is most apparent in leaves, sepals and petals which are flattened in a plane perpendicular to the stem or floral axis.

Although clear differences exist between the SAM and the lateral organs, it must be kept in mind that all lateral organs originate on the flanks of the SAM. There is strong dependency between the SAM and lateral organs during the initial phases of primordia formation. Therefore, changes in the morphogenetic state of the SAM may be reflected in the lateral parts of the plants. This inter-relationship between lateral organs and the SAM is evident in a number of dominant mutations that affect leaf morphology in maize (Freeling and Hake, 1985; Freeling, 1992).

1.2.1: A historical note

The founder of scientific morphology, Johann Wolfgang von Goethe, recognised these similarities between leaves and floral organs, and proposed that all the lateral organs of plants were homologous (Zecchi, 1989). He assumed that the leaf represented the base state of a lateral organ, and that floral organs were more advanced forms which arose from the contraction of leaves. To explain the transition from leaves to floral organs, Goethe proposed that nutrients from the roots were purified on passing up the stem, and that the refined components induced the production of reproductive organs rather than base leaves.

Although no evidence has yet been found in support of Goethe's theory of plant humours, many observations have supported the idea of homology between leaves and floral organs. In their early stages of development, the primordia of all lateral organs are similar (Steeves and Sussex, 1989). In *Impatiens balsamina*, a change in day length after floral initiation can lead to the production of organs containing both leaf and petal tissues (Battey and Lyndon, 1984). Perhaps the strongest evidence for the homology between leaves and floral parts has been provided by genetic analysis of the floral organ identity genes. A number of homeotic genes have been identified in *Antirrhinum* and *Arabidopsis* which act in combination to specify the identity of floral organs. Loss of one of these genes by mutation can alter the identity of one or more whorls of the flower. For example, *Antirrhinum* mutant plants for the *DEFICIENS* gene is characterised by the homeotic transformation of the second whorl organs, the five petals, in five correspondent sepaloid organs morphologically indistinguishable to the first whorl organs the five sepals. In addition, the third whorl results in a chimney like structure due to the fusion of the four stamens and one stamenoid, which strongly resembles to the fourth whorl the carpel. The genuine fourth whorl is missed (Sommer *et al.* 1990). This suggests that all the floral organs are homologous, and that differences in their identity are dependent on the expression of a few genes. Loss of the floral homeotic genes necessary to determine the identity of all four floral whorls, results in a flower composed entirely of leaves (Bowman, 1991). This finding not only supports the idea that leaves and floral organs are homologous, but also that leaves represent a developmental ground state.

It is therefore possible to say that studies of leaf morphogenesis may be equally applicable to the development of other lateral organs, and ultimately to morphogenetic changes in the SAM. Growth control, pattern formation and cell and tissue differentiation can all be studied in the context of leaf development.

1.3: The determinate structure of the leaf

The leaf is a determinate organ with a development that has a defined beginning and end. Once the leaf of a dicot has reached a certain length, incorporation of cells from the shoot meristem into the leaf primordium ceases, and the leaf can be considered an autonomous meristem, depending on the remainder of the plant only for nutrients. Experiments with the fern *Osmunda cinnamomea* support this view (Steeves and Sussex, 1957). When immature leaves (including those as small as 1 mm in length) were explanted to a culture medium containing simple nutrients, they were able to complete

their characteristic pattern of development. This experiment demonstrates that early in its development, the leaf becomes essentially self-controlling, but this was not necessarily so at its inception. In fact, when the ten youngest primordia in the shoot apex (P1 to P10) were explanted to a culture medium, many gave rise to shoots and ultimately to whole plants, rather than leaves. The proportion of primordia that lead to shoots was very high in the case of P1 and P2 (the youngest primordia), and diminished progressively in older primordia. P10 invariably developed as a leaf (Steeves and Sussex, 1957).

The determinacy of lateral organs, such as leaves, has an important consequence. The leaf primordium, which can be regarded as a meristem, will produce only a single leaf. Therefore its developmental program could be changed without any effect on the remainder of the plant. For instance, the genetic programme/s that produce the shape of the leaf may be modified in response to environmental stimuli, or may change rapidly on an evolutionary scale. In contrast to leaves, the developmental possibilities of the stem are restricted to the production of the axis and lateral organ primordia. It is therefore not surprising that modification of leaves in response to environment or developmental state of the plant is a common phenomenon, and that massive differences exist between the leaf shapes of different plants. The most extreme modification of the leaf is represented by the evolution of floral organs (Weigel and Meyerowitz, 1994). In contrast, apical meristems and newly initiated lateral organ primordia of different species are almost indistinguishable, and change little during the life of the plant (Smith and Hake, 1992).

The determinacy of leaves has another important implication, that is the establishment of regional identities within the leaf. Collections of leaf-shape mutants of pea (Marx, 1977; 1987), tomato (Mathan and Cole, 1964; Caruso, 1968) and maize (Freeling, 1992) demonstrate the existence of regional identities, and that their determination is under genetic control. For instance, in pea plants homozygous for the recessive mutation *afila* (*af*), each lateral leaflet is converted to a branched system of tendrils. The mutation can therefore be considered homeotic, though loss of leaflet identity also causes an increase in the degree of indeterminacy. In contrast, homozygous *tendrilless* (*tl*) mutant plants produce a single leaflet in place of each tendril. The phenotype of the double mutant (*af,tl*) could not be predicted from the phenotypes of the single mutations. It consists of a highly branched rachis structure, each axis of which terminates in a small leaflet. Studies of *af* and *tl* mutants have shown that there are no morphological differences between the wild type and the two mutants in their shoot

apical meristems or in the leaf primordia at their initiation. Differences become detectable only after plastochron two (i.e. when two subsequent primordia have been initiated at the apex).

The conclusion that can be drawn from these studies is the following: the developmental programme/s that lead to the formation of a compound pea leaf can be modified before a certain time, after which a regional identity is determined. One convincing but largely untested hypothesis to explain the effect of these mutations suggests that the size of the leaf meristem plays a role in the determination of organ identity (Young, 1983).

1.3.1: Regional identities in the maize leaf

Work on dominant leaf mutants in maize has led to a functional definition of leaf regional identities or leaf domains. The maize leaf consists of a basal sheath domain and a distal blade domain separated by an auricle and ligule, a flap of epidermally derived tissue located in the dorsal (abaxial) surface of the leaf. Sheath and blade domains have distinct morphological features such as venation pattern, internal anatomy, epidermal cell shape and epidermal hair pattern (Russell and Evert, 1985; Sylvester *et al.*, 1990). Several dominant mutations of maize cause alterations of the distal blade domain to sheath. One group of these dominant mutations is represented by three homeobox genes: *KNOTTED1* (*KN1*) (Vollbrecht *et al.*, 1991), *ROUGH SHEATH1* (*RS1*) (Becraft and Freeling, 1994) and *LIGULESS3* (*LG3*) (Fowler and Freeling, 1996). In the mature leaves of any of these mutants, part of the blade domain is transformed into sheath. The transformation is caused by the ectopic expression of any of these three homeobox genes. Mutations having the opposite effect, transforming blade to sheath, have not yet been observed, attributing features of polarity to these dominant mutations. As a consequence of this transformation, the ligule region is altered with its boundary displaced towards the blade. In the leaf of *Kn1* mutant plants there are often immature cells (knots) associated with the region of transformation. Moreover, the mutants differ in which part of the blade is altered. *Lg3* mutation alters the midrib and the central zone around the midrib. *Rs1* mutation seems to affect cells in the entire lateral dimension of the maize leaf blade, although *Rs1* is very specific to the ligular region (Fowler *et al.*, 1996). *Kn1* alters strips of cells around lateral veins preferentially in internal regions (Freeling and Hake, 1985; Sinha and Hake, 1990). These three maize leaf mutations are dominant and, at least in the case of *Kn1* and *Rs1* mutants, involve gains-of-function. Consequently it is not so straightforward to gain information about the WT functions of the genes from their mutant phenotypes. They may have general roles in the

development of the WT plant, but little to do with leaf development. Nevertheless, dominant mutations in maize have clearly demonstrated that regional identities exist. Both in monocots and dicots, recessive mutations affecting leaf shape have been identified and some of the genes have been cloned, as in the case of the *PHANTASTICA* (*PHAN*) gene in *Antirrhinum* (A. Hudson, pers. comm.). Loss of *PHAN* due to transposon insertion, leads to a complete or partial replacement of the lamina with midrib tissue, suggesting that *PHAN* is necessary for the determination of the laminal domain. The recessive mutation *narrow sheath* of maize leads to loss of leaf margin identity (Scalon *et al.,* 1996). Loss of the marginal domain is already detectable in mutant P2 leaf primordia. This finding provides further evidence for the existence of domains within the leaf, and that the specification of regional identities happens very early in leaf development.

1.3.2: How are regional identities established?

Once a leaf has become a determinate organ, it might be possible to deduce the fate of any particular cell in the growing leaf. However, clonal analysis has shown that cell lineage plays a minor role in determing cell fate in the leaf and that the development and final form are largely positional dependent (Poethig, 1984a; Poethig and Sussex, 1985; Poethig and Szymkowiak, 1995). This means that when a cell divides to give rise to a daughter cell, the fate of the new cell is related to its position more than its developmental lineage. Also, plant cells, unlike animal cells, are cemented together by their cell walls, and cannot change their position relative to their neighbours. When a plant cell from a putative leaf domain invades an adjacent domain due to the orientation of cell division, it changes its fate and adopts the identity appropriate to its new position (Langdale *et al.*, 1989). As a consequence, the plant cells must respond to signals which tell them how to interpret or at least reinterpret their position (Poethig, 1989; Dawe and Freeling, 1991).

Compartmentalisation is a common developmental strategy used by animals for the formation of organ primordia (Garcia-Bellido *et al.*, 1973). Compartments were first defined by boundaries of cell-lineage, and were later shown to originate by the expression of transcriptional activators in regions of animal embryos (Dinardo and Heemskerk, 1990). However, the boundary of two adjacent compartments may work as an organising centre for pattern formation in the developing organs. Many examples exist in *Drosophila* where compartmentalisation is known to be important in the

formation of the adult fly body (Lawrence, 1992). Cells acquire a positional value with respect to compartment boundaries and then interpret this in terms of their genetic constitution or developmental history (Wolpert, 1996).

The nature of the signals and the mechanisms of perception that allow a plant cell to interpret its position, still remain elusive. However, several scenarios can be envisaged. First, long-range signalling mechanisms may use small diffusible molecules or morphogens that can be transmitted via plasmodesmata or the apoplast. Calcium is an obvious candidate (Neuhaus *et al.*, 1993; Pooviah and Reddy, 1993) as are plant hormones, although there is little evidence that hormones are actually involved in pattern formation (Schawbe, 1971; Maksymowych and Erickson, 1977; Meicenheimer, 1981; Marc and Hachett, 1991).

A gradient of morphogen/s might be established in a growing leaf primordium so that different threshold concentrations of morphogen/s activate different genes which determine domains within the leaf. Recently it has been shown that transcription factor genes like the homeobox gene *KN1* (Lucas *et al.*, 1995) and the two MADS-box genes *DEFICIENS* and *GLOBOSA* (Perbal *et al.*, 1996) can move via plasmodesmata to exert their action in a polar non-cell-autonomous fashion. However, how the plasmodesmatal transport might be controlled to create developmental domains, is still unclear. Another mechanism might rely on short-signalling between adjacent cells, by means of components located on the extracellular matrix (i.e. cell wall). Different polysaccharides present at the cell wall in many species have been implicated in cell fate determination (Knox, 1993; Brownlee and Berger, 1995).

1.4: The leaf as a geometrical system

The leaf is a vital organ for efficient photosynthesis. Its thin, flat shape and structure is closely related to its function. Its often large surface area to volume ratio maximises the photon trapping surface. In practical terms, this allows the leaf to be described as a two-dimensional structure. Furthermore, the leaves are almost symmetrical along their main axis. In terms of developmental timing this could mean that the same spatial and temporal processes happen on both sides of the leaf to give the final shape.

Treating leaves as two dimensional allows their development to be described more simply. Measurement of the length of the leaf axis allows the rate of leaf growth and the plastochron index to be determined. The plastochron index is defined as the

interval between the initiation of any two successive leaves (Maksymowych, 1973). It is a measure of the developmental age (in terms of developmental time) of one plant and consequently of one leaf. The leaf plastochron index (LPI) is important when it is necessary to establish, for example, the moment of initiation of a new leaf, or when cell divisions cease and the leaf develops only by cell enlargement. LPI is most commonly determined by measuring the growth of emerged leaves, and assumes that the time between two subsequent emerged leaves reaching the same length is equivalent to the time between initiation of subsequent primordia at the apex (Erickson and Michelini, 1957). The term plastochron is now commonly used to identify the position of a primordium relative to the SAM, such that plastochron zero (P0) represents the site of an incipient leaf primordium, P1 the leaf primordium closest to the SAM, P2 the next oldest leaf primordium and so on.

In addition, the growth of the lamina can be followed by marking the leaf (for example with spots of India ink in a grid pattern) and calculating the relative area growth rate for the different parts of the leaf. It is possible to calculate the relative rate of extension of the leaf in the same way (Poethig and Sussex, 1985a).

1.5: Practical implications of leaf shape.

All aspects of agricultural production and the industrial transformation of its products are intimately associated with the growth of the leaf. In fact, plant shape is an important agronomic characteristic in several respects. The shape of leaves can have a marked effect on yield and biomass production. The understanding of developmental processes in leaves would allow the artificial manipulation of the shape of plant organs for agronomic ends. There is evidence to suggest that narrower leaves are more advantageous in drier conditions and are more resistant to mechanical damage by weather and machinery. If it proves possible to identify the factors which regulate the phases of leaf development, genetic manipulation of the shape of other plant organs may be achieved.

1.6: Why use *Antirrhinum majus* to study leaf development?

Antirrhinum majus (snapdragon) belongs to the large family of *Scrophulariacae*. Its main advantage as an experimental organism is that it has been well characterised genetically. *A. majus* has been subjected to the attention of geneticists for over a century, and the first systematic study dates back to that of De Vries, who investigated

the inheritance of a variegated floral phenotype in 1890 (Coen *et al.*, 1989). *A. majus* offers several advantages as a genetic system: it propagates well vegetatively, and it has flowers that are easy to emasculate and cross. Both RLFP and chromosome maps are available. Although the generation time is relatively long, the plants are large and provide substantial amounts of tissue for analysis. Its two major advantages are perhaps that: i) it contains a number of mutagenic transposable elements. These can be used to induce mutation in the genes of interest, and the affected loci can then be cloned by transposon tagging (e.g. Hudson *et al.*, 1993), and ii) a large collection of leaf-shape mutants is available (Stubbe, 1966).

Nine different *Antirrhinum* transposable elements (transposons) have been identified concomitantly in genes encoding a regulatory factor of the anthocynin pathway (Goodrich *et al.*, 1992), three enzymes of the same pathway (Upadhyaya *et al.*, 1985; Almeida *et al.*, 1989; Luo *et al.*, 1991; Nacken *et al.*, 1991; Sommer *et al.*, 1985) and two homeotic genes *DEFICIENS* and *GLOBOSA* (Schwarz-Sommer *et al.*, 1992; Trobner *et al.*, 1992). They have been named Tam 1 to Tam9 ("Tam" stands for Transposon *Antirrhinum majus*). Except for Tam 3, the remaining *Antirrhinum* transposons share a conserved sequence in their 13 bp terminal inverted repeats ending in the sequence 5'-CACTA-3'. Due to the high similarity in this region they are generally referred to as CACTA transposons or the CACTA family.

The structure of the *Antirrhinum* plant can be considered typical of many dicots (Fig. 1). It is composed of repeating structures called phytomers, produced continuously by the SAM. In *A. majus*, the phytomer consists of a pair of opposite leaves at a node in decussate phyllotaxis, an internode separating the node from that of the adjacent phytomer, and two axillary buds. The leaf is simple in outline with an entire margin. After an early vegetative phase of about 5 nodes (depending on environmental factors), leaves are produced singularly in spiral phyllotaxis. This phyllotaxis is maintained into the inflorescence where leaves are replaced by bracts. The bracts are separated by short internodes and at each node a floral meristem forms. *Antirrhinum* plants also show changes in the dimension of the leaves along the nodes. The first two nodes have leaves that are broader and shorter than leaves at intermediate nodes. Leaves produced immediately before the transition to inflorescence are narrower and shorter than the lower ones (Fig. 1).

Figure 1: A WT *Antirrhinum majus* plant. The phytomer (ph) unit consists of a pair of opposite leaves (l) in decussate phyllotaxis at a node (n), with two axillary meristems (am) and an internode (i). Leaves at the 5th node begin to undergo phyllotactic change from decussate to spiral. This phyllotaxis is maintained into the inflorescence.

1.7: Leaf Development

Leaf development can be divided into two phases: initiation and subsequent development from the point at which the primordium becomes autonomous.

1.7.1: Initiation and determination of leaves.

It is not easy to give a clear description how leaf initiation occurs, because this process is very complex and has been studied in different species often with contradicting results. It is, however, possible to put these findings together and attempt to give a generalised view of leaf initiation.

In the shoot apical meristem of angiosperms, such as *A. majus,* at least three distinctive cell layers can be recognised: two layers of tunica (L1 and L2) and one layer of corpus (L3) (Fig. 2) (Satina *et al.*, 1940). All three layers are involved in the initiation of the leaf, and they undergo several divisional changes in the process.

Periclinal chimeras, in which individual meristem layers are genetically different, have demonstrated that each layer makes a predictable contribution to the formation of leaves. In dicots, the L1 layer contributes only to the epidermis, whereas the L2 and L3 layers contribute to the inner tissues (Satina *et al.*, 1940).

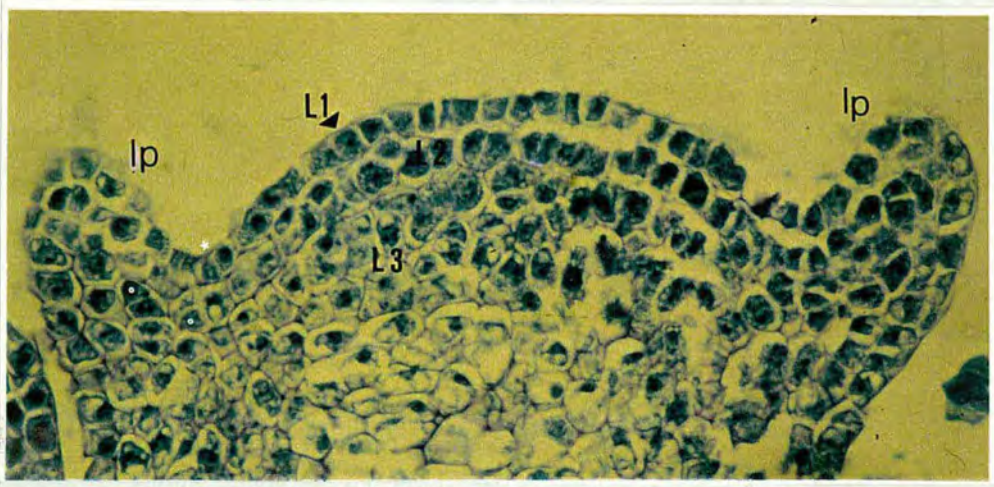

Figure 2: A WT *Antirrhinum* Shoot Apical Meristem (SAM). L1 and L2 are the two tunica layers, and L3 is the corpus layer. Two young leaf primordia are emerging in the flanks of the SAM. Only anticlinal division are seen in L1 layer (*), whereas periclinal (°) and anticlinal divisions are recognisable in layers L2 and L3 of the primordia (X40). lp= leaf primordium.

The SAM has also been divided into zones, reflecting the cytological features and cell division rates and patterns of its cells. Figure 3 shows a diagram of the zones of the SAM. The central zone at the distal end of the apical meristem includes cells from all three layers. Cells in the central zone divide less frequently and have more prominent nuclei than cells in the sides of the SAM (Rembur and Nougarede, 1977; Steeves and Sussex, 1989; Lyndon, 1990). The function of the central zone cells is regarded as mainly one of autorenewal by cell division and maintenance of an undifferentiated state. At the base of the SAM, the rib zone serves as a transition between the central zone and the plant stem. In the rib zone, cells are arranged in longitudinal files and contribute to tissue in the central portion of the stem (the pith). The third zone is the peripheral zone, located in the flanks of the SAM. The peripheral zone is implicated in the formation of lateral organs (Medford, 1992).

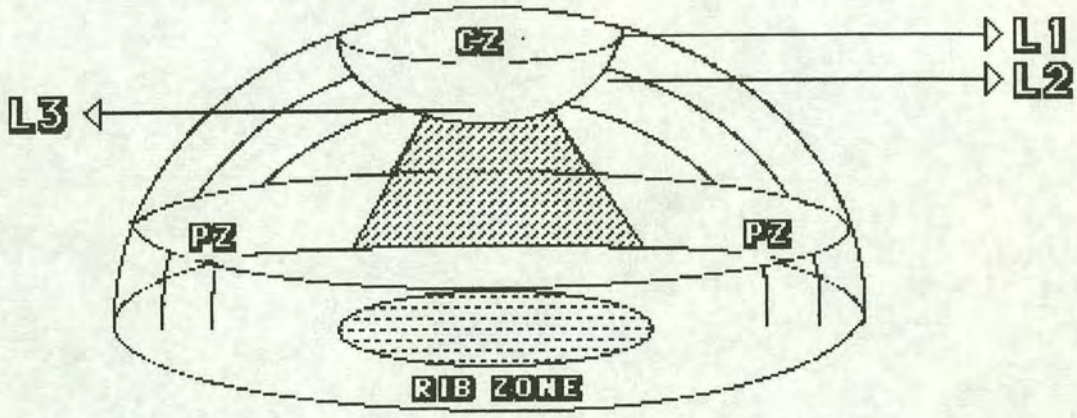

Figure 3: Schematic representation of zones in the SAM. The central zone (CZ) is a distally located group of cells that serve as a source of cells for the other parts of the SAM. The peripheral zone (PZ) is located to the side of the SAM and beneath the central zone. Organ initiation takes place in the peripheral zone. The rib zone forms the boundary between the SAM and the rest of the plant stem and is a source of the interior tissue of the stem. (Figure adapted from Medford, 1992.)

Leaf initiation is achieved through coordinated changes in the polarity and rate of cell division, and enlargement in a group of founder cells located at the peripheral zone of the SAM. Analysis of leaf sectors arising from single cells genetically marked in the meristem have suggested that approximately 100 to 200 cells on the flanks of the meristem give rise to a leaf primordium in both tobacco and maize (Poethig, 1984a, 1984b). The earliest indication of leaf initiation is a protrusion in the peripheral zone of the apical meristem, called the foliar buttress. In *Pisum sativum*, leaf initiation begins with an increase in the frequency of periclinal division (new cell walls parallel to the surface of the apex) in the L1 layer about half a plastochron before the leaf primordium appears, without any increase in the rate of cell division. An increase in the rate of cell division is observed only once the bulge in the shoot apex can be seen (Cunninghame and Lyndon, 1986). In the shoot apex of *Silene*, on the other hand, there is no apparent change in the polarity of cell division, but the rate of growth and division is increased (Lyndon, 1990). However, in L1 of *Solanum tuberosum*, only anticlinal division occurs (that is new cell walls perpendicular to the surface of the shoot meristem), but in the underlying layers both anticlinal and periclinal division can be recognised (Steeves and Sussex, 1989). Therefore *Silene* and *Pisum* seem to exemplify the different extremes, whereas potato is placed between them.

There is however, one observation which suggests that cell division plays no part in leaf initiation. Irradiation of grains of *Triticum vulgare* with a dose of gamma rays sufficient to inhibit cell division, did not prevent the formation of leaf buttresses from the next prospective leaf site. In absence of cell division, the initial protrusion was formed by polarised cell expansion (Foard, 1971). These observations led to the idea that the primary morphogenetic event in the initiation of leaves is a regional shift in the polarity of cell expansion which is normally accompanied by - but not caused by or dependent on - a change in the plane of cell division. This shift in polarity presumably requires an increase in the plasticity of the apical surface (Green 1992).

Insight into the mechanisms governing the polarity of cell expansion in the shoot apex, its reorientation during leaf initiation, and the determination of the cellular plane of division, has come from studies of cytoskeletal components and cell wall architecture. Changes in microfibril orientation may facilitate the changes in the direction of growth and help to determine the shape of the emerging organ (Hardham *et al.*, 1980; Green and Lang, 1981; Jesuthasan and Green 1989).

One of the main proteins with a fundamental role in the process of cellular division and expansion, is tubulin. Tubulin is a dimer formed by α-tubulin and β-tubulin, with an axial spacing of 8 nm arranged in longitudinal rows called

protofilaments. 13 protofilaments give a microtubule with a diameter of 25 nm (Salinsbury and Ross, 1992). A remarkable characteristic of the microtubules is that they can be assembled and disassembled by globular proteins called Microtubule Associate Proteins (MAPs), and thus form dynamic structures within the cell (Amos and Bradshaw Amos, 1991). The plant cell wall is composed of polysaccharides, of which cellulose is the most abundant. It appears that deposition of cellulose microfibrils is oriented by microtubules. This was suggested by the observation that microtubules were coaligned with newly synthesised cellulose microfibrils, and that the pattern of cellulose microfibril deposition could be disrupted by treatment with drugs which cause microtubule breakdown (Salisbury and Ross, 1992). As illustrated in figure 4, cellulose microfibrils within cells of the L1 layer of the shoot apex of *Vinca major*, are aligned in parallel arrays that encircle the apex forming "hoops of reinforcement". When the shoot apex forms a lateral organ, the hoop-reinforcement pattern undergoes a 90° shift locally. Plant cells tend to expand perpendicularly to the axis of cellulose microfibrils, since this growth can be accommodated by slippage of microfibrils, whereas growth in other dimensions is limited by them. As considered above, this shift in the reorientation of cellulose microfibrils is thought to result from a corresponding shift in the orientation of cortical microtubules (Green, 1992). In other words, the angle at which cellulose microfibrils are deposited may be an important part of leaf morphogenesis, and seems to depend on the angle of microtubules in the peripheral cytoplasm. How the cortical microtubules influence the orientation of cellulose microfibrils is still not known. It has been proposed that the microtubules guide the translocation of cellulose synthase through the plasma membrane, trailing cellulose microfibrils along behind them (Hardham, 1980; Gunning and Hardham, 1982).

At present, very little is known about the mechanisms that bring about these co-ordinated changes within leaf founder cells on the flanks of the shoot apex. Experiments where plant hormones and inhibitors of hormone synthesis or transport were applied to the shoot apex, resulted in stable changes in phyllotaxis or influenced leaf growth. However, these treatments also altered the formation or maintenance of the shoot apex itself (Schawbe, 1971; Maksymowych and Erickson, 1977; Meicenheimer, 1981; Marc and Hachett, 1991). Hormones might therefore not be directly implicated in the control of leaf initiation. Several mutants which fail to initiate leaves have been characterised in the same way, but these mutations alter the normal growth of the shoot apex (Caruso, 1968; Clark and Sheridan, 1986; Sheridan and Thorstenson, 1986; Mayer *et al.*, 1991).

An unexpected clue to the genetic control of leaf initiation has come from analysis of the expression pattern of the maize gene *KNOTTED1* (*KN1*) (Smith *et al.*, 1992; Jackson *et al.*, 1994). *KN1* is expressed at high levels in the apical meristem, but is down-regulated at the sites of leaf initiation. It therefore seems to be the first gene for which a change in the pattern of expression is correlated with and occurs before the earliest morphological events in leaf initiation. Ectopic expression of *KN1* later in leaf development causes meristematic proliferation of leaf tissues, suggesting that the function of *KN1* is to maintain cells in a meristematic state, and that loss of meristematic potential is necessary for leaf initiation.

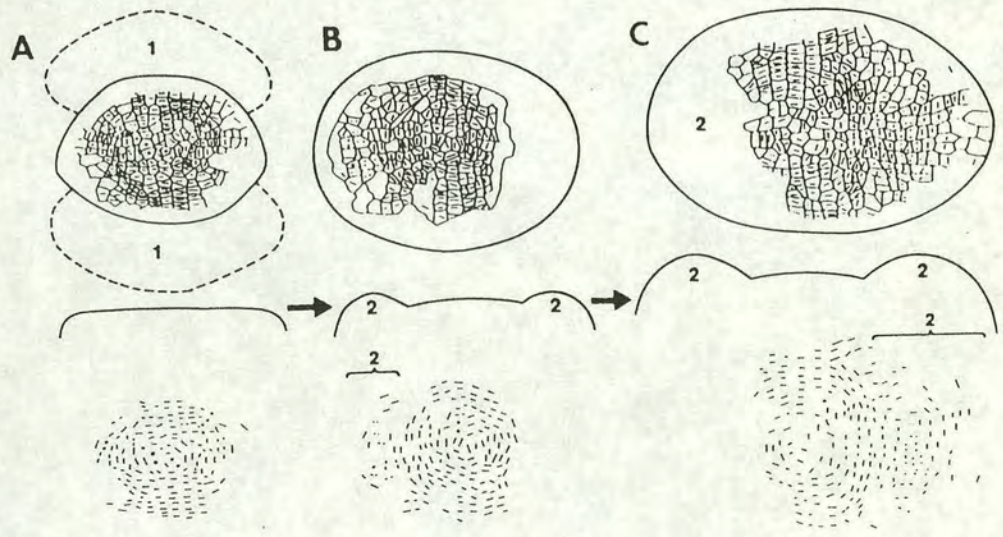

Figure 4: Alignment of cellulose microfibril arrays in the L1 layer in the shoot apex of *Vinca major*. A, B and C show three successive stages in the leaf initiation. The predominant orientation of microfibrils is shown by short bars. (Figure adapted from Jesuthasan and Green, 1989.)

1.7.2: Later development

In *Solanum tuberosum*, meristematic activity in the shoot apex continues to contribute cells to the leaf primordium until it achieves a length of 1 mm, and then the leaf develops in an autonomous manner (i.e. entirely from cells within the primordium). This is typical of most dicots. Two exceptions are represented in *Nicotiana tabacum* and *Angelica archangelica* in which the primordia reach 3 mm and 15 mm respectively (Steeves and Sussex, 1989). Once the leaf develops autonomously from the shoot apex, the first activity of the primordium is to promote the formation of the lamina. This involves a combination of cell division and cell enlargement and is complicated by the fact that these processes do not occur uniformly throughout the leaf primordium at any one time (Steeves and Sussex, 1989).

At the level of gross morphology, the continuing development of the leaf proceeds as follows. The lamina, in tobacco at least, arises at the boundary between the adaxial and abaxial faces of the leaf axis (fig. 5). Initially it extends in a smooth curve from the tip to the base of the leaf axis (fig. 6). Soon after initiation, the lamina stops expanding in a narrow region located near the base of the axis which will give rise to the petiole (Poethig and Sussex, 1985). Although geometrically simple, this process involves a complex sequence of events at the cellular level.

One widely accepted view of laminal development which accounted for its dorsoventral characteristic, was that the lamina is formed by the activity of marginal meristems consisting of one or two of rows of initial cells, located along the two lateral edges of the leaf primordium at the junctions of adaxial and abaxial faces. This activity was assumed to continue late into leaf development (Avery, 1933; Foster, 1936). This concept of marginal activity has been discredited by the studies of Poethig and Sussex (1985) using the technique of clonal analysis in *Nicotiana tabacum*. Plants heterozygous for a semidominant mutation which reduces chlorophyll synthesis were irradiated with X-rays at different times during development. In some leaf cells this resulted in mitotic recombination or breakage of the chromosome carrying the chlorophyll locus, and restored their potential to produce wild-type levels of chlorophyll. The subsequent fate of the labelled cells could then be determined by analysis of the pattern of dark green sectors within the otherwise light green leaf (Poethig, 1984a; Poethig, 1987). Clonal sectors located near to the leaf margin were found to be oriented parallel to the margin rather than perpendicular to it, a finding which was not consistent with the existence of marginal meristems. In fact clones immediately next to the margin were isodiametric,

indicating that marginal cells had made an equal contribution to the increase in leaf width and length (Poethig and Sussex, 1985). The overall pattern of clones indicated that all the leaf initials functioned as a generalised meristem.

Dolan and Poethig (1991) have carried out similar studies of cotton leaf development. Although their findings support the concept that the leaf margin does not contribute enormously to the formation of the lamina, the orientation of cell division at the leaf margin in cotton is significantly different from that of tobacco. Mesophyll sectors originating at the leaf margin tend to be oriented perpendicular to the margin rather than parallel as is the case in tobacco, which suggests that cells at the margin do contribute to an increase in the width of the leaf.

Mitotic activity ceases relatively early in leaf development. In tobacco, for example, cell division is over by the time the leaf has reached 20 % of its final size (Poethig and Sussex, 1985). The remaining growth is attributable to cell expansion which accompanies differentiation of the specific leaf-cell types. However, cell division and expansion do not show the same timing throughout the leaf. Within the layers of the tobacco leaf, division ceases first in the two epidermal layers and in the ventral layer that will become the spongy mesophyll, but continues in the dorsal layer of cells that will become the palisade tissue. Subsequent cell expansion stops first in the spongy mesophyll. This results in the spongy mesophyll cells being pulled apart and to some extent distorted by the continuing growth of the other cell layers. Growth of the epidermis keeps pace with that of the palisade mesophyll, although the relative contribution of cell division and expansion to this growth varies between the two layers. After the spongy mesophyll, cell division stops next in the epidermal cells which then expand as the palisade continues to divide. The phase of palisade cell expansion is relatively short, and ends slightly before that of the epidermis. Palisade cells expand relatively little in the direction parallel to the leaf surface, but show significant elongation in the anticlinal direction which produces their characteristic columnar form (Steeves and Sussex, 1989). The time at which this sequence of events occurs in the different cell layers varies along the length of the leaf. Growth stops first at the tip of the leaf, and this cessation of growth proceeds basipetally. The gradient in the duration of cell division partly accounts for the shape of the mature leaf. Therefore in tobacco, as in many other plant species, the number of palisade cell per unit area is fairly uniform throughout the lamina, and the narrower parts of the leaf have fewer cells. However, cell size does decrease slightly toward the tip and the base of the lamina, but this difference accounts for only a small part of the variation in width (Poethig and Sussex, 1985).

Figure 5: Transverse section of a leaf primordium of tobacco, just prior to (left) and during (right) the initiation of the lamina. (Poethig and Sussex, 1985)

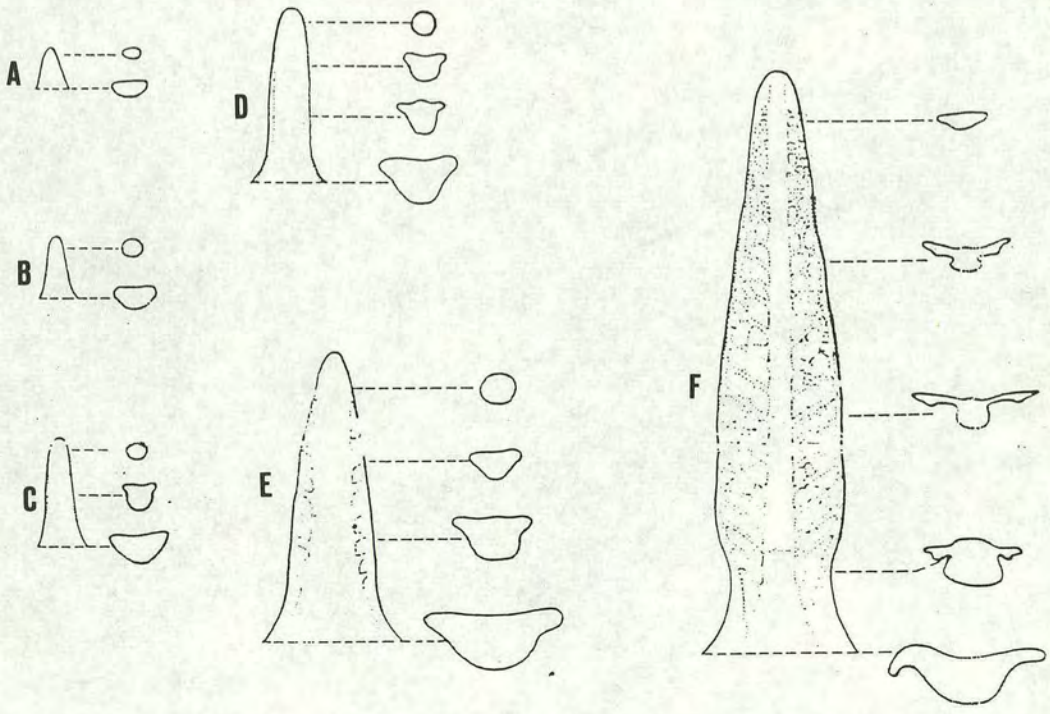

Figure 6: Stages in the development of tobacco leaf. A-F show successive stages. (Avery, 1933)

1.8: Leaves and vascular tissue: good companions

The vascular tissue has many important functions in the maintenance of the integrity of the plant. The most important are: distribution and relocation of water and inorganic and organic solutes (minerals, sugars, hormones, proteins). The array of vascular bundles contributes to the mechanical support of the aerial plant body, and the production of wood is closely related to the secondary growth of vascular tissue (Esau, 1977).

A bidirectional flux of organic and inorganic compounds is established between lateral organs and vascular tissue in order to exchange not only nutrients but also signal molecules. For instance, floral induction in many flowering plants is apparently due to signals which come from leaves and which are translocated through the vascular system to terminal meristems (Salisbury and Ross, 1992; Bernier *et al.*, 1993).

The leaf itself consisting of a fine network of veins. The relationship between leaf vasculature and that of the stem is interesting. So it seems appropriate to describe the development of leaves also taking into account development of the vascular system.

The organisation of the vascular system in stems of *Antirrhinum* is similar to that of many dicot plants. Transverse sections of the *Antirrhinum* stem at an internode reveals the anatomy of the mature vascular system (Fig. 7). It is organised in a system of discrete strands or vascular bundles. Each vascular bundle consists of xylem and phloem tissues, with the xylem differentiating near the pith (inside), and phloem near the cortex (outside). The xylem has two main roles: transport of large quantities of water from the root to the shoot in the tracheary elements, and mechanical support of the aerial plant body. Phloem is a complex tissue composed of sieve elements, companion cells, parenchyma and sclerenchyma cells, and it is responsible for the translocation of organic solutes. The vascular bundles are separated from each other by groups of parenchymal cells that interconnect the pith and the cortex (Fig. 7). The vascular bundles extend along the axis of the stem as a system that forms a ring around the central pith. The branching bundles are often interconnected, forming what are named *sympodia* (Esau 1977). An important feature of the vascular system is that at each node, one bundle diverges from the central ring and extends across the cortex into the leaf attached at the node. The extension of a vascular bundle from the stem towards a leaf is referred to as leaf trace (Fig. 8). A region without bundles is found above the leaf trace, before adjacent bundles reform a continuous cylinder. This is termed the leaf gap. If the vascular system is followed acropetally along the stem axis, it may be seen as branching

bundles. When the apex of *A. majus* is analysed in medial longitudinal sections, the uppermost limits of the vascular bundles merge into strands of densely cytoplasmic cells which are the precursors of vascular tissues. This procambium is identifiable by both the shape of the cells and by their strong staining reaction to the O-toluidine blue and other stains (Fig. 8).

The procambium cells are elongated along the main axis of the plant and they are longer than they are wide. However, they are initially not necessarily longer than the surrounding cells of the SAM, although they still show more intense staining. The uppermost limit seems to be localised exactly below the site of initiation of a leaf primordium (Steeves and Sussex, 1989). The close relationship between leaves or lateral organs and the procambium seems to have its origin at this level. Each leaf primordium has associated with it and extending into it a recognisable strand of procambium (Fig. 8).

From these observations a fundamental question arises: is the first stage of procambium differentiation dependent on the formation of a lateral primordium, or is a group of undifferentiated cells of the SAM committed to become procambium at an earlier stage? Alternatively, the vascular system might develop in response to a combination of meristematic pattern and the influence of leaf initiation.

There is much experimental evidence which supports the existence of an incipient vascular or provascular stage, preceding the leaf-related procambium stage in the shoot apex. For instance, in a transverse section of *Geum chiloense*, a ring of small densely staining cells that are cytologically very similar to the procambial cells is recognisable. Since the leaf-oriented procambium strands arise as part of this ring, it does not seem likely that the ring itself is related to differentiation of the leaf (McArthur and Steeves, 1972). Also in *A. majus* it is possible to detect a ring of cells that give rise to the procambium (Fig. 9). This ring appears to be the forerunner of the vascular system and has been designated provascular tissue in *A. majus* as well as in other plants. However, it is plausible that this ring of cells represents an uncommitted meristematic tissue which is recognisable only because the ground tissue of the pith and cortex mature more precociously (Esau 1965). In this view, the procambium is the very first step towards differentiation and the tissue ring consists of cells in a yet uncommitted state (Kaplan 1937). Observations in the fern *Osmunda cinnamomea* revealed the existence of provascular tissue above the site of leaf initiation (Stevees 1963). Moreover, experiments where leaf primordia were ablated provided evidence that in absence of leaves, the SAM can produce a ring of vascular tissue uninterrupted by leaf gaps (Wardlaw 1946).

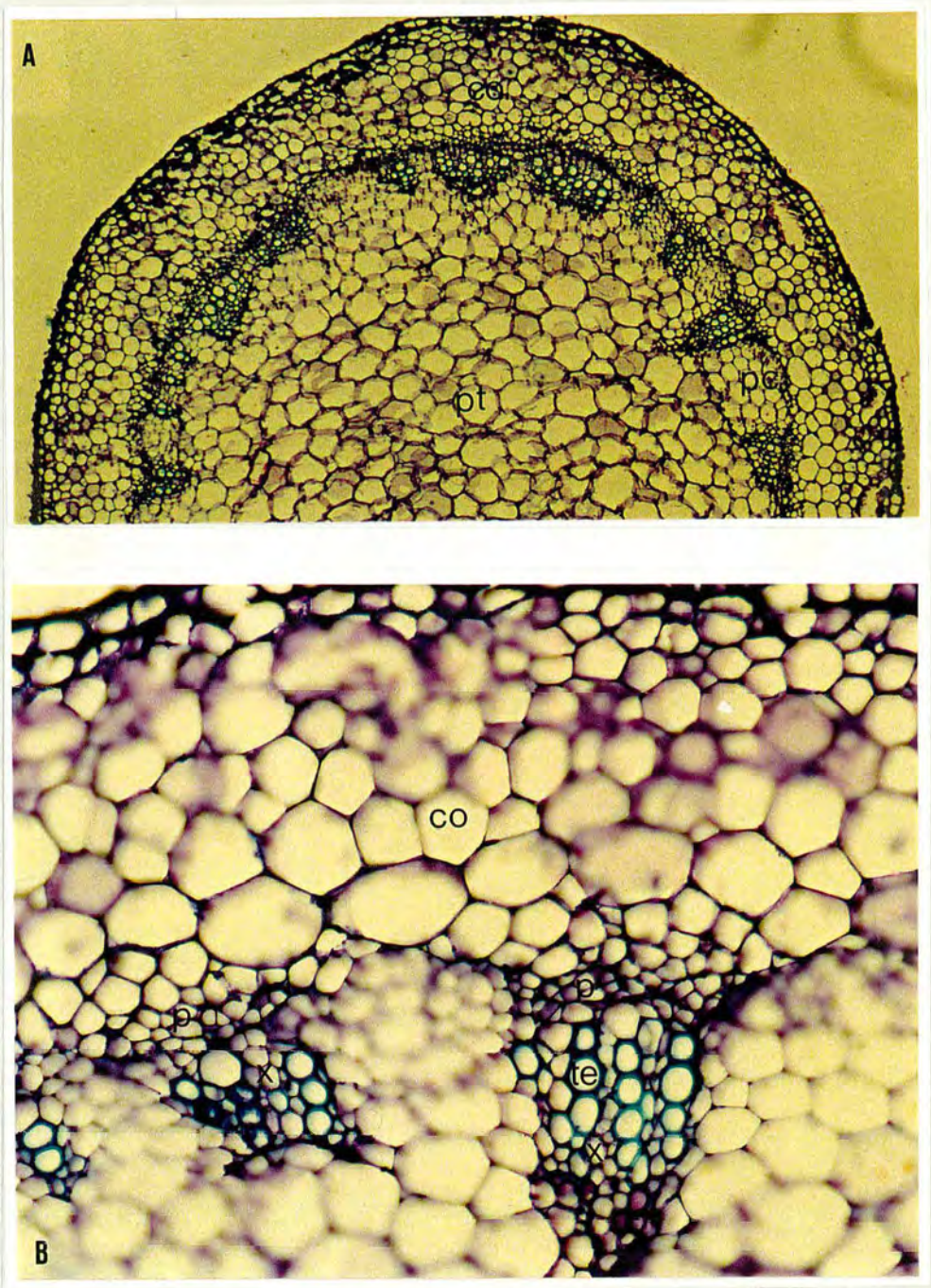

Figure 7: Transverse sections at internode of a WT *A. majus* stem showing the anatomical organisation of the mature vascular system. (A) The vascular system forms a ring of discrete bundles separated from each other by parenchymal cells (pc) (X23). (B) Higher magnification of vascular bundles: xylem (x) differentiates near the pith (pt) and phloem (p) near the cortex (co). Mature tracheary elements are stained in blue (te) (X40).

On the other hand, in *Lupinus* the removal of all leaves lead to a formation of a distinct provascular ring, but this tissue could not differentiate further into a more mature vascular tissue (Young 1954). This finding suggested that the leaf seems essential for development beyond the provascular stage.

Since developing leaves were known to be the primary source of auxin, an auxin source was supplied to the site of an ablated leaf. This allowed the ring of tissue to be more easily recognised, but no further differentiation was detected (Young 1954). However, when sucrose was applied together with the source of auxin, the ring of tissue differentiated into mature vascular tissue. Extensive studies on the influence of auxin flux and polarity in the differentiation of vascular bundles has been done by T. Sachs (1981; 1991). Although these studies have assigned to auxin a fundamental role in promoting vascular differentiation, the mechanism of auxin action still remains unclear. For instance, it is not known whether auxin is confined to developing vascular bundles, and if it is why does it not leak out? Vascular induction experiments were done in tissue that normally can give rise to vascular tissue. New induced vascular bundles form most easily in the region where procambium is present. This suggests that cells in the apical meristem have been predisposed to sense hormonal stimuli, coming from leaves or from exogenous sources. The stimuli later lead to the differentiation of a mature vascular system. How the SAM predisposes a group of cells to became a meristematic source of procambium is still unknown.

In addition to this, another question needs to be answered: does the provascular tissue perform a regulatory role in the leaf development in addition to demarcating the prospective vascular tissue?

Sharman (1942) suggested that in *Zea* the midvein is specified first, and thus it could send inductive signals which may promote leaf initiation. The idea that provascular cells could be inducers is only a speculation and experimental work is absent. However, in maize, studies of clonal analysis (Cerioli *et al.*, 1994) have addressed the possibility that leaf epidermal cells between veins behave as clonal compartments, or modules. Modules must form before epidermal differentiation when two lateral veins are separated from each other by just a few cells. This finding raises once again the question whether veins act as organisers. Yet it is not known if a module defined by two adjacent lateral veins is induced at an early stage by veins, or whether their clonal relatedness is merely a consequence of the pattern of cell division.

In conclusion, we can regard the leaf as one of the simplest plant organs in which to study the development of shape. Development of the leaf from the apical meristem involves a number of changes in the predominant patterns of cell divisions occurring in the primordium and the establishment of regional identities, and they must be closely controlled in order to form the leaf shape characteristic of the particular species. There is little evidence for the nature of the mechanisms which regulate these processes, although these processes can be disrupted by mutations.

CHAPTER 2

Material & Methods

Materials & Methods

2.1: Plant stocks

2.1.1: Nomenclature

All inbred lines of *A. majus* were referred to by their place of provenance. For example, the two wild type (WT) lines of plants coming from the John Innes Institute, Norwich, were labelled JI 98 and JI 75. Individual plants were referred to by a four part code (two letters and two numbers). The first letter indicated the place were the plant was maintained ("E" for Edinburgh) and the second letter indicated the time of sowing, so that the plants bearing the same second letter were raised at the same time. The first number referred to the plant family, that is all the plants grown from the seeds of a single capsule. The second number referred to a member of a family, and this number appeared as a superscript.

An example of numbering is given below:

ED 211^{7}: was the seventh plant of family 211. "D" denotes the set of plants, all of which were grown at the same time, and "211" the number of the family within the set. Plants grown by cutting were distinguished from the original plant by the suffix "C" (cutting), and if insufficient seedlings were obtained for a family, seeds from another capsule were sown, and the resown family distinguished from the original by the suffix "R" (resown).

2.1.2: Culture conditions

Seeds were germinated on the surface of moist vermiculite at 20°C under metal halide illumination, with a cycle of 16 hr light and 8 hr dark. Two weeks after germination, the seedlings were transferred to plug trays containing Levington M3 compost (Fisons) and grown under greenhouse conditions (mean temperature 18°C). After a period of about three weeks, they were transferred to 10 cm pots of John Innes No. 1 compost (300 l peat: 100 l sand: 100 l grit: 320 g Enmag fertiliser (ICI) and 250 g lime). In *A. majus* the transition from vegetative to inflorescence meristem is advanced by long days, and supplementary lighting was given in the evenings to keep the daylength above 16 hr and promote flowering.

2.1.3: Pollination

For outcrossing, immature anthers were removed from the female parent when the flower was still closed. Pollination was carried out using pollen from a dehiscent anther of the male parent once the emasculated flower had opened. Self-pollination was performed when the anthers of the flower were mature. Emasculation and pollination were carried out using forceps which were sterilised in 70% ethanol between each manipulation to prevent pollen contamination. Care was taken to remove excess alcohol which may have damaged the stigma or pollen. Cross-pollinated flowers were labelled around the pedicel (flower stalk) to allow identification of mature seed capsules. In summertime, the pollinated flowers were protected from insect pollinators by paper bags. Seeds were collected as soon as the fruit began to dehisce.

2.2: Preparative treatments of leaf tissue for microscopy and in situ hybridisation

2.2.1: Sampling the leaves

Because the mutant leaves showed different rates of growth, only fully expanded leaves were taken for microscopic analysis. Three or four leaves were taken from mutant plants. To provide a consistent comparison, leaves were harvested from the 5^{th} and 6^{th} nodes from the stem base. The external appearance of each mutant leaf was described qualitatively. Each leaf was divided into three regions (Tip, Middle and Petiole) in order to standardise the areas examined and to allow comparison of sections. The regions of the leaf were cut across the width of the lamina into strips approximately 3-5 mm wide to allow the penetration of the fixative.

2.2.2: Fixation

The leaf strips were fixed by immersion in FFA solution (90 ml of 50% (v/v) absolute alcohol, 5 ml glacial acetic acid, 5 ml formaldehyde 40% (w/v)) for 24 hr.

For in situ hybridisation, shoot meristems and leaves were cut from the plant and immediately immersed in a vial containing ice cold fix solution (4% formaldehyde solution(w/v), 1% Triton (v/v), 1% Tween (v/v)), and then left at 4°C overnight in order to minimise any mRNA degradation. 4% formaldehyde solution was made by adjusting the pH of 100 ml of 1X PBS (see 2.8.3.) to 11.0 using 10N NaOH. The 1X PBS

solution was heated to 60°C and 4 g of paraformaldehyde dissolved in it by shaking. The solution was then cooled to 4°C on ice and the pH readjusted to 7.0 using H_2SO_4.

To allow penetration of the fixative, the tissues were vacuum infiltrated. To do this, the shoot meristems and leaf material were forced down under the surface of the fixative solution using a piece of wire gauze, then placed in a vacuum desiccator and a vacuum created using an oil vacuum pump. Care was taken to ensure that the solution did not boil under reduced pressure. Since the formaldehyde is volatile, the fixative solution was replaced after vacuum treatment.

All the steps following tissue fixation until sectioning were the same for histological and in situ hybridisation protocols.

2.2.3: Dehydration

To dehydrate the tissues, shoot meristems and leaf strips were removed from fixative and immersed in 0.85% (w/v) NaCl solution (saline solution) for 30 min, on ice. Then the tissues were paused through series of solutions as follows:

50% (v/v) ethanol/0.85% saline solution	1.5 hr on ice
70% (v/v) ethanol/0.85% saline solution	1.5 hr on ice
85% (v/v) ethanol/0.85% saline solution	overnight 4°C
95% (v/v) ethanol	1.5 hr on ice
100% ethanol	1.5 hr on ice
100% ethanol	overnight 4°C

2.2.4: Addition of wax

Once dehydration was complete a solvent, Histoclear (Cell Path plc, Hemel Hemstead, UK), was used to replace ethanol in the tissue and allow the introduction of wax (Gurr Paramat Extra, pastillated, BDH). After the last change of 100% ethanol, fresh ethanol was added at room temperature and left for 2 hr. The tissues were then taken through steps of increasing histoclear concentration: 25:75 (v/v) histoclear:ethanol at room temperature for 1-2 hr; 50:50 (v/v) histoclear:ethanol for the same time; then three changes of 100% histoclear at room temperature each for 1 h. Molten wax was then added, dissolved in Histoclear in the proportion 50:50 (v/v), and tissues were left at 55-60°C for an overnight. On the two following days, the mixture was replaced each

morning and evening with 100% molten wax, poured slowly into the vials to avoid bubbles.

2.2.5: Embedding

Brass moulds chilled on ice were filled with molten wax. The tissues were then transferred into the molten wax and placed in appropriate orientations for sectioning. Flamed forceps were used to prevent rapid cooling of the wax surrounding the tissue during the transfer. The wax was left to cool on ice until it became a solid block. The blocks were stored at 4°C until use. Alternatively, thermo-resistant plastic moulds were used in the same way.

2.2.6: Preparation of slides and coverslips

In order to ensure the absence of any RNase in the in situ hybridisation experiments, slides were soaked in concentrated nitric acid for 30 min. They were then washed for at least 1 h in several changes of sterile distilled water, and drained. Finally they were washed in acetone for 15 min, dried and baked at 180°C overnight.
When the slides were cool, 8-10 µl of poly-L-lysine (1 mg ml^{-1} in DEPC water) was added to one side of the slide, and spread into a film over the slide using a coverslip. The slides were left on a 42°C hotplate overnight to dry, and stored at 4°C in a box with desiccant. Under these conditions the slides were stable for at least one week. The coverslips were washed in acetone for 15 min and baked as the slides.

For histological microscopy, the slides were washed in distilled water and dried. A film of glycerine albumen was spread on one surface of the slide to ensure that the sections stuck to it.

2.2.7: Sectioning

The wax block was trimmed to allow the tissue to be localised and ensure that it was lying straight in the block. The block was then cut to a trapezoid shape to ensure that a straight ribbon of sections would be obtained. The tissue was sectioned on a microtome (R. Jung-AG, Heidelberg) to produce a ribbon of longitudinal sections of the shoot meristems and transverse sections of leaf blade of 5-10 µm thickness. Ribbons of section were laid onto slides. Sterile distilled DEPC-treated water was dropped onto the slides to float the sections, and the slides were placed on a hotplate at 42°C. Once

the sections had spread out, the excess water was drained off and the slides were left to dry on the 42°C hotplate overnight.

2.2.8: Staining and de-waxing for histological analysis

The embedded plant material was stained using toluidine blue-O for histological analysis (Sakai, 1973). The slides were placed in 0.05% toluidine blue-O in distilled water for 2-10 min. They were periodically removed from the stain, rinsed in water, and viewed to check the intensity of the staining. When the staining was satisfactory, the slides were rinsed in water for 1 min and allowed to air dry. The wax was removed with two changes of Histoclear. The cover slips were mounted with a synthetic neutral resin (Entalan). Other stains including safranin or fast green were sometimes also used.

Safranin was prepared as follows: 50 ml of (0.1%) safranin in Cellosolve (2-ethoxythanol) was stirred overnight and filtered through Whatman paper. 25 ml of 90% alcohol, 25 ml of 4% sodium acetate and 1 ml of 40% formaldehyde were then added, and the solution mixed.

Fast Green at 5% (w/v) was dissolved in a mixture of equal parts of Cellosolve, absolute alcohol and oil of cloves.

2.2.9: Histological analysis of sections

Microscopic analysis was used to produce qualitative descriptions of the leaf sections. Photographs of representative areas of the sections were taken using a Polyvar Widefield Photomicroscope (Reichert-Jung,) and Kodak Ektachrome T64 film.

2.2.10: Scanning electron microscopy (SEM)

SEM of leaf surfaces and plant apices was carried out on resin replicas made using a modification of the method described by Green and Linstead (1990). Specimens of plant material were coated in Extrude vinylsiloxane dental impression medium (Kerr UK Ltd., Peterborough, UK), which polymerised to form moulds. After about 30 minutes, the moulds were removed and infiltrated with Agar 100 epoxy embedding resin for 15 min at 70°C under vacuum. The vacuum was then released, the moulds drained of excess resin, and the remaining resin allowed to polymerise at 65°C for 16-24 hr. Resin replicas were gold coated before examination at ambient temperature in the scanning electron microscope.

Freeze fractured sections were prepared as follows: a mature leaf from each mutant was mounted on an SEM stub, frozen in nitrogen slush, and broken to give a transverse section of the lamina. The broken surface was carbon coated and examined whilst still frozen in the cryo-SEM.

2.2.11: Statistical analysis

[1]Analysis of Variance was applied to different morphological parameters chosen to represent the major differences observed between transverse sections of mutant and wild-type leaves. The parameters were:

1) Midrib height, measured vertically from the middle of the dip on the dorsal surface to the ventral surface, as shown in Fig 10.

2) Midrib width, measured at the midpoint of the midrib height. If the midrib was less pronounced, then the distance between the first palisade cells on each side of the blade was measured, as shown in Fig 10.

3) Number of cells in the ventral epidermis of the lamina (Fig 10).

4) Number of cells in the ventral epidermis of the midrib (Fig 10).

5) Thickness of the lamina at the distal-point (Fig 10)

Variance Analysis (one way) was applied to the data using the Statgraphics program (Statistical Graphics System).

2.3: Gene nomenclature

Attempts have been made to unify the system of gene nomenclature in line with that adopted by *Arabidopsis* workers from yeast. Wild-type loci and phenotypes are shown in italic capitals, recessive mutant loci and phenotypes in lower-case italics. In the case of dominant mutant the nomenclature is given in lower case italics except for the first letter which is upper case italics. The allele name is given in lower case Roman. Proteins are shown in Roman capitals.

---

[1] The analysis of variance allows differences or equality between two or more samples of data coming from the measurement of one parameter to be define. It is a way of testing a null-hypothesis.

1) Midrib Height

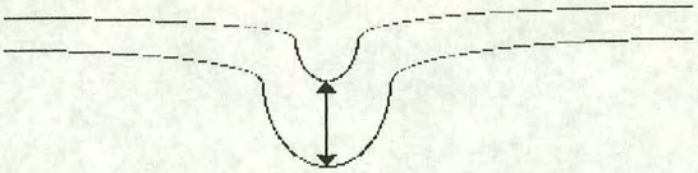

2) Midrib Width

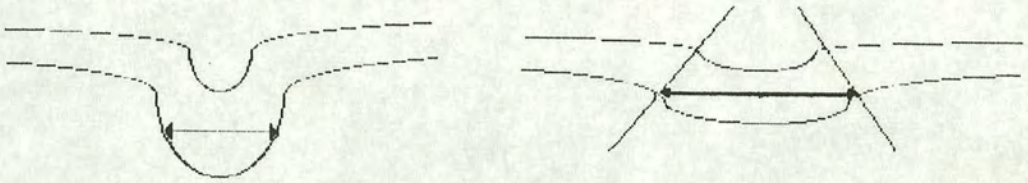

3) Number of cells in the ventral epidermis of the leaf lamina

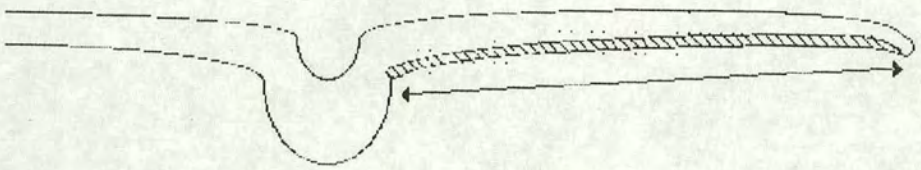

4) Number of cells in the ventral epidermis of the midrib

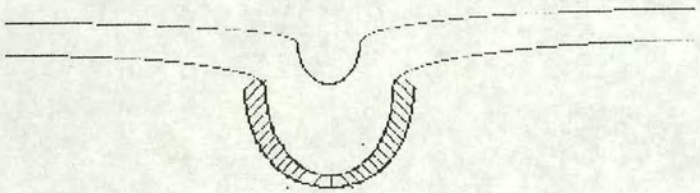

5) Thickeness of the leaf lamina at the distal point

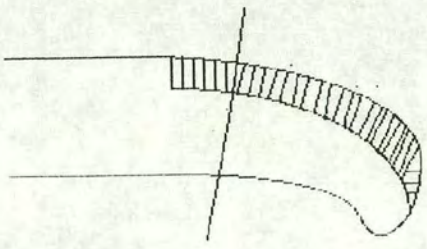

Figure 10: Criteria for taking measurements from transverse section of leaves.

2.4: DNA and RNA extraction and detection.

2.4.1: DNA Extraction

DNA extractions were performed using the method of Coen *et al.*, (1986). 3-5 g of leaves were harvested and frozen in liquid nitrogen. Tissue not for immediate use was stored at -70°C. The foliar tissues were ground for 1 min in a chilled coffee grinder to produce a powder. The powder was thawed in 25 ml of DNA extraction buffer (see 2.10) in a sterile tube. The resulting mixture was extracted once with 20 ml of chloroform, once with 25 ml of phenol:chloroform (1:1), and finally with an equal volume of chloroform. Each extraction involved vigorous shaking for a few minutes. The aqueous phase was separated from the organic phase and debris by centrifugation at 3600 rpm for 5-10 min in a MSE Mistral 1000 between each extraction. Nucleic acids were then precipitated with an equal volume of ethanol, recovered by centrifugation, and left to dry at room temperature. The nucleic acid pellet was dissolved in 5 ml of TE solution containing 25 $\mu g\ ml^{-1}$ RNase A (DNase free) to degrade RNA, and left for either 30 min at room temperature with occasional shaking, or at 37°C for 10-15 min with continuous shaking. 0.7 ml of 5 M NaCl was added to the solution, followed by 5.7 ml of CTAB solution, in order to precipitate DNA. The precipitate was pelleted by centrifugation at 3600 rpm for 5 min, and the resulting pellet washed overnight with 10 ml of 70% ethanol and 30% 0.5 M NaCl to displace CTAB. The DNA was recovered by centrifugation, air dried and then dissolved in 0.5 ml of TE pH 8.0.

2.4.2: RNA extraction

Total RNA was extracted from different parts of the plant. Tissues were collected and immediately frozen in liquid nitrogen. To avoid any exogenous RNase contamination of the RNA sample, all the plasticware and glassware were first autoclaved and then baked at 120° C overnight. For the preparation of the solutions required for the extraction, DEPC-treated water was used.

The tissue was ground with a pestle in a sterile mortar. The resulting powder was resuspended in RNA extraction buffer (see 2.9.), extracted three times with equal volumes of phenol-chloroform and finally with chloroform. The supernatant was transferred in a fresh tube and the total RNA precipitated by adding one third of the volume of 8 M LiCl and left at 4°C overnight. The RNA was pelleted by centrifugation for 15 min at 3,600 rpm in a MSE Mistral 1000 centrifuge, the supernatant discarded

and the pellet washed several times with a solution of 70% ethanol and 0.15 M NaCl. After the final centrifugation, the pellet was redissolved in DEPC-treated water.

2.4.3: Estimation of DNA and RNA yields

The concentration of DNA or RNA in a solution was estimated by measuring the difference between the absorption of light of 260 nm and 280 nm wavelength.

$$\text{concentration } (\mu g\ \mu l^{-1}) = \frac{2 \times (A260 - A280)}{a\ X}$$

Where *a* is 20 for DNA and 25 for RNA. X is the dilution factor. This minimised the effect of absorption by compounds other than nucleic acids, which may have remained in the preparation. Estimates of nucleic acid concentrations were also obtained by visual comparison in ethidium bromide stained agarose gels.

2.4.4: Digestion of Plant DNA with Endonucleases

For Southern blots 5-6 µg of DNA was digested for 2-2.5 hr at 37°C in 25 µl final volume containing 2.5 µl of 10X buffer of the appropriate salt concentration, 1.25 µl of 50 µM spermidine solution and 10-25 units of restriction endonuclease. For visualisation of digested DNA in minigels, the reaction was scaled down according to the amount of DNA digested so that the DNA concentration never exceeded 0.5 µg μl^{-1}.

2.4.5: Agarose Gel Electrophoresis of DNA

For Southern hybridisation of plant DNA, one tenth volume of loading buffer was added to the digested sample. The digested solutions were loaded into submerged 8 mm thick gels of 0.5 % or 1.2 % agarose in 1X TBE. Electrophoresis was carried out in 1X TBE at 50 mV cm^{-1} for 1.5 -2 days. Gels were stained with 10 µg ml^{-1} ethidium bromide in TBE, the DNA visualised on a 610 nm UV transilluminator, and photographed on Mitsubishi video copy processor (Mitsubishi Electric Corporation).
To check for the presence and digestion of DNA, or to estimate the size of recombinant DNA fragments, meniscus minigels 2-4 mm thick were used. These were treated as large agarose gels except that they were run at 75-100 mV cm^{-1} for 15 min to 1 hr.

2.4.6: Agarose Gel Electrophoresis of RNA

Total RNA was fractionated by electrophoresis through horizontal gels containing 1.2% agarose in 7% formaldehyde and 1X MOPS buffer (Sambrook *et al.*, 1989). Samples contained up to 10 μg of total RNA in 25% (v/v) formaldehyde, 50% (v/v) formamide, 0.5 μg ml^{-1} ethidium bromide and 1X MOPS in a final volume of 25 μl. Before loading, 2.5 μl of loading buffer (see 2.10) were added and the samples heated at 55°C for 10 min. Electrophoresis was carried out in 1X MOPS buffer at 40 mV cm^{-1} for 4 hr.

2.4.7: Southern blotting

Transfer of DNA from agarose gels to Hybond-N filters (Amersham) was carried out using the method described in Sambrook *et al.* (1989). DNA in the gels was partially nicked by depurination caused by soaking in 0.25 M HCl for 10 min, and denatured in 0.5 M NaOH, 1.5 M NaCl for 30 min, with gentle shaking. The alkali was neutralised by washing the gel for 30 min in 1 M Tris-HCl pH 7.0, 1.5 M NaCl with shaking. Transfer to the Hybond-N filter wetted in 20X SSC, was carried out overnight in 20X SSC. Several pieces of Whatman paper were cut to the size of the gel, as was the piece of Hybond-N nylon. Two large gel plates were placed inside a plastic tray containing 20X SSC, and two pieces of Whatman paper were draped over the opposite sides of the plates into the SSC. The gel was placed upside down on the Whatman papers, then the piece of Hybond-N was placed on top of the gel with care to avoid bubbles. Three layers of wetted Whatman paper followed by seven dried ones were placed above the Hybond-N, followed by a thick layer of paper towels and a weight of about 0.5 kg. After the transfer had taken place, the filter was removed from the gel, washed gently in 2X SSC, and the DNA on the filter cross linked to it by exposure to 0.40 $mWcm^{-2}$ of UV light.

2.4.8: Labelling of the probes with radioactive isotope

50-100 ng of DNA was labelled in a random primer reaction (Feinberg and Vogelstein, 1983). The purified DNA probe was diluted with water to a final volume of 27 µl, and denatured by boiling at 100°C for 5 min. After chilling on ice, 6.0 µl of OLB (see 2.10), 1.0 µl of BSA (10 mg ml^{-1}), 3.0 µl of α-(^{32}P)dCTP (3000Ci mM^{-1}) and 1.5 units of Klenow fragment of DNA Polymerase I (1 U μl^{-1}) were added. The reaction was incubated at 37°C for 45 min. The radiolabelled probe was then separated from the unincorporated α-(^{32}P)dCTP by chromatography on a small column of Sephadex G-50 DNA grade (Pharmacia). The Sephadex was prepared as follows: the resin was washed with distilled, sterile water several times to remove soluble dextran (10 g of Sephadex G-50 yields 160 ml of slurry). Then the resin was equilibrated in TE pH 7.6, autoclaved at 15 psi for 30 min and stored at 4°C. The column was made using a 1 ml plastic syringe barrel plugged with a small piece of Whatman paper. Using a Pasteur pipette, the syringe was filled with TE and then with the Sephadex slurry until it packed to a level about 1 cm below the top of the syringe. The solution containing the labelled probe was mixed with a solution of Dextran Blue and Orange G (~25 µl) and loaded onto the column which was run by adding TE. The Dextran Blue co-migrates with DNA and the Orange G with unincorporated nucleotides allowing separation on the column to be visualised. The localisation of labelled DNA was further monitored with a Geiger counter. The probe, which eluted first, was collected in a sterile Eppendorf tube, and care was taken to avoid collecting unincorporated nucleotides.

2.4.9: Pre-hybridisation and Hybridisation

Nitrocellulose or Hybond-N filters were pre-hybridised by incubation for 30 min at 65°C in 50 ml of 3X SSC, 0.1% SDS, 0.2% Ficoll and 0.2% Polyvinilpyrrolidone with the addition of 0.5 ml salmon-sperm DNA (10 mg ml^{-1}), freshly denatured by heating to 100°C for 10 min before use. The probe was denatured by boiling for 10 min with 0.5 ml of 10 mg ml^{-1} salmon-sperm DNA, mixed with 50 ml of hybridisation solution (as pre-hybridisation solution) at 65°C, and used to replace the pre-hybridisation solution. Hybridisation was carried out in sandwich boxes with shaking at appropriate temperatures for 10-16 hr. After hybridisation, the filters were washed in 0.5X SSC, 0.1% SDS for 5-10 min at the same temperature as hybridisation. After this first wash, the filters were monitored with a Geiger counter and where required a second wash carried out. Washed filters were partially air dried, wrapped in Saranwrap (Dow

Chemical Company, UK) and exposed at -70°C, to X-ray film (Cronex blue base X-ray film, Dupont, UK) using intensifying screens.

2.4.10: Northern hybridisation

After electrophoresis, RNA was transferred to nitrocellulose filters as described for DNA, except that the gel was not subjected to any prior treatment and the transfer was carried out in 10X SSC. The nitrocellulose filter was viewed on a UV transilluminator after blotting to locate ribosomal RNA band, and to examine the quality of the RNA. Detection of the RNA was made using DIG Northern Luminescent Detection Kit (Boehringer Mannheim, UK). The preparation of the hybridisation solution was carried out according to the manufacturer's instructions as were all the steps for hybridisation and detection of the labelled RNA.

2.5: Preparation of plasmid DNA

2.5.1: Small scale preparation

Plasmid DNA was prepared on a small scale by a modification of the rapid extraction alkaline lysis method of Sambrook *et al.*, (1989).

A single bacterial colony was used to inoculate 5 ml of L-broth, supplemented with appropriate antibiotics when required, and grown with vigorous shaking at 37°C overnight. Cells from a 1.5 ml aliquot of this culture were pelleted in a MSE microfuge at 13,000 rpm for 2 min, and the supernatant discarded. The cells were resuspended in 100 µl of 50 mM glucose, 10 mM EDTA, 25 mM Tris-HCl pH 8.0. Then 200 µl of 0.2M NaOH 1% SDS was added and the contents mixed by inverting the tube five or more times. The tube was then incubated on ice for 5-10 min before the addition of 150 µl of 3 M potassium acetate pH 4.8. The tube was inverted a few times and after a further 10 min incubation on ice, the sample was centrifuged in a cooled micro centrifuge for 5 min at maximum speed and the supernatant transferred to a fresh tube. The sample was then extracted with phenol-chloroform, centrifuged 2 min and the supernatant placed in a fresh tube. The DNA was precipitated with an equal volume of 100% ethanol, centrifuged and the pellet rinsed with 1 ml of 70% ethanol. Once the ethanol had been removed, the pellet was left to air dry and redissolved in 20 µl of TE buffer. Aliquots of 2 µl were used for restriction digestion together with RNase-A added to a final concentration of 0.1 µg ml^{-1} in the reaction mixture. Alternatively a small scale

procedure to extract plasmid DNA for sequencing, was performed using the Wizard^{TM} DNA Purification System from Promega. The method was carried out according to the manufacturer's instructions.

2.5.2: Extraction of DNA from agarose gel

Three methods were used:

a) Freeze-squeeze

This is a rapid DNA purification method with a recovery of approximately 60%, although the efficiency drops for large DNA fragments. A small hole was made in a 0.5 ml Eppendorf tube with a hot needle. The bottom of the tube was filled with glass beads to make a filter, and the gel slice cut in small cubes and loaded into the tube. The tube was then placed inside a 1.5 ml microfuge tube and spun at 13,000 rpm for several minutes. The aqueous solution containing the DNA was recovered from the lower tube, transferred into a fresh tube, phenol-chloroform extracted, and the DNA precipitated with ethanol. The DNA was dissolved in 10-20 µl of water or TE, and used directly in probe synthesis.

For ligation reactions, the DNA was purified from the aqueous solution using the Magic^{TM} DNA Clean-Up System from Promega following the manufacturer's instructions.

b) Geneclean

Geneclean kits were supplied by BIO 101 Inc, UK. This method utilises DNA binding affinity for silica in the presence of a chaeotrope, and the efficiency of recovery for DNA fragments over 500 bp is 80%.

The agarose slice was melted at 55°C with 3 volumes of the 6 M NaI stock solution and TBE modifier. 5 µl of Glassmilk was added (to purify up to 5 µg of DNA) and allowed to bind for 5 min. While the Glassmilk was present in the solution it was not vortexed to avoid shearing the DNA. The Glassmilk/DNA was pelleted for 5 sec by centrifugation and washed three times with the supplied "New Wash". The DNA was eluted in 10 µl of water at 55°C, the Glassmilk spun down and the DNA solution transferred to a fresh tube. The sample was re-spun to remove all traces of the silica matrix before using it in ligation reactions, since the Glassmilk could inhibit this process.

c) NACS Prepac^{TM} columns

NACS columns (Gilbo BRL) were used when a large amount of pure DNA was required. The NACS column is an ion exchange resin that can bind up to 40 µg of DNA in a low salt concentration (0.1-0.5 M NaCl) and release them in a high salt concentration (0.7-2.0 M NaCl). All steps of the DNA isolation with this column were carried out as indicated in the manufacturer's instructions.

2.5.3: Ligation of DNA molecules

The vector and DNA insert were cut to completion with the appropriate endonuclease(s). Endonucleases were removed by phenol extraction and the DNA precipitated with ethanol. Typically between 200-600 ng DNA insert was ligated with a linearised vector in a 3:1 insert:vector molar ratio (Sambrook *et al.,* 1989). Ligation was carried out in 10 µl reaction volume containing 1X ligation buffer (66 mM Tris-HCl pH 7.5, 5 mM $MgCl_2$, 1 mM dithioerythritol (DTE), 1 mM ATP), and incubated overnight at 12°C. The ligation products were then transformed into an *E. coli* strain.

2.5.4: Phenol Extraction and Chloroform Extraction

Organic solvents enable separation of nucleic acids from contaminating proteins. Redistilled phenol saturated with water was purchased from Raithburn Chemicals. It was equilibrated with 0.1 M Tris-HCl pH 8.0 and 8-hydroxyquinoline was added to 0.1% (w/v). Solutions of nucleic acids were deproteinised by shaking or vortexing, with an equal volume of phenol or phenol/chloroform (1:1 v/v). The phases of the emulsion were separated by centrifugation. Samples less than 1 ml in volume were centrifuged in a MSE microfuge (Fisons) at 13,000 rpm for 2 min at room temperature. Samples over 1 ml were centrifuged in a Mistral 1,000 centrifuge at 3,600 rpm for 20 min at room temperature or in a Sorrall RC-5B centrifuge, using a SorrallR HB4 (swing out) rotor, at 13,000 rpm for 5-10 min at 4°C. The aqueous phase which contained the nucleic acid was retrieved.

Chloroform extractions were performed following phenol extraction to remove residual phenol from the sample (Sambrook *et al.*, 1989).

2.5.5: Precipitation of nucleic acids

Under high salt conditions, nucleic acids precipitate from solution upon addition of ethanol. 0.1 volumes of 3 M sodium acetate pH 5.0 (Na-Ac) and 2.5 volumes of ice cold 100% ethanol were added to a nucleic acid solution and incubated at -70°C for 30 min. The precipitate was collected by centrifugation in a MSE microfuge for 1 ml volume at 13,000 rpm for 30 min at 4°C. For larger volumes, a Sorrall RC-5B centrifuge with a Sorrall SS34 rotor was used at 10,000 rpm for 30 min at 4°C. The supernatant was discarded and the pellet of precipitated nucleic acids retrieved. To wash away contaminating salts, 1-2 ml ice cold 70% ethanol was gently added to the pellet and incubated on ice for 5 min. The supernatant was discarded and the pellet desiccated under a vacuum of -1 bar (Gyro Vap, Howe). The pellet was finally redissolved in TE buffer or sterile distilled water.

2.6: Transforming *E. coli*

2.6.1: $CaCl_2$ method

L-broth (100 ml) was inoculated with 1 ml of an overnight culture of the relevant bacterial strain and grown at 37°C with shaking until the OD 600 reached 0.2-0.3 (measured using a Philips PU 8625 UV/VIS spectrophotometer). The culture was chilled on ice for 10 min. The cells were pelleted by centrifugation (4,000 x g max., 10 min 4°C) and re-suspended in 50 ml of ice-cold, sterile 50 mM $CaCl_2$. The suspension was left on ice for 15 min and the cells then repelleted and resuspended in 2.5 ml of ice-cold 50 mM $CaCl_2$. One 0.1 ml aliquot of this suspension was removed into a 1.5 ml tube for each transformation and stored at -70°C. The transformation was carried out as follows: 10-100 ng of DNA from the ligation reaction were mixed with the aliquot of the competent cells, and incubated on ice for 30 min. The cells were then heat-shocked at 42°C for 90 sec and returned to ice for a further 15 min. 0.9 ml of L-broth including 10 mM glucose was added to each tube and the cells incubated at 37°C for 1 hr. Samples of 100-200 µl of each transformation were then plated out on L-agar plates supplemented with ampicillin (to final concentration of 150 µg ml^{-1}). The plates were inverted and incubated at 37°C overnight.

2.6.2: Electroporation method

L-broth (1 litre) was inoculated with 1/100 volume of fresh overnight culture of the relevant bacterial strain, and grown at 37°C with vigorous shaking to an OD 600 of 0.5-0.6. The culture was chilled on ice for 15 to 30 min and centrifuged in a cold rotor at 4,000 x *g* for 15 min. Once the supernatant had been removed, the pellet was resuspended in 1 l of ice-cold sterile 10% glycerol and centrifuged as before. After removal of the supernatant, the pellet was resuspended in 0.5 l of the same glycerol solution and centrifuged. The same steps were repeated twice more, using 20 ml of ice-cold 10% glycerol followed by a final step using 2-3 ml of the same solution. This suspension was frozen in aliquots of 100 µl (in liquid nitrogen), and stored at -70°C. For the transformation step, 40 µl of cell suspension were placed in a cold 1.5 ml microfuge tube and mixed with 10-100 ng of DNA. The mixture was placed on ice until transferred to a chilled cuvette (Bio-Rad gene pulser/*E. coli* pulser^{TM} cuvette). The Gene Pulser apparatus (Bio-Rad) was optimised for *E. coli* electroporation following the manufacturer's instructions with resistance set at 200 Ohm and capacitance at 25 mF. The cuvette was placed in a chilled safety chamber slide and a single electric pulse of 2.5 kV was administered to the bacteria for 3-5 msec. Once the pulse had been given, 1 ml of SOC medium was immediately added to the cuvette and cells quickly re-suspended with a Pasteur pipette. The mixture was transferred to a microfuge tube and incubated at 37°C for 1 h. Samples of 100-200 µl of each transformation were then plated out on to L-agar plates supplemented with ampicillin to a final concentration of 150 µg ml^{-1}. The plates were inverted and incubated at 37°C overnight.

2.6.3: Colour selection of transformant bacteria

Bacteria transformed with pBluescript acquired ampicillin resistance. In addition, pBluescript allowed for blue/white transformant selection when plated on medium with IPTG and XGal (BioGene. UK) at final concentrations of 40 µg ml^{-1}. Bacteria in which the plasmid contains an insert in the multiple cloning sites usually produce white colonies, whereas those in which the plasmid remains unaltered produce blue colonies (Sambrook *et al.*, 1989).

2.7: DNA sequencing

2.7.1: Generation of nested set of deletions with Exonuclease III

Nested deletions of DNA fragments were required for DNA sequencing when the cloned DNA was bigger then 250 bp. Deletions of cloned DNA fragments were generated using Exo III and S1 nucleases. The Exo III removes 5' mononucleotides from recessed or blunt 3' termini, whereas protruding 3' termini are completely resistant to the action of the enzyme. To create various nested deletions, the plasmid was digested between the target DNA and the plasmid sequences with two restriction endonucleases which did not cleave the cloned insert. One cut nearer the plasmid sequence, generating a protruding 3' terminus, thus protecting the plasmid from deletion in this direction, and the other cut next to the target DNA generating either a blunt or recessed 3' terminus. Digestion therefore occurred unidirectional into the target DNA sequence. The protruding single strands were then removed by digestion with S1 nuclease, and the plasmid recircularised. Digestion with Exo III nuclease occurs at a uniform rate allowing the production of nested deletions of the required size. 10-20 µg plasmid DNA were digested with the two restriction endonucleases for 2 hr at 37°C. The enzymes were extracted from the sample with an equal volume of phenol-chloroform, the sample mixed and the two phases separated by centrifugation at 13,000 rpm for 5 min. The aqueous phase was transferred to a fresh tube. The DNA was ethanol precipitated, the pellet washed with 70% of ice-cold ethanol and then dried. It was redissolved in 60 µl 1X Exonuclease III buffer (66 mM Tris-HCl pH 8.0, 6.6 mM $MgCl_2$) and preincubated at 37°C for 5 min. In the meantime, 25 microfuge tubes each containing 7.5 µl S1 reaction mixture (30 mM potassium acetate, pH 4.5, 50 mM NaCl, 10 mM $ZnSO_4$, 0.6% (v/v) glycerol, 0.6 U μl^{-1} S1 nuclease) were stored on ice. 150 U Exo III per pmole of recessed 3' termini were added to the linearised DNA, the sample mixed and incubated at 37°C. Under these conditions, Exo III nuclease removes approximately 200 nucleotides per minute from the recessed 3' end. 2.5 µl samples were removed at 15-30 sec intervals, added to 7.5 µl S1 reaction mix and kept on ice. After all 25 samples had been taken, the tubes were incubated for 30 min at room temperature. The reactions were stopped by addition of 1 µl S1 STOP mixture (0.3 M Tris base, 50 mM EDTA, pH 8.0). Aliquots of each sample were analysed by electrophoresis through 1% (w/v) agarose to check the rate of deletion. The samples of the desired size were pooled, phenol-chloroform extracted, ethanol precipitated and the pellet redissolved in 10 µl of sterile distilled water. To this solution, 1 µl of Klenow mixture (0.2 M $MgCl_2$, 10 mM

Tris-HCl, pH 7.6, 0.1 U μl^{-1} Klenow fragment of *E.coli* DNA polymerase) was added and incubated for 5 min at 37°C. After incubation, 1 µl of a solution containing the four dNTPs, each at a concentration of 0.5 mM, was added to each of the pooled samples, and the incubation carried on for a further 15 min at room temperature. To recircularise the linear DNA, 2 µl of 10X ligase buffer (500 mM Tris-HCl, pH 7.6, 100 mM $MgCl_2$, 100 mM DTT, 50 mg ml^{-1} BSA), 3 µl of 15% polyethylene glycol (PEG 8000), 5 Weiss units T4 DNA ligase and sterile distilled water to final volume of 20 µl, were added to each sample and incubated at room temperature for 3-4 hr. 2 µl aliquots were used to transform competent *E. coli* by electroporation. Those colonies containing plasmids of the desired size detected by restriction endonuclease digestion and gel electrophoresis, were used to prepare plasmids for sequencing.

2.7.2: Sequencing

The nested set of deletions were sequenced using T7 Sequencing Kit (Pharmacia). Each DNA template was sequenced from -40 or Reverse priming sites of pBluescript, according to the orientation of the cloned DNA and therefore to the orientation of the deletions.
The method yielded ^{35}S-labelled, dideoxy base terminated DNA fragments which were separated by electrophoresis in a 5% polyacrylamide-TBE denaturing gel containing 7 M urea.

2.7.3: Sequencing reaction 1: primer annealing

DNA was purified for sequencing as described in 2.5.2. For each sequencing reaction, 2 µg template DNA was dehydrated under vacuum and dissolved in 10 µl of water. To denature DNA and also hydrolyse any RNA present in the solution, 2 µl of 2 M NaOH was added to the DNA and incubated at room temperature for 15 min. Solutions of denatured DNA were neutralised with 3 µl 5 M K-Ac, and ethanol precipitated. The pellet was washed with 70% ethanol, dried under vacuum, and re-dissolved in 10 µl of water plus 2 µl of annealing buffer and 1 µl of primer (10 µM). The annealing was performed by placing the tube into a block preheated to 65°C, then removing the block from the source of heat and leaving it until the temperature reached 37°C.

2.7.4: Sequencing reaction 2: labelling and extension reactions

Sequencing reactions were performed following the manufacturer's instructions in the T7 Sequencing Kit. The method is based on two-stage extension of primers by T7 polymerase. First, a single labelling reaction was carried out in the presence of all deoxynucleotides, one of them radiolabelled (^{35}S-dATP). Secondly, four separate extension and termination reactions were carried out, each with one quarter of the labelling reaction and including a single dideoxynucleotide. The addition of the dideoxynucleotide to the end of DNA polymer caused extension to terminate. Incorporation into the DNA strand was random for each dideoxynucleotide, hence all fragments between approximately 50-500 bp were represented.

2.7.5: Denaturing polyacrylamide gel electrophoresis

Chain terminated reaction products were separated by electrophoresis in 5% polyacrylamide denaturing gels (5% acrylamide, 0.3% N,N,-methylenebisacrylamide, 7 M urea, 1X TBE, 0.04% AMPS w/v, 0.2% TEMED). The sequencing gel apparatus (Sequi-gen nucleic acid sequencing cell, Bio-Rad, UK) was mounted and sequencing gels poured according to manufacturer's instructions. Gels 0.4 mm thick were run in 1X TBE and heated to 50°C prior to sample loading. Samples were incubated at 80°C for 3 min to denature DNA, and loaded onto sequencing gels in the order T-C-G-A (nucleotide bases represented by their initials). Samples were subjected to electrophoresis at an appropriate current to maintain gels at a temperature of 50°C. Gels were fixed in 2.5 l 10% v/v methanol, 10% acetic acid solution for 30-45 min. Gels were drained for 2 min, blotted dry and transferred to Whatman 3 MM paper. Mounted gels were dried under vacuum (Model 583 Gel Dryer, Bio-Rad) at 80°C for 1 h and allowed to cool before autoradiography using Cronex blue base X-ray film (Dupont).

2.8: Manipulation of phage Lambda

2.8.1.: Plating of phages

An appropriate strain of bacterial plating cells was grown in 50 ml L-broth supplemented with 0.2% maltose and 10 mM $MgSO_4$, at 37°C overnight. The cells were pelleted by centrifugation at 3,600 rpm for 10 min in a MSE mistral 1000, resuspended in sterile 10 mM $MgSO_4$ to give an OD 600 of 2 and stored at 4° C. Series

of phage dilutions were mixed with 150 µl of plating cells and incubated for 20 min at 37°C to allow the phage to infect the bacteria. The mixture of phage and cells was added to 3 ml of molten BBL top agar at 47°C and quickly poured onto dried BBL agar plates (9 cm diameter). The plates were allowed to set, inverted and incubated at 37°C overnight. Titres of phage were calculated from the number of plaques produced by a given dilution.

2.8.2: Picking of plaques and small-scale liquid culture of bacteriophage

A well isolated phage plaque was picked into 0.5 ml of phage buffer with 2 µl of chloroform and the phage left to elute from the agar plug at 4°C for 4-6 hr. 5 ml of L-broth was inoculated with 100 µl of phage solution and 250 µl of host plating cells in the presence of 10 mM $MgSO_4$ and 0.1% glucose. The culture of phage and cells was incubated at 37°C overnight with constant shaking. After lysis had taken place, the cell debris was removed by centrifugation. The supernatant was transferred in a fresh tube and the phage DNA extracted as in 2.8.3.

2.8.3: Bacteriophage DNA purification

Two different methods were used to purify phage DNA. The first was used for general screening and restriction analysis of recombinant phage DNA. The second method was used when a higher grade of purity and good yield were required.

1) Bill's phage miniprep

1 ml of lysate was placed in an microfuge tube, and 2 µl of DNase I and 2 µl of RNase I added (each 5 mg ml^{-1} in 50% glycerol stored at -20°C). The mixture was incubated at 37°C for 30 min. After incubation the mixture was centrifuged for 5 min in a microfuge at maximum speed to pellet cell debris. Once the supernatant was recovered in a fresh tube, 50 µl of 0.5 M EDTA and 20 µg Proteinase K (10 mg ml^{-1} in 50% glycerol) were added, and the solution incubated for 30 min at 37°C. The phage DNA was then precipitated adding 100 µl 3 M NaOAc and extracted with 0.5 ml phenol-chloroform (1:1) for 2-3 min. After 3 min of centrifugation, 1 ml of the aqueous phase was transferred to a fresh tube and the phage DNA precipitated with 600 µl of isopropanol and pelleted by 5 min centrifugation at 13,000 rpm in a microfuge. The pellet was washed in 70% ethanol, air dried and dissolved in 30 µl of TE containing

BSA at 0.1 mg ml^{-1} to complex polysaccharides. 15 µl of this solution was used for restriction analysis.

2) Qiagen affinity column

Qiagen DNA affinity columns (Qiagen inc.) were used in the isolation of phage DNA from 10 ml liquid cultures. The phage DNA purification steps were performed according to the manufacturer's instructions.

2.8.4: Screening libraries and plaque lifts

DNA from phage plaques were transferred to Hybond-N nylon membrane filters (Amersham). For the primary screens, approximately $1x10^4$ plaques were plated on each petri dish (9 cm diameter), using the appropriate plating cell strain. After incubation at 37°C overnight, the plates were cooled for 1 h at 4°C and a single sheet of Hybond-N membrane laid on the surface for 1 min, avoiding bubbles. The sheet of membrane was marked with needle holes for subsequent orientation. The membrane was removed and placed plaque side up on blotting paper soaked in denaturation solution (0.5 M NaOH, 1.5 M NaCl) for 5-7 min. Then the membrane was neutralised by placing on blotting paper soaked in 1 M Tris-HCl pH 8.0, 1.5 M NaCl for 10 min, and finally placed on blotting paper soaked in 2X SSC for 5 min. The filter was air dried and the phage DNA fixed by incubation under vacuum in an oven at 80°C for 30 min. Hybridisation of the filters was carried out as in section 2.4.9.

2.9: In situ hybridisation

2.9.1: Preparing the digoxigenin-UTP probes

Kits for synthesis of digoxigenin labelled RNA probes and for their detection were obtained from Boehringer Mannheim. Labelled RNA was detected using anti-DIG-antibody conjugated to alkaline phosphatase. A subsequent enzyme-catalysed colour reaction with 5-bromo-4-chloro-3-indolyl phosphate (X-P) and nitroblue tetrazolium salt (NBT), produced an insoluble blue precipitate which visualised digoxigenin-labelled molecules.

Usually, 1 µg of template DNA was used. The template DNA was linearised by cutting it with an appropriate enzyme (restriction enzymes leaving 3' overhangs were not used). After phenol/chloroform extraction and ethanol precipitation, the

linearised template was transcribed according to the polymerase manufacturer's instructions. The transcription reaction was carried out in 20 µl final volume, in a sterile centrifuge tube containing the following reagents: 2 µl 10X transcription buffer, 2 µl NTP labelling mixture (10 mM ATP, 10 mM CTP, 10 mM GTP, 10 mM DIG-UTP, pH 7.5), 1 µg linearised DNA, 2 µl T7 or T3 polymerase (10U μl^{-1}), and 1 µl of RNase inhibitor (20U μl^{-1}). The tube was incubated at 37°C for 2 hr. 1 µl of the mixture was removed, added to 9 µl of water, and examined in a minigel for the synthesis of RNA. The reaction was stopped by adding 75 µl 1X MS buffer (10 mM Tris-HCl pH 7.5, 10 mM $MgCl_2$, 50 mM NaCl), 2 µl tRNA (100 mg ml^{-1}), 1 µl DNase (RNase free) and incubated for 10 min at 37°C. The absence of remaining DNA which could contribute to background was confirmed by electrophoresis. The newly synthesised RNA was then precipitated with 100 µl NH_4Ac (3.8 M) and 600 µl ethanol (ice cold), and left overnight at -20°C or for 15 min at -70°C. The sample was then spun down and the resulting pellet washed with 100-200 µl of 70% EtOH/0.15 M NaCl (ice cold). After centrifugation at 13,000 rpm for 30 min, the supernatant was poured off, the pellet left to air dry, and finally redissolved in 50 µl of RNase free water. The sample was hydrolysed using 50 µl of 1X carbonate buffer (80 mM $NaHCO_3$, 120 mM Na_2CO_3, pH 10.2), incubating it at 60°C for a period of time given from the following formula :

$$t(min) = [(kb) - 0.15] / [0.11 \times kb \times 0.15]$$

In practice, longer times were found to be better (50-60 min for 0.4-0.5 kb, 80-90 min for 0.7-1.0 kb) to avoid background.
The RNA was then precipitated with 10 µl of 10% Acetic acid (kept frozen), 12 µl 3 M NaAc, pH 4.8 and 312 µl EtOH and incubated for 15 min at -70°C or at -20°C overnight. The sample was spun down and re-suspended in 50 µl TE before storage at -20°C. 2 µl of probe were used for each slide.

2.9.2: Assaying the probe

1 µl of 1:5 dilution of labelled control DNA from the kit and 1 µl of synthesised probe were spotted on nitrocellulose filter. After UV crosslinking, the filter was wetted in DIG buffer 1 (100 mM Tris-HCl pH 7.5, 150 mM NaCl), and then left for 30 min in DIG buffer 2 (as buffer 1 with 0.5% (w/v) Boehringer blocking reagent). The filter was washed again in DIG buffer 1, and left for 30 min in 5 ml DIG buffer 1 with 1 µl anti-DIG antibody. Then the filter was washed twice for 15 min in DIG buffer 1 and briefly

washed in DIG buffer 5 (100 mM Tris-HCl, pH 9.5, 100 mM NaCl, 50 mM $MgCl_2$). Finally it was incubated for 10 min in DIG buffer 6 (7 ml NBT, 5 ml X-P in 5 ml buffer 5), and the intensity of purple precipitate produced by the probe was compared to that of the control RNA.

2.9.3: Preparation of sections for in situ hybridisation

In order to prepare tissue sections for hybridisation, they were treated to remove the wax, hydrolyse proteins and acetylate any positive charges in the tissue or in the slides which could give background. All these steps were performed in plastic containers free of RNase containing 300 ml of the appropriate solutions (except for the histoclear steps and the first 100% ethanol which were performed in glass troughs, since Histoclear is a solvent for the plastic). The steps were carried out as follows:

Histoclear	10 min
Histoclear	10 min
100% Ethanol	1 min
100% Ethanol	30 sec
95% Ethanol in 0.85% Saline Sol.	30 sec
85% Ethanol in 0.85% Saline Sol.	30 sec
50% Ethanol in 0.85% Saline. Sol.	30 sec
30% Ethanol in 0.85% Saline Sol.	30 sec
0.85% Saline Sol.	2 min
PBS_1	2 min
Pronase (0.125 mg ml^{-1}, in pronase buffer)	10 min
0.2% Glycine (in PBS)	2 min
PBS_1	2 min
4%Formaldehyde (in PBS)	10 min
PBS_1	2 min
PBS_2	2 min
Acetic anhydride	10 min
(3 ml in 600 ml 0.1M Triethanolamine pH 8.0)	
PBS_2	2 min
0.85 Saline Sol.	2 min

Then the slides were dehydrated through the ethanol series up to the first 100% ethanol, washed in fresh ethanol and stored for up to several hours at 4°C in a plastic box with a little ethanol to maintain a saturated atmosphere.

Acetic anhydride is very unstable in water, thus for the acetilation step, the triethanolamine solution was stirred over a magnetic stirrer as the acetic anhydride was added immediately before treatment of the slides. Fresh triethanolamine buffer and acetic anhydride was used for each subsequent set of slides. Formaldehyde and acetic anhydride steps were carried out in a fume hood.

The stock solutions used at this stage of in situ hybridisation are listed below:

		Dilution for pre-treatments
10X Saline Solution		
85 g NaCl in 1 l of H_2O		30 ml to 300 ml
10X PBS		
1.3 M NaCl	74 g }	
70 mM Na_2HPO4	9.94 g }	in 1 l of H_2O.
30 mM NaH_2PO4	4.14 g }	(30 ml to 300 ml)
20X Pronase buffer		
1.0 M Tris-HCl pH 7.5		16 ml to 320 ml
0.1 M EDTA		+ 1 ml Pronase

Pronase (Sigma)

Made up to 40 mg ml^{-1} in H_2O.

Pre-digested by incubating for 4 hr at 37°C.

Stored at -20°C in 1 ml aliquots.

4% Formaldehyde

As detailed in fixation section (2.2.2).

Triethanolamine 2M

149 g of triethanolamine was poured into an autoclaved bottle. The volume was brought to 500 ml with H_2O and the pH adjusted to 8.0 using HCl.

2.9.4: Hybridisation

Riboprobes are most commonly used at a concentration of 0.1-0.3 ng μl^{-1} kb^{-1} probe length. 2 µl of probe was used for each slide. 4µl de-ionised formamide and 2 µl of water was added to 2 µl of probe and heated to 80°C for 2 min. It was then chilled on ice and briefly spun, and 38 µl of hybridisation buffer was added. The hybridisation buffer was made as follows for 25 slides:

Hybridisation buffer

10X Salts	100 µl
(10X Salts: 3 M NaCl, 0.1 M Tris-HCl pH 6.8, 0.1 M $NaPO_4$ buffer, 50 mM EDTA)	
($NaPO_4$ buffer: 7.8 g NaH_2PO_4-$2H_2O$, 7.1 g Na_2HPO_4 in 1 l with H_2O)	
Formamide (de-ionised)	400 µl
50% Dextran sulphate	200 µl
100 mg ml^{-1} tRNA (Sigma)	10 µl
100X Denhardt's	10 µl
H_2O	80 µl

40 µl of riboprobe and hybridisation buffer mixture was added to each slide so that it surrounded the tissues. A coverslip was placed onto each slide to spread the mixture uniformly. Special care was taken to avoid bubbles and damage to the tissues. The hybridisation was performed overnight at 50°C in an oven, with the slides in sealed plastic boxes (RNase -free) on tissue paper soaked in 2X SSC, 50% formamide.

2.9.5: Washing the slides

Once the hybridisation was concluded, the slides were washed to remove unhybridised probe that would contribute to high background. The slides were put back into the stainless steel racks, and immersed in 300 ml of wash buffer (2X SSC, 50% Formamide) for 30 min at 50°C with gently stirring so that the coverslips fell off. Coverslips that remained attached to the slides were removed by hand. After this first wash, the slides were re-washed twice for 1 h each time in a fresh wash solution.

Then the slides were washed twice for 5 min each at 37°C in 1X NTE (10X NTE: 5 M NaCl, 100 mM Tris-HCl pH 7.5, 10 mM EDTA) to equilibrate them for the next step which consisted of RNase treatment. The slides were incubated in 1X NTE solution containing 20 μg ml^{-1} of RNase (1.2 ml of 10 mg ml^{-1} stock solution for 600 ml of 1X NTE solution) at 37°C for 30 min. To remove excess RNase, the slides were washed for 5 min at room temperature in 1X NTE followed by a wash in wash buffer at 50°C for 1 h. Finally the slides were washed for 2 min in 1X SSC at room temperature and 5 min in PBS. If the slides were not processed immediately for the colour reaction, they were stored overnight at 4°C.

2.9.6: Detecting the probe.

The solutions required to visualise the probe are listed below:

Buffer 1: 0.1M Tris-HCl, 0.15M NaCl, pH 7.5

Buffer 2: Buffer 1 containing 0.5% (w/v) blocking reagent (Boehringer) dissolved for 1 h at 60-70°C. It was prepared fresh daily.

Buffer 3: Buffer 1, with 1% (w/v) BSA (Sigma) and 0.3% (v/v) Triton-X-100.

Buffer 4: Buffer 3 containing Anti-digoxigenin-AP antibody (Boehringer Anti-digoxigenin-Fab-fragments, linked to alkaline phosphatase) at 1:300 dilution. This buffer was made shortly before use.

Buffer 5: 0.1 M Tris-HCl, 0.1 M NaCl and 0.05 M $MgCl_2$, pH 9.5.

Buffer 6: Buffer 5 with 2 μl NBT and 1.5 μl X-P per ml of buffer 5.
NBT: 75 mg ml^{-1} nitroblue tetrazolium salt in 70% (v/v) dimethylformamide
X-P: 50 mg ml^{-1} 5-bromo-4-chloro-3-indolyl phosphate in dimethylformamide

All the solutions and chemicals were stored at room temperature, except for the blocking reagent and the anti-digoxigenin-AP which were stored at 4°C, and the NBT and the X-P which were stored at -20°C.

For the detection of the riboprobe, slides were placed in square sterile petri dishes (5 slides for each dish) and incubated as follows with gentle shaking in 20 ml of each buffer:

Buffer 1	5 min
Buffer 2	1 h
Buffer 3	1 h
Buffer 4	1 h

They were then washed 4 times for 20 min each in Buffer 3, equilibrated for 5 min in Buffer 1 and 5 min in Buffer 5.

Buffer 5 was discarded and replaced with 20 ml of Buffer 6, and each dish sealed with parafilm to avoid evaporation. The slides were left to incubate in the dark at room temperature for at least 36 hr. For the first 12 hr they were gently agitated.

Once the signal had developed sufficiently, the slides were placed back in the rack, and treated in order to stop the enzymatic reaction and to wash off background. The treatment consisted of a series of washes in 300 ml of each of the following solutions:

dd H_20	5 min
70% EtOH	5 min
95% EtOH	5 min
100% EtOH	5 min
100% EtOH	5 min

At this point, the slides were immersed again in ddH_2O, stained in 0.1% Calcafluor (Sigma) for 2 min, briefly washed in ddH_2O and left to air dry. Then coverslips were mounted with Entalan (Merck), and dried overnight. The day after, the slides were ready for viewing under the microscope.

2.9.6.: Photography

Photos of in situ hybridisation were taken using Polyvar Widefield Photomicroscope (Reichert-Jung) and Kodak Ektachrome T-64 transparency film.

2.10: Solutions

Chemicals were supplied from Sigma, Fisons, BDH, Aldrich, Boehringer, Pharmacia and Anachem.

Enzymes (Restrictions Endonucleases, Exonucleases, T3 and T7 Polymerase, Klenow fragment of DNA Polymerase, DNase I, RNase A, T4 DNA Ligase, Proteinase K RNase Inhibitor) were supplied from NBL, Pharmacia, BRL and Boehringer.

Radioisotopes were provided by Amersham as were Hybond-N nylon membranes.

Standard solutions were made according to Sambrook *et al.*, (1989) using sterile distilled water, and were sterilised by autoclaving (15 psi, 30 min). Common solutions not detailed in the text are described below.

TE :	10 mM Tris-HCl pH 7.4-8.0, 1 mM EDTA pH 8.0.
0.5 M EDTA :	0.5 M Diaminoethanetetra-acetic acid disodium salt, pH 8.0.
10X TBE :	0.9 M Tris, 0.89 M Boric Acid, 25 mM EDTA.
10X DNA gel loading buffer:	Type III: bromophenol blue 0.25% (w/v), xylene cyanol FF 0.25% (w/v), glycerol 30% in water. stored at 4 °C .
10X RNA gel loading buffer	30% (w/v) Ficoll, 0.25% (w/v) Bromophenol blue.
10X MOPS gel buffer :	0.2 M Na-MOPS pH 7.0, 50 mM Na-Acetate, 10 mM EDTA.
RNA Formaldehyde : Sample Buffer	50% (v/v) formamide, 25% (v/v) formaldehyde (at 4% w/v), 25% (v/v)10X MOPS buffer.

20X SSC :	3M NaCl, 0.3M Na_3-Citrate, adjusted pH 7.2.
CTAB Solution :	2% (w/v) cetyltrimetilammonium bromide, 50 mM Tris-HCl pH 7.5, 10 mM EDTA pH 8.0.
DNA extraction buffer :	3X SSC, 0.1M EDTA, 0.1M Na-diethyldithiocarbamate and 10% SDS (w/v).
RNA extraction buffer :	50 mM Tris pH 9.0, 150 mM LiCl, 5 mM EDTA and 5% SDS (w/v).
OLB (oligo labelling buffer): 100 µl solution A 250 µl solution B and 150 µl solution C were mixed together.	Solution 0 : 0.125 M $MgCl_2$, 1.25 M Tris-HCl pH 8.0. Solution A : 0.95 ml solution 0, 18 ml 2-Mercaptoethanol, 25 ml 20 mM dATP, 25 ml 20 mM dTTP, 25 ml 20 mM dGTP. Solution B : 2 M Hepes pH 6.6. Solution C : Hexadeoxyribonucleotides (Pharmacia) suspended in TE buffer at 90 OD units ml^{-1}.
Salmon Sperm DNA :	10 mg ml^{-1} stock which was sonicated, phenol extracted and ethanol precipitated. Purchased from SIGMA.
100X Denhardt's :	2% (w/v) Ficoll 400, 2% (w/v) polyvinyl pyrrolidone, without BSA.
Acrylamide stock:	29.2% (w/v) Acrylamide, 0.8% (w/v) N-N-methylene-bisacrylamide.
Spermidine:	Spermidine-Cl 5 mM, pH 7.4.

2.11: Bacterial strains and relevant genotypes

Escherichia coli:

JM101: *supE thi* D(*lac-proAB*) *F'* [*tra*D*36 proAB*$^{+}$ *lacI*^{q} D(*lacZ)M15*] Used as a host for recombinant manipulation.

XL1-Blue: *supE44 hsdR17 recA1 endA1 gyrA46 thi relA1 lac*$^{-}$ F' [*proAB*$^{+}$ *lacI*^{q} *lacZDM15* Tn*10* (*tet*^{r}). Used to propagate pBluescript clones.

C600: F^{-} *thi-1 leub6 lacY*^{1} *tonA21 supE44*. Used for growth of λ.

C600 hflA: *SupE hsdR hflA*. Used to select recombinant λ.

2.12: Bacterial plasmid and bacteriophage

Vector:	**Source:**	**Use:**
pBluescript SK/KS	Stratagene	General subcloning; Sequencing.
pBS+	Stratagene	General subcloning.
λgt10	Murray (1982)	cDNA library vector.
λNM1149	Murray (1982)	Library vector.

2.13: Media

All the media used (listed below) were sterilised by autoclaving. Antibiotics and sugars were made up in dH_2O and filter sterilised. The only antibiotic used was Ampicillin (stock solution, 150 mg ml^{-1} in water to a final concentration of 150 $\mu g\ ml^{-1}$).

L-broth	10 g Difco Bacto-Tryptone, 5 g Difco Bacto-Yeast Extract, 10 g NaCl per litre, pH 7.2.
L-agar	15 g Bacto-Agar added to 1 litre of L-broth.
BBL agar	10 g Baltimore Biological Laboratory trypticase, 5 g NaCl, 10 g Difco agar per litre.
BBL top agar	As BBL agar except only 6.5 g Difco agar per litre.
SOC	2% Bacto tryptone, 0.5% Bacto yeast extract, 10 mM NaCl, 250 mM KCl, 10 mM $MgCl_2$, 10mM $MgSO_4$, and 20 mM glucose
Phage buffer	3 g KH_2PO_4, 7 g Na_2HPO_4, 5 g NaCl, 10 ml 0.1M $MgSO_4$, 10 ml 0.1M $CaCl_2$, 1 ml 1% (w/v) gelatine per litre.

CHAPTER 3

Results

3.1: Screening for leaf-shape mutants

The purpose of this research was to identify genes involved in specifying leaf shape. In order to achieve this aim, a collection was made of *Antirrhinum* leaf shape mutants.

Nine leaf shape mutants were recovered from a screening of over 60,000 plants in a transposon mutagenesis programme at the John Innes Institute in Norwich. Lines of *Antirrhinum* plants carrying active transposons (M0) were first grown at 15°C to increase the frequency of transposition, and then self pollinated. The M1 generation was grown and self pollinated to allow the segregation of mutated alleles which were heterozygous in this generation. The seeds from the M1 were then bulked (usually 18 capsules from 18 different M1 plants) forming subpopulations of the M2 generation. Bulk seeds were then sown and screened for homozygous mutant plants showing altered leaf development.

A further five mutants (*Graminifolia*^{constants}, *Graminifolia*^{mutabilis}, *hirzina, latifolia* and *phantastica*) came from the collection of *Antirrhinum* mutants maintained in Gatersleben, Germany. A new allele of *Graminifolia* was recovered later from another mutagenesis programme conducted at the John Innes Institute.
All these leaf-shape mutants can be divided into three general classes (Fig. 11):

1- Broader than WT

2- Narrower than WT

3- Mutants with distorted leaves.

This classification is arbitrary, and the 14 mutants could be grouped differently. For instance, only a few of these mutants could be considered true leaf-shape mutants. Others showed pleiotropic effects in other parts of the plant. Moreover, some other mutants could be listed in different classes, for instance *Spissifolia, asperfolia* and *wavy* which have thicker leaves than WT.

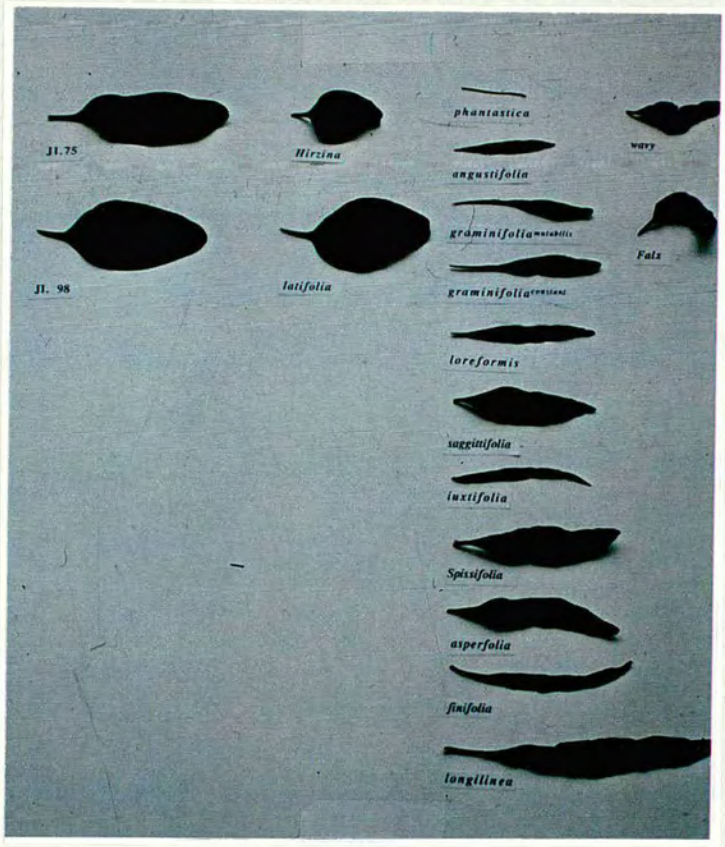

Figure 11: Leaf-shape mutants of *A. majus*. They are grouped in three classes: broader, narrower and more distorted than WT. The two WT line (JI 75 and JI 98) are to the left.

3.2: Phenotypic description and morphogenetic characterisation of *Antirrhinum* leaf-shape mutants.

In order to know how the mutations affected the shape of the lamina, nine of the 14 leaf mutants were characterised morphologically. Wax-embedded material was used for histological analysis and freeze-fracture or resin replicas for SEM analysis. This allowed the internal and external structure of the different mutant leaves to be compared to that of WT. For six of the leaf mutants genetical analysis was carried out, by crossing each mutant with WT plants and with other leaf-shape mutants. The phenotypic and morphological descriptions of the nine mutants and WT leaves are reported below. Where possible, the results of genetical characterisation and statistical analysis of morphological characteristics have also been included.

3.2.1: The wild-type leaf

The leaves of wild-type (WT) *Antirrhinum* plant are simple in outline and they have entire margins (Fig. 1). The leaf is wider than it is thick reflecting its function of trapping sunlight. Early in vegetative development pairs of opposite leaves are produced at each node of the stem in decussate phyllotaxis. The first indication of leaf initiation is a protrusion from the flanks of the apical meristem. In *A. majus*, like in other monocot and dicot plants (Stevees and Sussex, 1989), the initiation of a leaf primordium is accompanied by both periclinal and anticlinal cell divisions in the L2 and L3 layers of the corpus, and only anticlinal division in the L1 tunica layer (Fig. 2). In monocot plants the youngest leaf primordium (P1) is present as a ring that encircles the meristem (Poethig and Szymkowick, 1995), whereas in *Antirrhinum* the opposite primordia are separated by 4-5 files of cells, 30-32 μm measured from the nearest points at both sides of the shoot apical meristem (Fig. 12). These are the sites where the next two leaf primordia (P0) will arise.

When the shoot apical meristem (SAM) of *A. majus* was analysed in histological sections, a distinctive feature of differentiation in the stem immediately below the SAM became evident. Cells of the pith begin vacuolation very close to the summit of the apex and enlarge faster than those that surround them peripherally. Moreover, on the surface of the apical flanks, the protoderm forms a distinctive superficial layer. Between the pith and the protoderm regions, there are unvacuolated cells that will give rise to the cortex and the vascular tissue. It is from the peripheral zone of the SAM that leaf primordia arise.

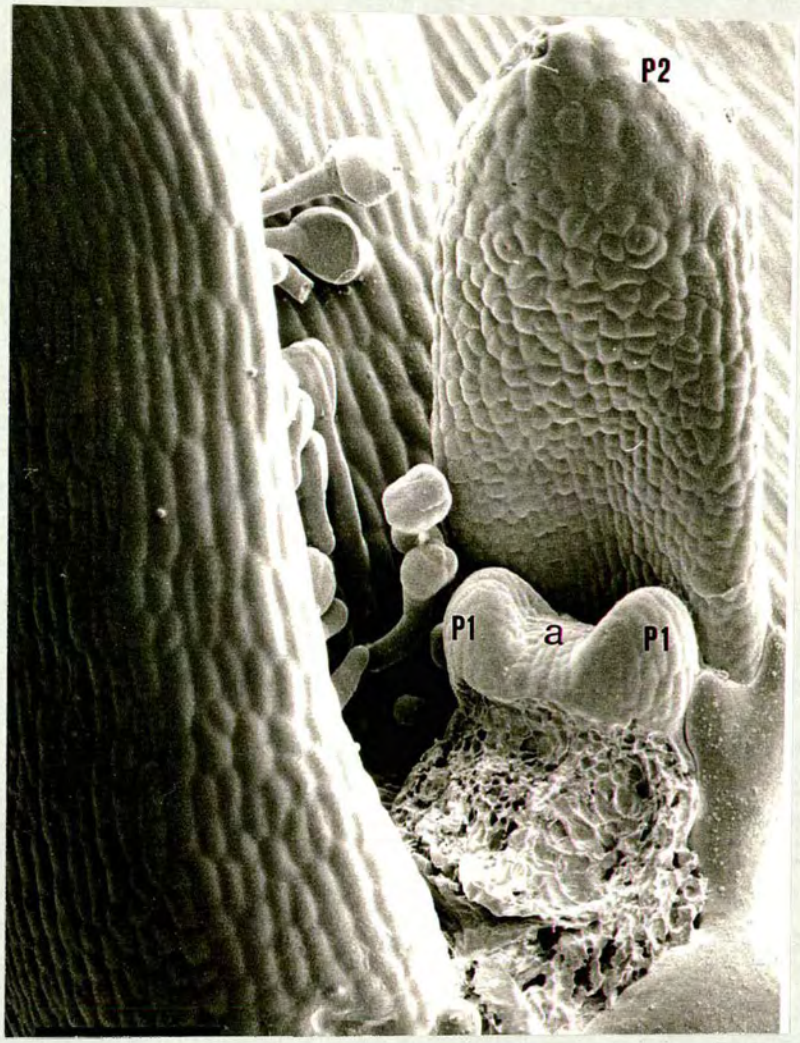

Figure 12: SEM photograph of a WT *A. majus* apex (a) during the vegetative phase. Two emerging leaf primordia (P1) flank the SAM. The older P2 leaf shows the characteristic flattened shape; anticlinal divisions contributing to increase in both lenght and width of the leaf, are seen in the dorsal epidermal cells of P2. (Scale bar 100 μm)

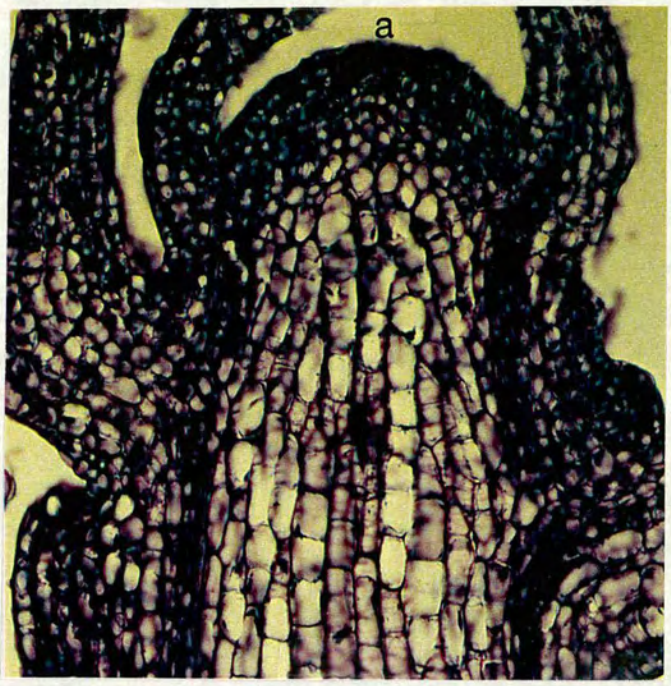

Figure 13: Longitudinal section of a WT *A. majus* apex (a) during the vegetative phase (X23). (See text for explanation)

The close relationship between the leaf primordia and the vascular tissue of the stem can be seen to have its origin at this level. Each pair of opposite *Antirrhinum* leaf primordia have associated with them and extending into them a recognisable strand of procambium (Fig. 13).

An important characteristic that differentiates a developing leaf from a shoot is its dorsoventrality, which is reflected both in its external morphology and in its anatomy. Soon after initiation, the leaf primordium shows the characteristic flattened shape. Cells in a young leaf divide in an anticlinal fashion with respect to the plane of the lamina (Fig. 12). The epidermal cells do not yet show the characteristic irregular shape of a mature lamina. When the leaf is about 900 µm in length, the epidermal cells at the tip of the lamina show the features of mature epidermal cells (Fig. 14). This could mean that cells at the apex of the leaf stop dividing and start to enlarge and differentiate much earlier than those in the central-basal part of the leaf lamina. A basipetal gradient of leaf expansion was seen in experiments where a leaf of 10 mm length was marked with small spots of ink. As the leaf grew, points became more widely spaced in the central-basal part of the lamina than those at the tip (data not shown). This is in agreement with what has been observed in tobacco and maize leaf, where a basipetal gradient of lamina maturation was described (Poethig and Sussex, 1985b; Freeling, 1992).

Analysis of histological and freeze fractured transverse sections of mature leaves as well as SEM of leaf surface, revealed differences in cell types and in the internal leaf structure.

The midrib is an obvious protrusion from the ventral (abaxial) surface. It consists of vascular tissue surrounded by parenchymal cells, forming the bundle sheath (Fig. 15 and 16). The vascular tissue in the midrib is compact with a clear region of xylem and phloem situated near the dorsal (adaxial) side. The ventral epidermal cells in the midrib are rounded and elongated in direction of the proximal-distal axis (Fig. 17). They are distinguished from the cells at the dorsal side of the midrib which are less elongated and include hair cells.

In the lamina, four distinct cell types are recognisable along the dorso/ventral (d/v) axis: dorsal epidermis, palisade mesophyll, spongy mesophyll and ventral epidermis (Fig. 18). The dorsal epidermal cells are bigger and more swollen than the ventral ones, which instead are more interlocked and appear more dendritic (Fig. 20 and 21). Moreover, the ventral epidermis is characterised by the presence of stomata which

are absent or very rare in the dorsal epidermis. The palisade mesophyll is made up of two or three files of cells elongated perpendicularly to the dorso/ventral axis.

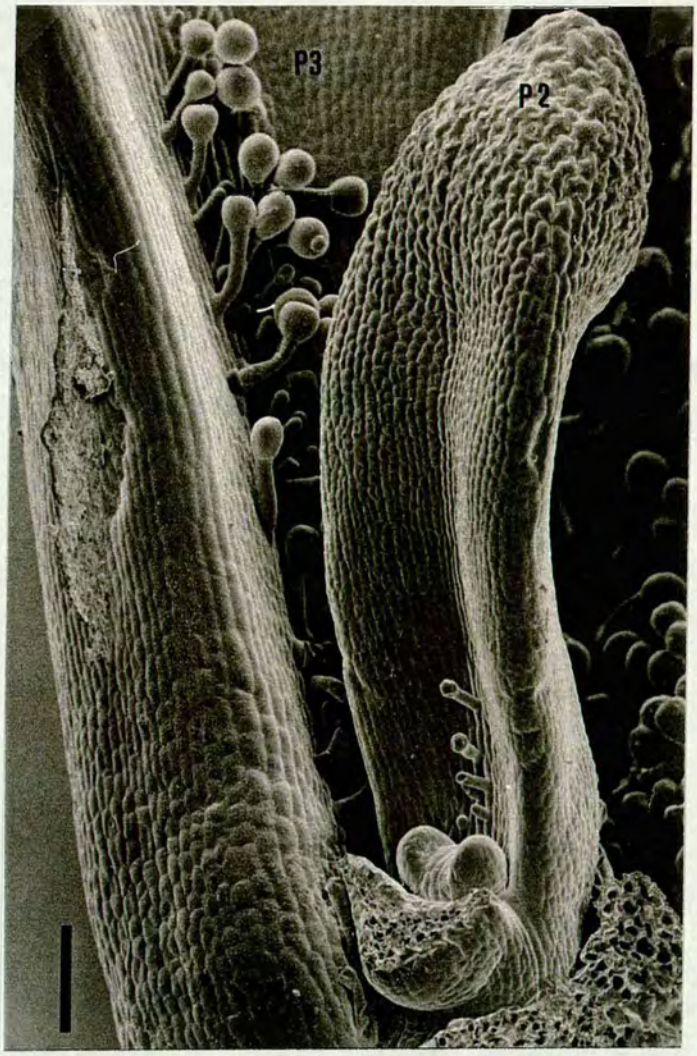

Fig 14: Later stage of a P2 leaf with the tip epidermal cells begin to differentiate in more mature irregular shaped cells. The epidermal cells of more basal region of the leaf, either in P2 or P3 leaves, are still dividing. The dorsal side of the midrib show hair cells for both P3 and P2 leaves. (Scale bar 100 μm)

Fig 17: SEM of the ventral surface of a WT *A. majus* leaf showing the midrib (m) and part of the ventral lamina. The ventral epidermal cells in the midrib are elongated in direction of the proximal-distal axis. (Scale bar 100 μm)

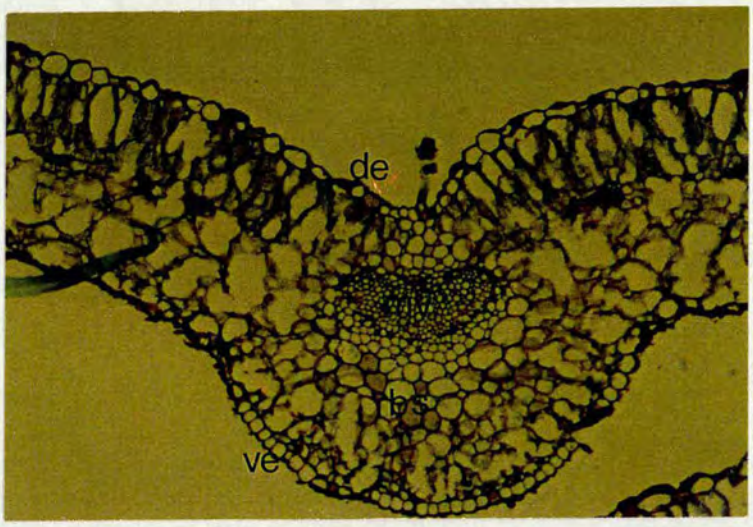

Figure 15: Transverse section of a WT *A. majus* leaf midrib (X23) (toluidine blue stain). mv= midvein, bs= bundle sheath, de= dorsal epidermis and ve= ventral epidermis.

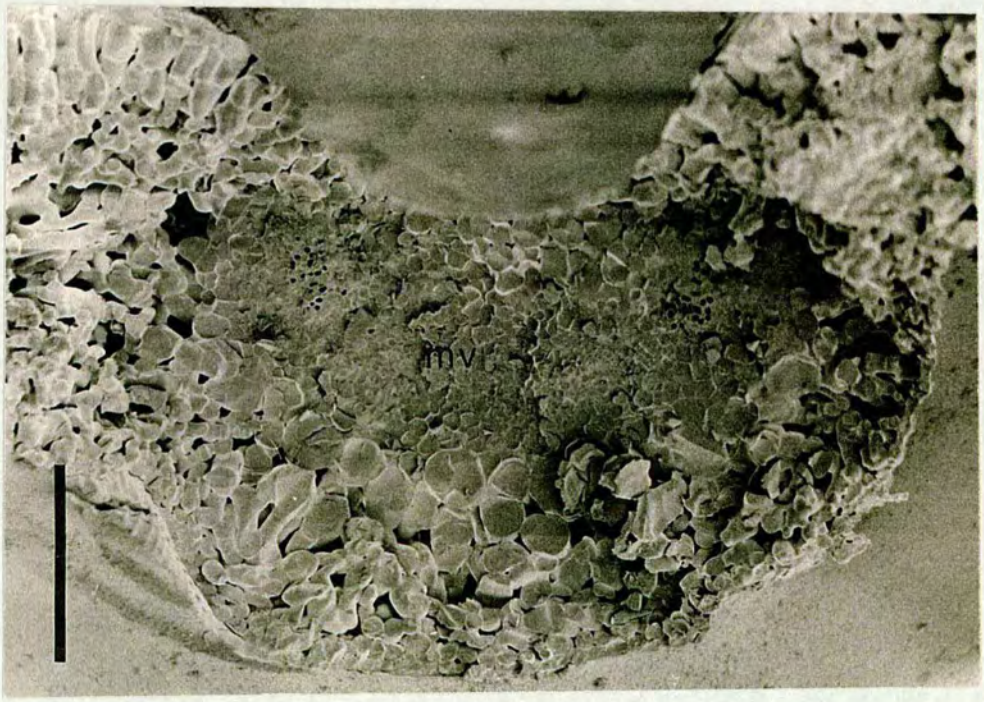

Figure 16: Cryo-SEM transverse section of a WT *A. majus* leaf midrib. (Scale bar 400 μm). mv= midvein.

The spongy mesophyll cells have their own irregular shape with large air-spaces between them. Minor veins are scattered along the lateral axis surrounded by parenchymal cells (Fig. 18 and 19).

At the edge of a mature leaf, the epidermal cells have a more rounded and regular shape and they tend to bulge more from the surface than the dorsal ones (Fig. 20). In a very young leaf, the margin does not show this epidermal cell type and the cells at the margin are elongated towards the proximal-distal axis (Fig. 14).

Dorso ventral epidermal cell type is also seen in other features like the colour of the two surfaces (the dorsal side appears greener than ventral side), or the foliar texture (the dorsal side appears smoother).

On the basis of these and other observations, (Waites and Hudson, 1995) the WT *Antirrhinum* leaf shows dorso-ventral asymmetry in several respects. Both lamina and midrib show a different array of tissue layers along the dorso/ventral axis. Therefore dorsal and ventral parts of the leaf are not mirror images of each other and the leaf presents only one plane of symmetry perpendicular through the mid vein, which divides the leaf in two equal parts.

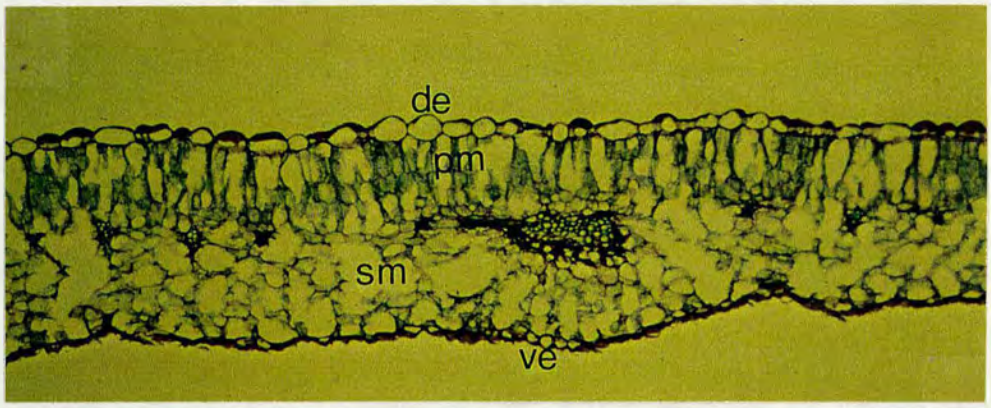

Figure 18: Transverse section of a WT *A. majus* leaf lamina (X23) (toluidine blue stain). The four characteristic layers that confer dorso-ventral asymmetry to the lamina are easily recognisable. de= dorsal epidermis, pm= palisade mesophyll sm= spongy mesophyll, ve= ventral epidermis.

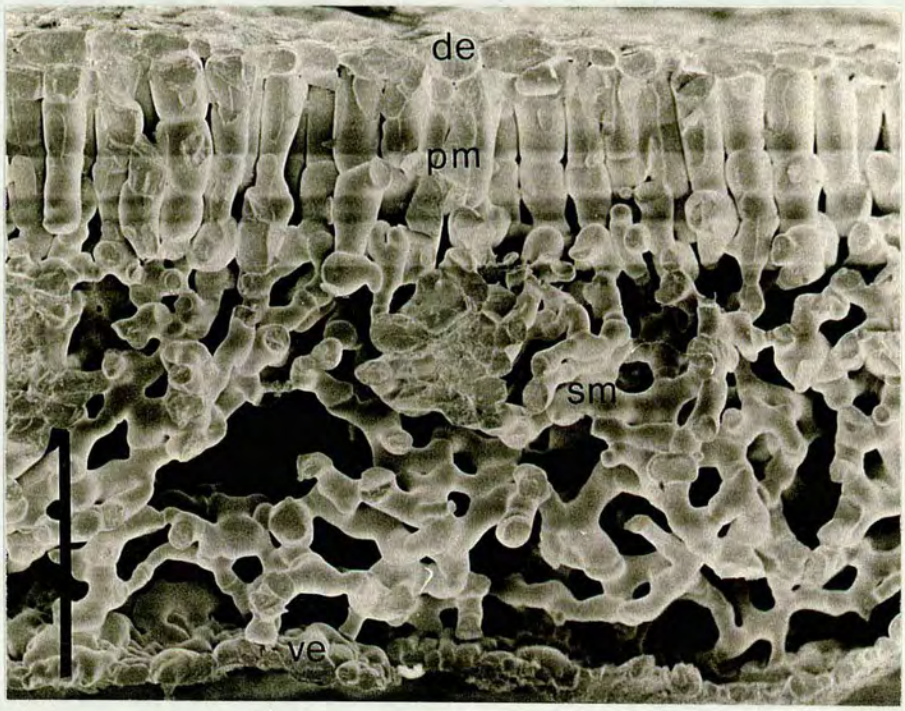

Figure 19: Cryo-SEM transverse section of a WT A. *majus* leaf lamina. (See text for explanation). (Scale bar 200 μm). Symbol as figure 18.

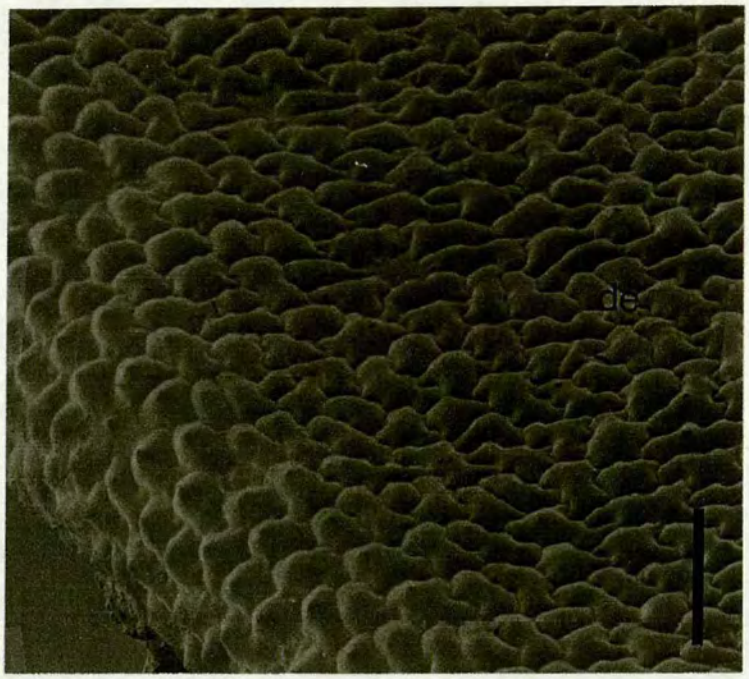

Figure 20: SEM of the dorsal epidermal surface of a WT *A. majus* leaf. Compare the shape of the dorsal epidermal (de) cells with those of the ventral epidermis in Fig. 21 that are flatter and more interlocked. (Scale bar 100 μm)

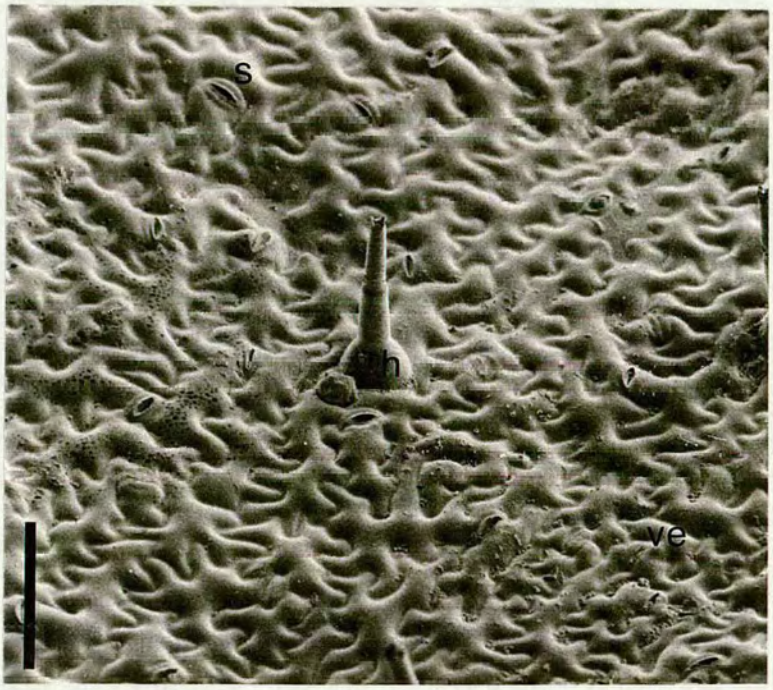

Figure 21: SEM of the ventral epidermal (ve) surface of a WT *A. majus* leaf. Stomata (s) and hair cells (h) are visible. (Scale bar 100 μm)

3.2.2: The *Graminifolia (Gram)* mutant

The *Graminifolia* (*Gram*) mutant was obtained from Zentralinstitut fur Genetik und Kulturflanzenforschung, Gatersleben Germany. E. Baur first described the *Gram* mutant phenotype in 1918. Later, H. Stubbe (1966) reported three different alleles of *Graminifolia*: *Gram*^{constants} (*Gram*^{const}), *Gram*$^{mutabilis-a}$ (*Gram*$^{mut-a}$) and *Gram*$^{mutabilis-b}$ (*Gram*$^{mut-b}$). He noted that one of the differences between *Gram*^{const} and the other two alleles was in the capacity of the others to give rise to reversion events germinally (with *Gram*$^{mut-b}$ having higher frequency of reversion than *Gram*$^{mut-a}$) (Stubbe, 1966). *Gram*^{const} is a stable mutation, and during the period required for this project, no revertant plants were recovered from *Gram*^{const}. Bags containing *Gram* seeds received from Gatersleben were marked as *Gram*^{mut} without indication if they were line-a or line-b, so it was decided to name these mutants *Gram*$^{-202}$. They were maintained by inbreeding as line E202, whereas *Gram*^{const} was named *Gram*$^{-203}$ and maintained by inbreeding line as E203.

A new allele of *Gram* was obtained from a transposon mutagenesis programme carried out at the John Innes Institute, in Norwich. Crossing it to Gatersleben E202 line gave only *Gram* mutant progeny. One explanation was that the new mutant was affected at the *Gram* locus. Alternatively, the new mutant may have carried a dominant mutant allele of another locus. To distinguish between these possibilities, the F1 progeny plants were self pollinated. All progeny showed a *Gram* mutant phenotype. This suggested that the Norwich allele did not carry a dominant mutation at another locus (in this case 3/16 of the progeny would have had at least one WT *GRAM* allele and no mutant allele of the second locus, and would therefore have been WT). Similarly back-crossing the F1 plants to WT plants produced only WT progeny (all assumed to be *GRAM/Gram* heterozygotes), a result incompatible with the involvement of a dominant mutation. This suggested that the *Gram*$^{-Norwich}$ allele was not a dominant mutation of another locus. Therefore it was concluded that the *Gram*$^{-Norwich}$ allele was indeed a new *Gram* mutant allele.

Reciprocal crosses made between WT lines and *Gram* mutant alleles suggested that the *Gram* mutation was semidominant. In the F1, plant heterozygous for *Gram* showed a phenotype intermediate between WT and *Gram* mutant homozygotes.

3.2.2: The *Graminifolia (Gram)* mutant

The *Graminifolia* (*Gram*) mutant was obtained from Zentralinstitut fur Genetik und Kulturflanzenforschung, Gatersleben Germany. E. Baur first described the *Gram* mutant phenotype in 1918. Later, H. Stubbe (1966) reported three different alleles of *Graminifolia*: *Gram*^{constants} (*Gram*^{const}), *Gram*$^{mutabilis-a}$ (*Gram*$^{mut-a}$) and *Gram*$^{mutabilis-b}$ (*Gram*$^{mut-b}$). He noted that one of the differences between *Gram*^{const} and the other two alleles was in the capacity of the others to give rise to reversion events germinally (with *Gram*$^{mut-b}$ having higher frequency of reversion than *Gram*$^{mut-a}$) (Stubbe, 1966). *Gram*^{const} is a stable mutation, and during the period required for this project, no revertant plants were recovered from *Gram*^{const}. Bags containing *Gram* seeds received from Gatersleben were marked as *Gram*^{mut} without indication if they were line-a or line-b, so it was decided to name these mutants *Gram*$^{-202}$. They were maintained by inbreeding as line E202, whereas *Gram*^{const} was named *Gram*$^{-203}$ and maintained by inbreeding line as E203.

A new allele of *Gram* was obtained from a transposon mutagenesis programme carried out at the John Innes Institute, in Norwich. Crossing it to Gatersleben E202 line gave only *Gram* mutant progeny. One explanation was that the new mutant was affected at the *Gram* locus. Alternatively, the new mutant may have carried a dominant mutant allele of another locus. To distinguish between these possibilities, the F1 progeny plants were self pollinated. All progeny showed a *Gram* mutant phenotype. This suggested that the Norwich allele did not carry a dominant mutation at another locus (in this case 3/16 of the progeny would have had at least one WT *GRAM* allele and no mutant allele of the second locus, and would therefore have been WT). Similarly back-crossing the F1 plants to WT plants produced only WT progeny (all assumed to be *GRAM/Gram* heterozygotes), a result incompatible with the involvement of a dominant mutation. This suggested that the *Gram*$^{-Norwich}$ allele was not a dominant mutation of another locus. Therefore it was concluded that the *Gram*$^{-Norwich}$ allele was indeed a new *Gram* mutant allele.

Reciprocal crosses made between WT lines and *Gram* mutant alleles suggested that the *Gram* mutation was semidominant. In the F1, plant heterozygous for *Gram* showed a phenotype intermediate between WT and *Gram* mutant homozygotes.

3.2.2.1: The phenotype of *Gram* mutants

The phenotype of *Gram* mutants showed several changes in the morphology, shape and phyllotaxis of leaves, and pleiotropic effects were also seen in the stem between internodes.

Gram leaves were narrower and slightly shorter than WT leaves (Fig. 22), with the dorsal surface texture similar to that of WT. The margins of *Gram* leaves, at least for all those above the second node, were not entire but slightly serrated, and hairs were present along them (Fig. 29). Hairs are not normally present on the margin of the WT leaf, but are found abundantly throughout both sides of the first pair of WT leaves, or along the dorsal midvein and ventral surfaces of subsequent leaves (P. Huijser, pers. comm.). In WT plants, hairs are also present at the base of the stem, and they become rare along the stem axis of the plant, to reappear again when the transition to inflorescence occurs. In *Gram* mutants hairs are present on the stem axis also above node three (data not shown).

The first pair of true leaves of *Gram* mutants was found to be a good indicator of phenotype (leaves are narrower than those of WT). This allowed screening for germinal revertants to take place at the seedling stage approximately 8-10 weeks after sowing, greatly reducing the space and time required.

The flowers of *Gram* mutants showed a slight reduction in the dimensions of sepals and petals. The reduction in the size of the petals was often accompanied by a split between the two dorsal (upper) petals (data not shown). The *Gram* mutant plants showed more branching than WT and as a result were smaller with a more bushy habit . Frequently, more than three leaves were formed at each node (data not shown).

Remarkably, a stripe of more green tissue, similar to dorsal epidermal tissue, was found along the ventral margin of mutant leaves (Fig. 23). Microscopical analysis of embedded tissues, freeze fractured transverse sections of the lamina and SEM on the surface of *Gram* mutant leaves, revealed differences in morphology. The midrib was much smaller and flatter than in WT (Fig. 24). There were more parenchymal cells above the midvein compared with WT, therefore the mid vein was in a more central position in the midrib. The palisade cells occupied a smaller part of the lamina depth and they appeared less elongated in the dorsoventral direction. The spongy mesophyll cells were small but nevertheless had air-spaces (Fig. 25).

The histological and SEM analysis revealed the cell type of the greener cells located at the margin of the leaf lamina. The cells were found to have the features typical

of dorsal epidermal cells (see WT for description) (Fig. 26 and 27). Moving towards the midrib the more characteristic ventral epidermal cell type was observed.

Figure 22: Phenotype of *Gram*$^{-202}$ mutant plant. The figure shows the vegetative and inflorescence apices.

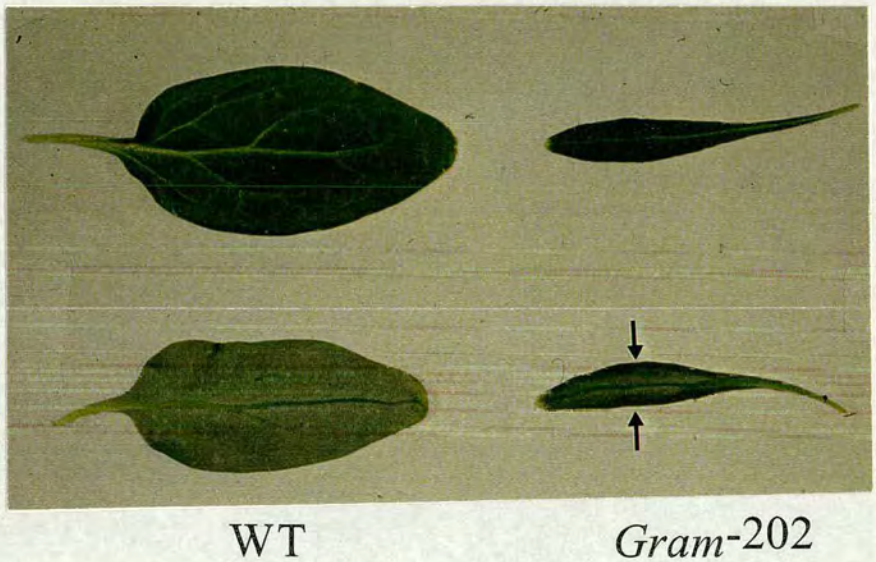

Figure 23: Dorsal and ventral surfaces of WT JI 75 line and *Gram*$^{-202}$ leaves. A greener stripe of tissue (marked with arrows) is visible in the ventral side of *Gram*$^{-202}$.

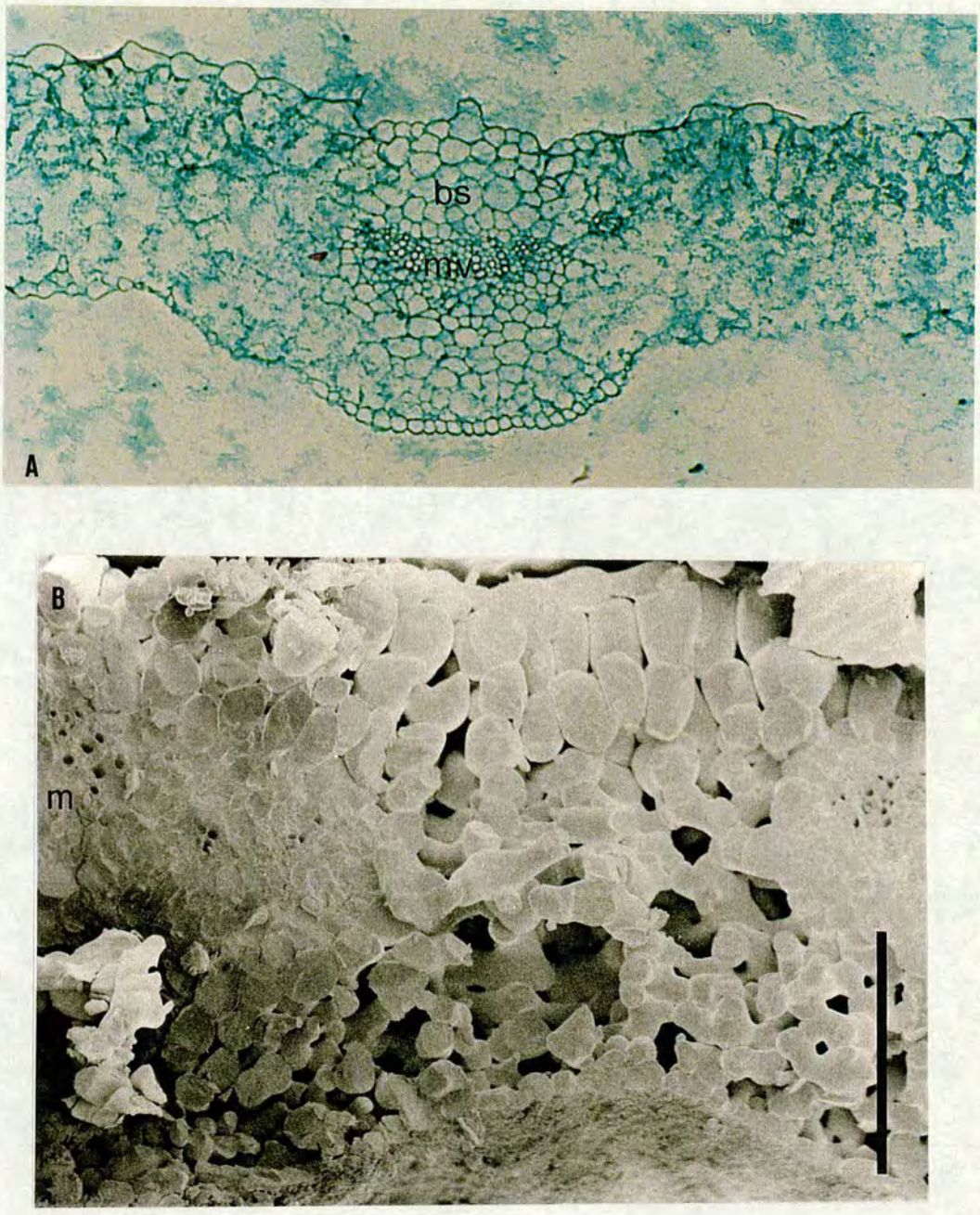

Figure 24: (A) Transverse section of a *Gram*$^{-202}$ midrib (X23) (Fast Green stain). (B) Cryo-SEM transverse section of a *Gram*$^{-202}$ midrib. (Scale bar 200 μm) (see text for explanation). m= midrib, mv= mein vein, bs= boundle sheath.

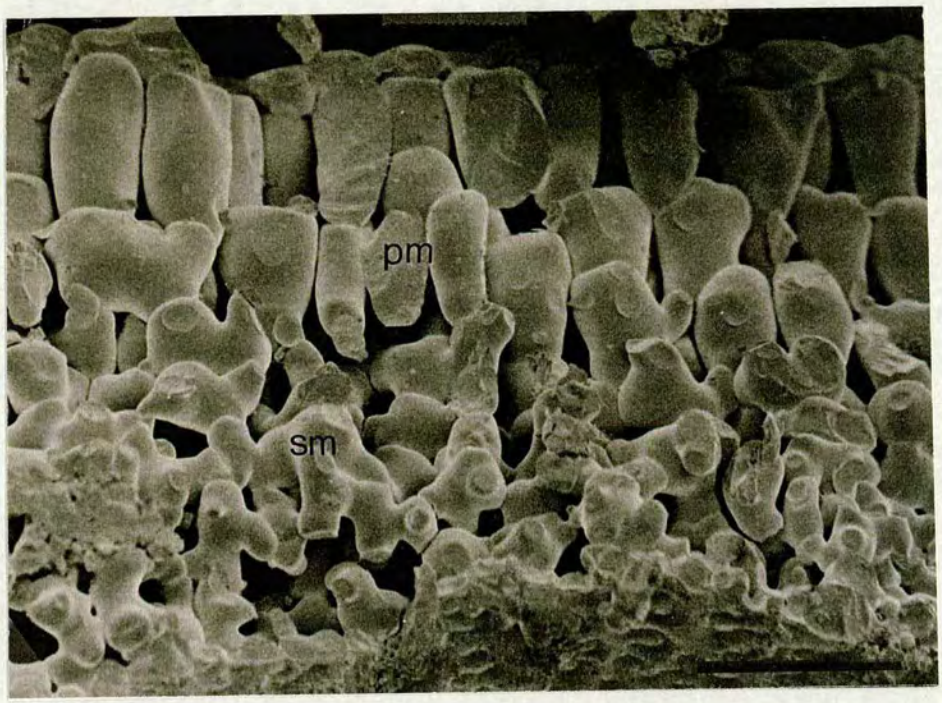

Figure 25: Cryo-SEM transverse section of a *Gram*$^{-202}$ leaf lamina. (Scale bar 100 μm) (see text for explanation). pm= palisade mesophyll sm= spongy mesophyll.

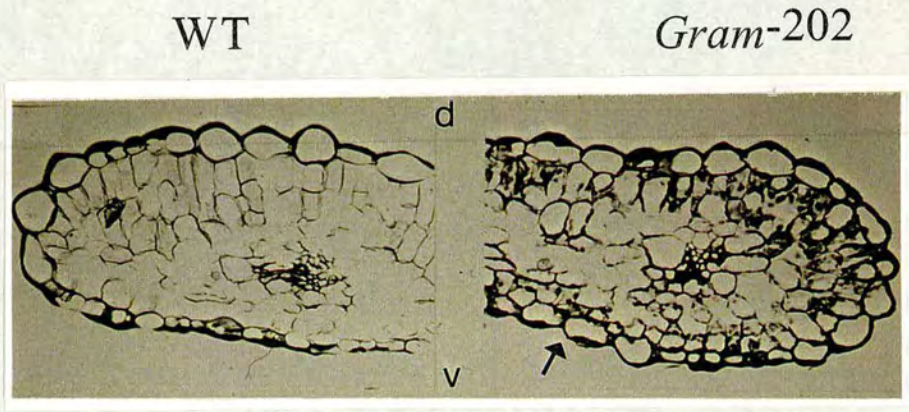

Figure 26: WT JI 75 and *Gram*$^{-202}$ leaf margins (X23). The *Gram*$^{-202}$ leaf margin shows dorsal epidermal cells in ventral position (arrow).

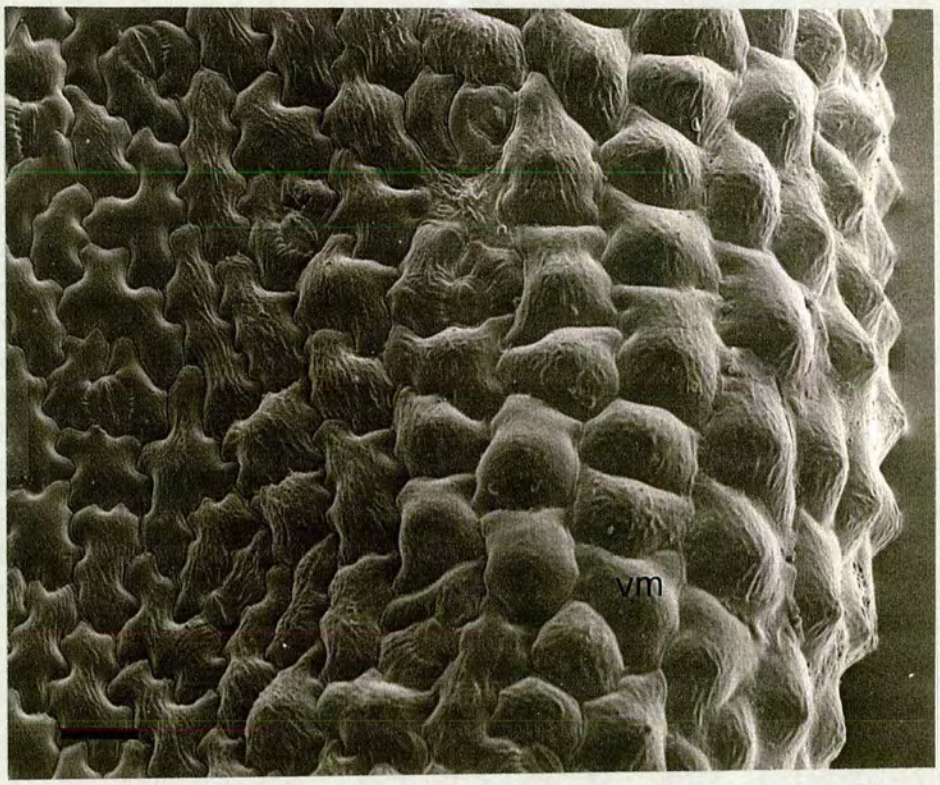

Figure 27: SEM of *Gram*-202 ventral leaf margins. In *Gram*-202, epidermal cells near the ventral margin (vm) have the shape characteristic of dorsal epidermal cells (see Figure 20 and 21). (Scale bar 40 μm)

In contrast to the WT leaf, in which palisade cells are confined to the dorsal region, palisade cells were found to extend ventrally around the margin of the *Gram* mutant leaf, in the region in which ectopic dorsal epidermis cell were observed. The lateral veins were surrounded by cells which looked more like palisade cell type than bundle sheath type. No spongy mesophyll was present in this lateral part of the lamina (Fig. 26).

A further feature in the ventral side of the leaf lamina was seen in *Gram* mutant plants heterozygous for *Eluta* (*El*). *Eluta/Eluta* genotype confers a pale pigmentation to the flowers, and a pale green colour to the ventral side of the leaf. Plants with *ELUTA/ELUTA* (*EL/EL*) genotype have flowers with a vivid red colour in the flower and a rusty red colour in the ventral side of the leaf, but the dorsal side has the typical green colour. Plant with *EL/El* genotype showed an intermediate phenotype, with the ventral side of the leaves showing the rusty colour, only paler than that in *EL/EL* leaves. Thus *ELUTA* acts as a marker for dorsal leaf epidermal cell type. The *Gram* mutants coming from the German collection are derived from *Sippe50* which has *El/El* genotype. The WT JI 75 is *EL/EL*. In F2 populations from crosses between *Gram* mutants in a *Sippe50* background and WT plants of line JI75, *Gram* mutants heterozygous for *EL/El* were identified and compared with WT *GRAM* siblings with the same *ELUTA* genotype. *Gram* mutants showed the red pigmentation characteristic of ventral epidermal cells near the ventral midrib, but epidermal cells along the ventral margins were green, suggesting dorsal cell type (Fig. 28). This finding, together with the microscopical analysis, strongly suggested that the cells at the ventral margins of *Gram* mutant leaves were dorsal cell types.

Other important phenotypic effects of *Gram* mutation were seen in the *Gram*$^{-}$ Norwich allele and rarely in *Gram*$^{-202}$ from the German collection. They included the alteration of the node/internode structure, the length of the petiole, the sporadic presence of a shoot growing at the margin of the leaf and alteration of the phyllotaxis (Fig. 29 and 32).

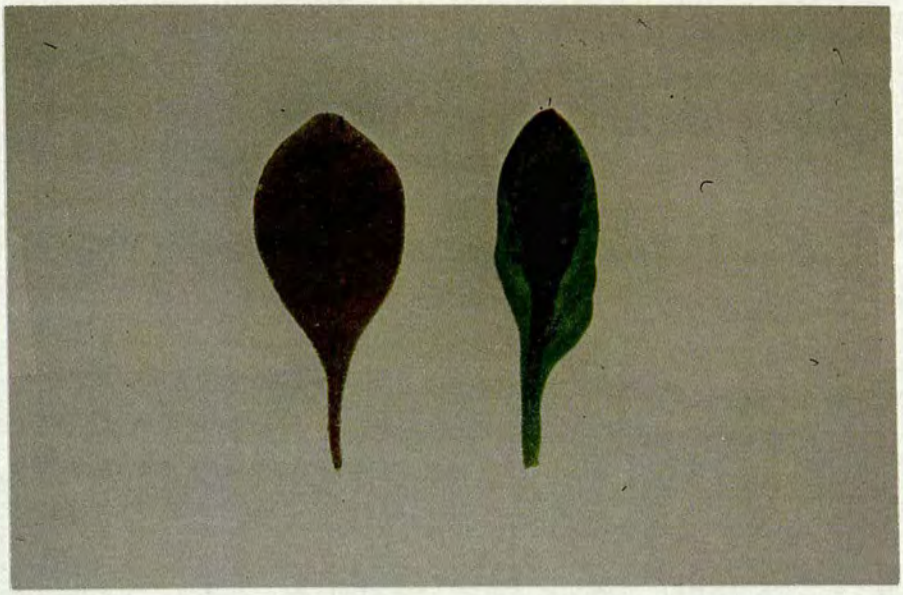

Figure 28: Ventral surfaces of a WT JI 75 (left) and a *Gram*$^{-202}$ (right) leaf mutant. Both leaves are heterozygous at the *ELUTA* locus (*EL/El*) and show the characteristic rusty colour in the ventral epidermis, but only near the midrib, whereas the margin still retains the stripe of green tissue.

Figure 29: A *Gram*$^{-202}$ mutant plant showing alteration of the node/internode (see text for explanation).

The internode of *Gram* mutants showed characteristics reminiscent of the sheath of monocot plants. This sheath-like structure encircled the stem and had hairs on the two sides where it diverged. Figure 29 shows a bizarre leaf to the right of the stem. This leaf might be the result of a fusion of two leaf primordia, or the split of one due to a displacement of part of the same primordium to a more apical region. At the corners of the triangle formed by the two fused leaves, a flag of epidermal tissue was present. Where the upper petiole of these fused leaves was attached to the stem, a file of hairs encircled the petiole. An axilary shoot had been produced below the lower petiole of the fused leaves, and had grown to give a long stem, whereas no axilary shoot was formed in the axil of the upper petiole. On the left side of the stem, a leaf had grown at a different node, located opposite but between the two petioles of the fused leaves. A leaf had been produced in its axil, rather than an axilary shoot.

Leaves with very long petioles were seen in all *Gram* mutants. Frequently, a shoot meristem developed at various positions along the margin of the leaves. Some shoots were located near the base of the lamina, whereas others were formed at more distal positions (Fig. 30 and 31). Ectopic shoots that formed at more distal positions appeared to have a phyllotaxy consistent with the position of the leaf from which they were formed. In Fig. 30 a leaf like-structure was initiated to the right of the ectopic shoot with hairs along the margin. The presence of ectopic shoot in the leaf lamina, clearly recalls the phenotype of tobacco plants overexpressing *KNOTTED1* (Sihna and Hake, 1992).

The number of cells in the ventral epidermis of the lamina and midrib was significantly lower than in WT (Table 3), with *Gram* mutants containing approximately 1/3rd of the cells present in a transverse-section of a wild-type leaf. It is not known if the reduction of cell number is due to a decrease in number of cell divisions or an alteration of earlier events in the formation of the leaf.

An interesting phenotype was seen as a results of the cross between *Gram* and *phantastica* mutants. Leaves of the *phantastica* mutant are typically needle-like and they lack the characteristic dorsoventrality of the WT leaf (Waites and Hudson, 1995). In the double mutant *Gram*$^{-202}$*/phan*, the primary shoot failed to develop, and a secondary shoot then developed from the hypocotyl (Fig. 33). Leaves with a typical *phantastica* phenotype were seen but with an additional feature. Some of the typical needle-like leaves ran parallel to the internode and were attached to it for about 2/3rd of their length. It was only the tip of these leaves which diverged from the internode (Fig. 34). The same happened for those leaves which were able to produce a lamina, but in this case it was only the petiole which remained attached to the internode for about half

of its length. Moreover the phyllotaxis was altered and needle-like leaves could be formed along the same axis (Fig. 34).

Complementation analysis suggested that the *Gram* locus was not represented by any of the other leaf mutants.

Figure 32: *Gram*-Norwich mutant plant showing alteration of phyllotaxis. The two nodes visible in the figure have at least 4 leaves in a spiral phyllotaxis which is different from the one present in the inflorescence of a WT plant.

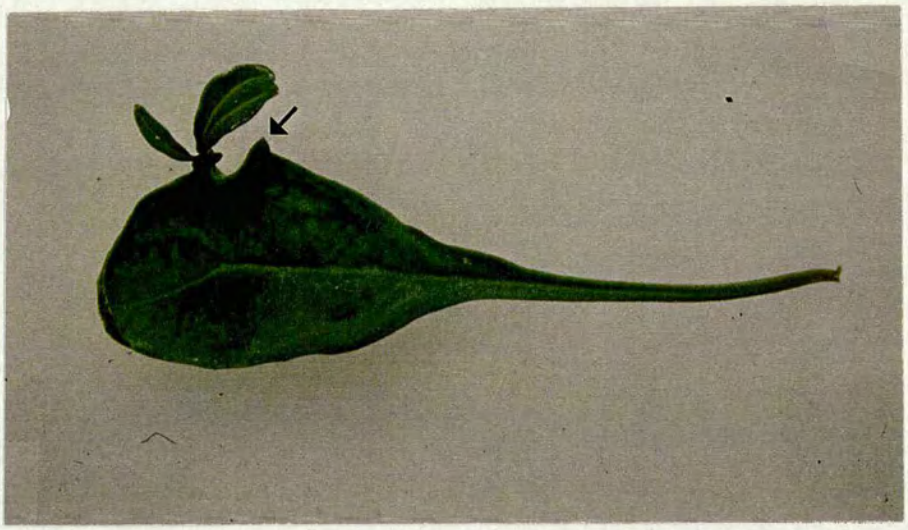

Figure 30: A *Gram*-Norwich mutant leaf bearing an ectopic shoot in the margin. A leaf like structure is visible (arrow) with hairs along its margin. The phyllotaxis of the newly formed shoot appears to be consistent with the position of the leaf from which it derived.

Figure 31: A *Gram*-202 mutant plant with very long petiole bearing an ectopic shoot.

Figure 33: A *Gram-202/phan* double mutant plant. The primary shoot fails to develop. A secondary shoot then develops from the hypocotyl.

Figure 34: Leaves of a *Gram-202/phan* double mutant plant run parallel to the internode and are attached to it for part of their length. Some needle-like leaves characteristic of the *phan* mutant phenotype are formed along the same axis showing alteration in the phyllotaxis.

3.2.3: The *longilinea* (ED 701) mutant

Apart from the shape of the leaves, the *longilinea* mutant resembled WT. The phyllotaxis was normal decussate. After the ninth or tenth node the vegetative meristem underwent the transition to inflorescence meristem. The flowers were normal in shape and structure. Thus the mutation appeared to affect only the shape of the leaves.

longilinea had narrow leaves, but unlike the other narrow leaf mutations, it showed a very long proximal/distal leaf axis. It had a similar venation pattern of the WT. The leaf lamina was not perfectly symmetrical along the midrib but showed an undulating margin (Fig. 35). The ventral surface was very similar to the WT JI 75 whereas the dorsal surface had an irregular texture and was slightly more lumpy than WT.

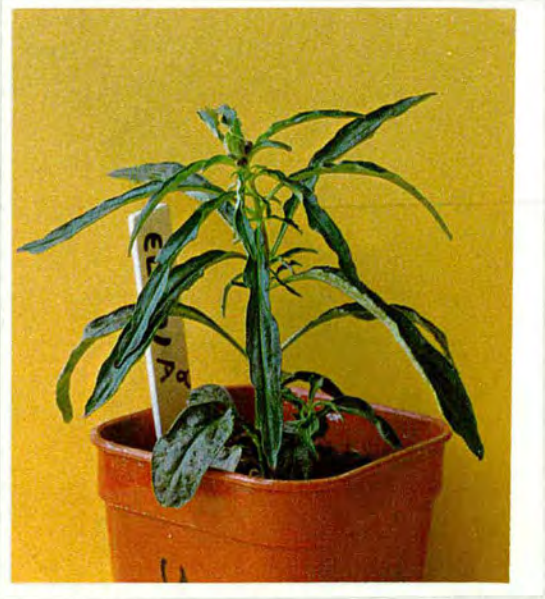

Figure: 35: Phenotype of the *longilinea* mutant.

The mutation appeared to affect both the width of the leaf and its length. The leaf contained significantly fewer cells in a plane across the middle of the blade (Table 3). The *longilinea* leaf was always longer than a WT leaf measured from the corresponding node. It was not established whether this was due to increased cell division or cell expansion along the proximal/distal axis of the leaf, but the growth curve of the mutant leaf suggested that *longilinea* increased in length at the same rate as WT but that the growing period was extended (Fig. 36).

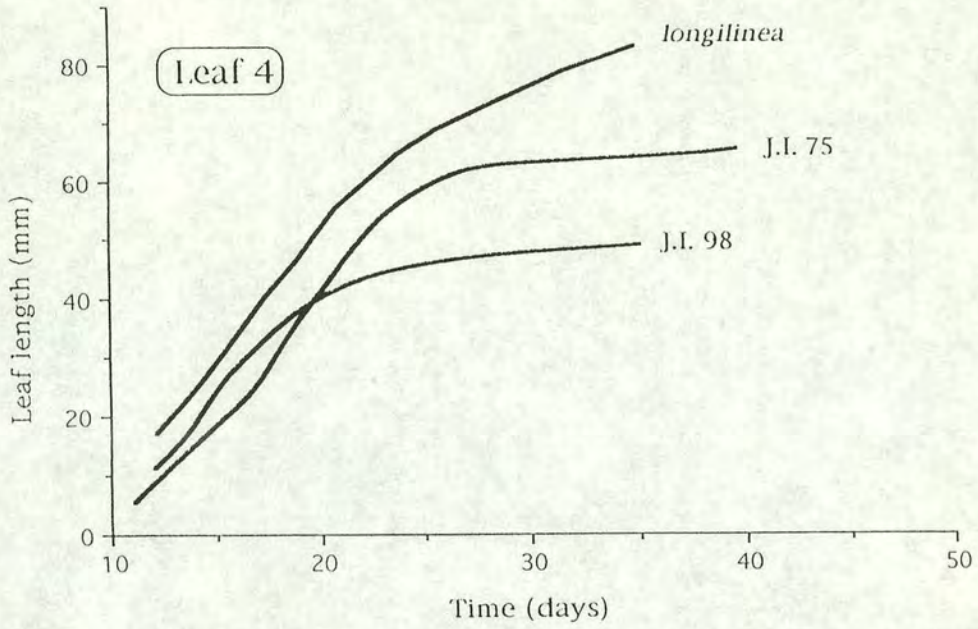

Figure 36: Growth curves of *longilinea* mutant and two WT lines for leaves attached at the 4th node.

The morphological analysis revealed that the midrib was less curved with the vascular tissue extending more towards the lamina. Parenchyma cells surrounding the midvein were less expanded along the dorso/ventral axis (Fig. 37), and the midrib was significantly wider than WT in the tip and middle regions (Table 2).

In the leaf lamina of *longilinea* there was a major difference in the gross morphology. In some parts of the lamina the spongy mesophyll was absent. In the tip and petiole regions, only small areas were devoid of spongy mesophyll, however in the middle region of the leaf, spongy mesophyll may have been missing from up to half of the lamina. Where this occurred, the overlying palisade cells contained more chloroplasts than WT (Fig. 38). The lack of mesophyll was confirmed by SEM analysis (Fig. 39). From the cross with wild-type plants *longilinea* appeared to be recessive. Complementation analysis has suggested that the *longilinea* locus was not represented by any of the other leaf mutants.

At least 5,000 plants from a self pollination of *longilinea* homozygote were screened in order to recover revertants. Unfortunately none of the screened progeny showed signs of reversion.

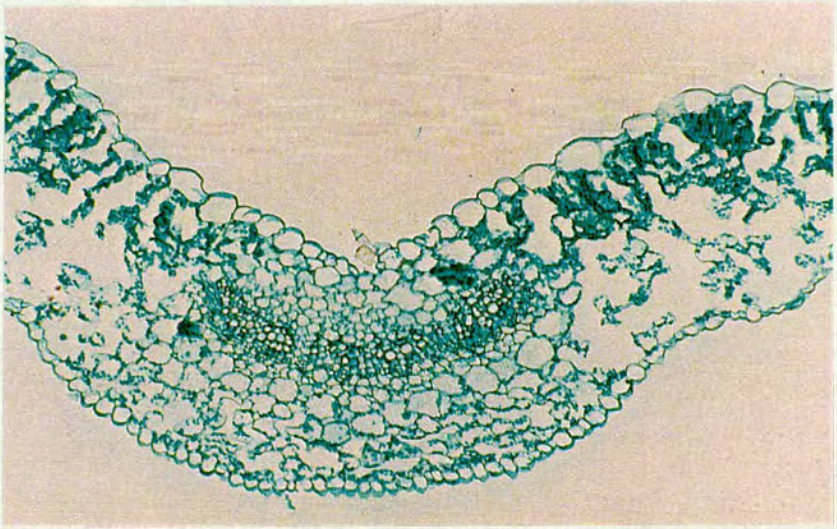

Figure 37: Transverse section of the midrib of a *longilinea* mutant leaf. (X23) (Fast Green stain)

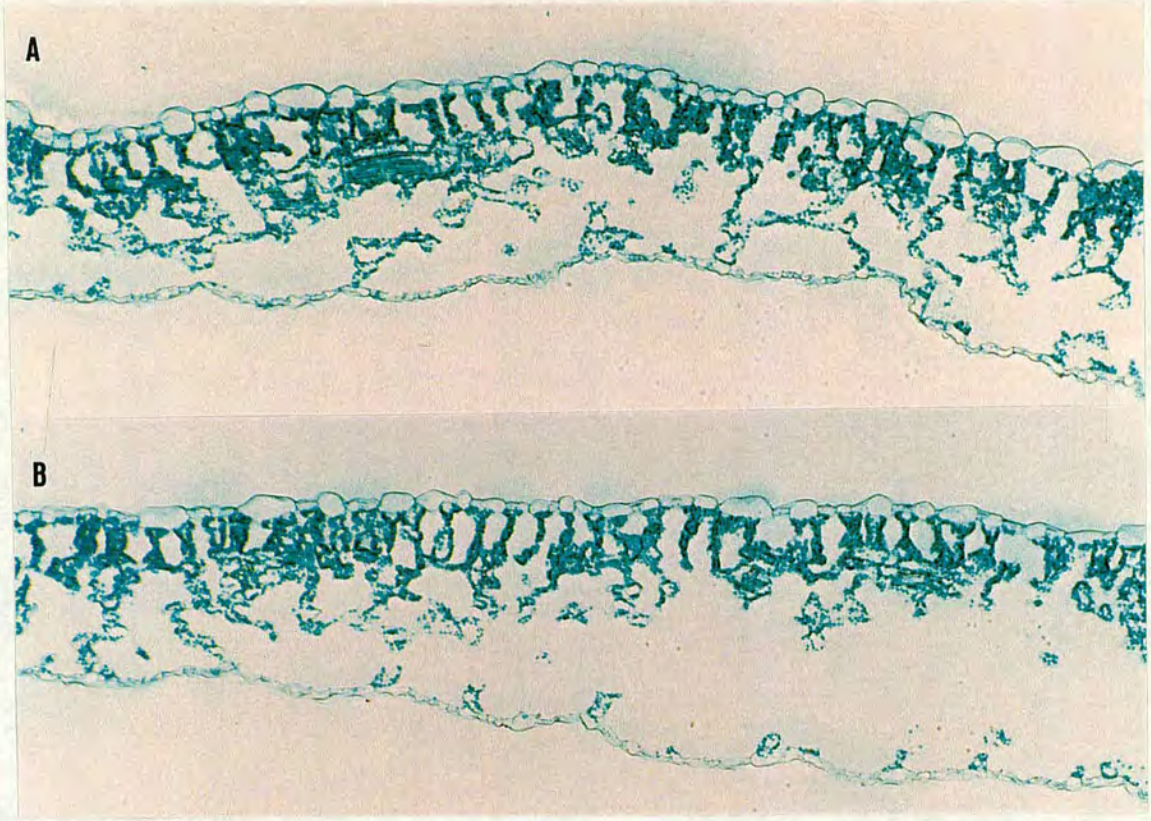

Figure 38: Transverse sections of the leaf lamina of the *longilinea* mutant. Very little spongy mesophyll is seen in A and even less in B. (X23) (Fast Green stain).

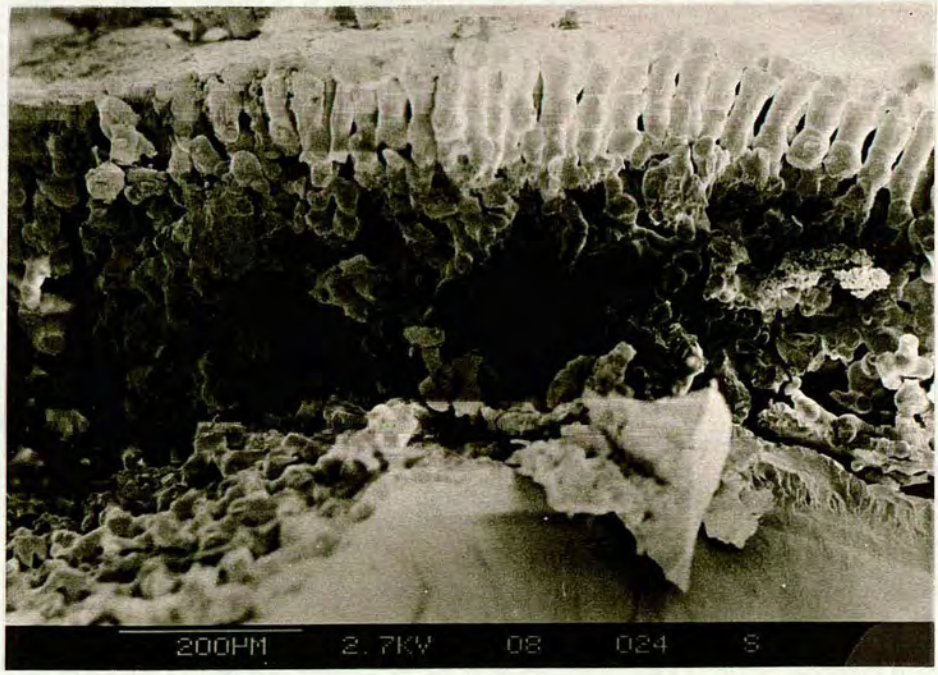

Figure 39: Cryo-SEM transverse section of *longilinea* mutant leaf lamina. A large area of the spongy mesophyll is absent from the lamina. (Scale bar 200 μm)

3.2.4: The *wavy* (ED 700) mutant

This leaf-shape mutant took over a year to produce flowers, since its development had been very slow. The plant appeared different to WT in several respects. The overall leaf surface was remarkably reduced. The *wavy* leaf had a distorted outline (Fig. 40) with indentations that always occurred opposite each other. The position of the indentations along the leaf axis varied from leaf to leaf. When they occurred distally, the effect was to produce a leaf which appears to have no tip. The dorsal surface was waxy, very lumpy, puckered and quite thick. Because the dorsal surface was rough, the venation pattern was not easily visible. The flowers were normal in shape and the phyllotaxis was unaffected, and the shoot meristem showed weak apical dominance.

Figure 40: Phenotype of *wavy* mutant leaves.

The histological analysis of lamina transverse sections revealed that midrib, palisade cells and spongy mesophyll were not well expanded or differentiated. Morphologically the mid vein was quite elongated towards the lamina and the midrib itself quite wide (Fig. 41) (Table 2). The cells below the vascular tissue were not expanded. In the lamina the palisade cells were irregular in width with space between them. Cells of the spongy mesophyll were smaller than wild-type with less air space between them (Fig. 42). The number of epidermal cells in the ventral side of the lamina

is significantly smaller than wild-type (Table 3), but the midrib has undergone more cellular division, as confirmed by the statistical analysis (larger midrib width and greater number of epidermal cells in the ventral side of the midrib) (Table 2 and 4).
It appeared, at least in the midrib, that an increase in cell division had compensated for the lack of expansion. In the lamina however, the number of the cells decreased suggesting that the final shape reflected a reduced cell number.

Crosses with WT plant suggested that wavy was a recessive mutation.

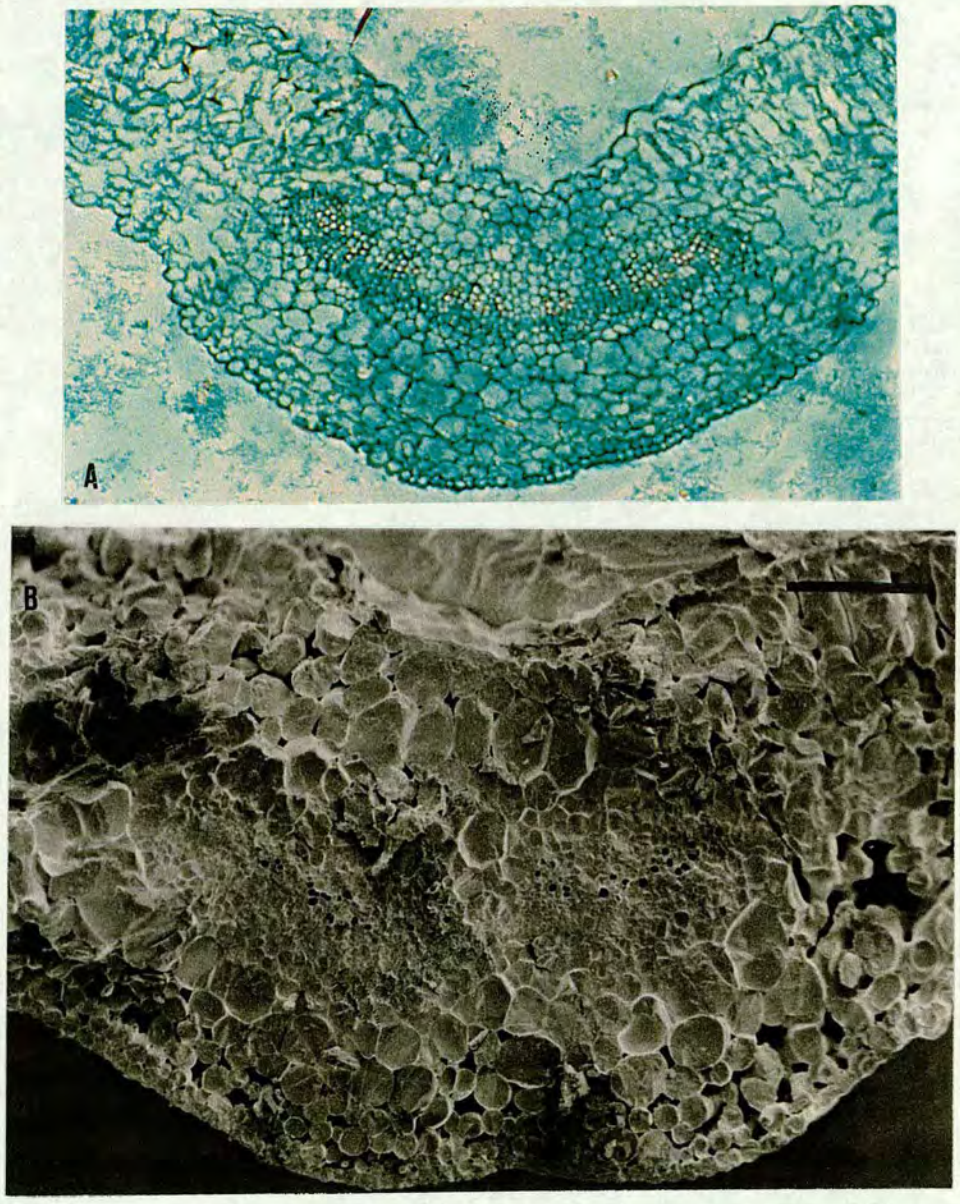

Figure 41: (A) Transverse section of the midrib of a *wavy* mutant leaf. (X23) (Fast Green stain). (B) Cryo-SEM transverse section of a *wavy* mutant midrib. (Scale bar 200 μm) (see text for explanation)

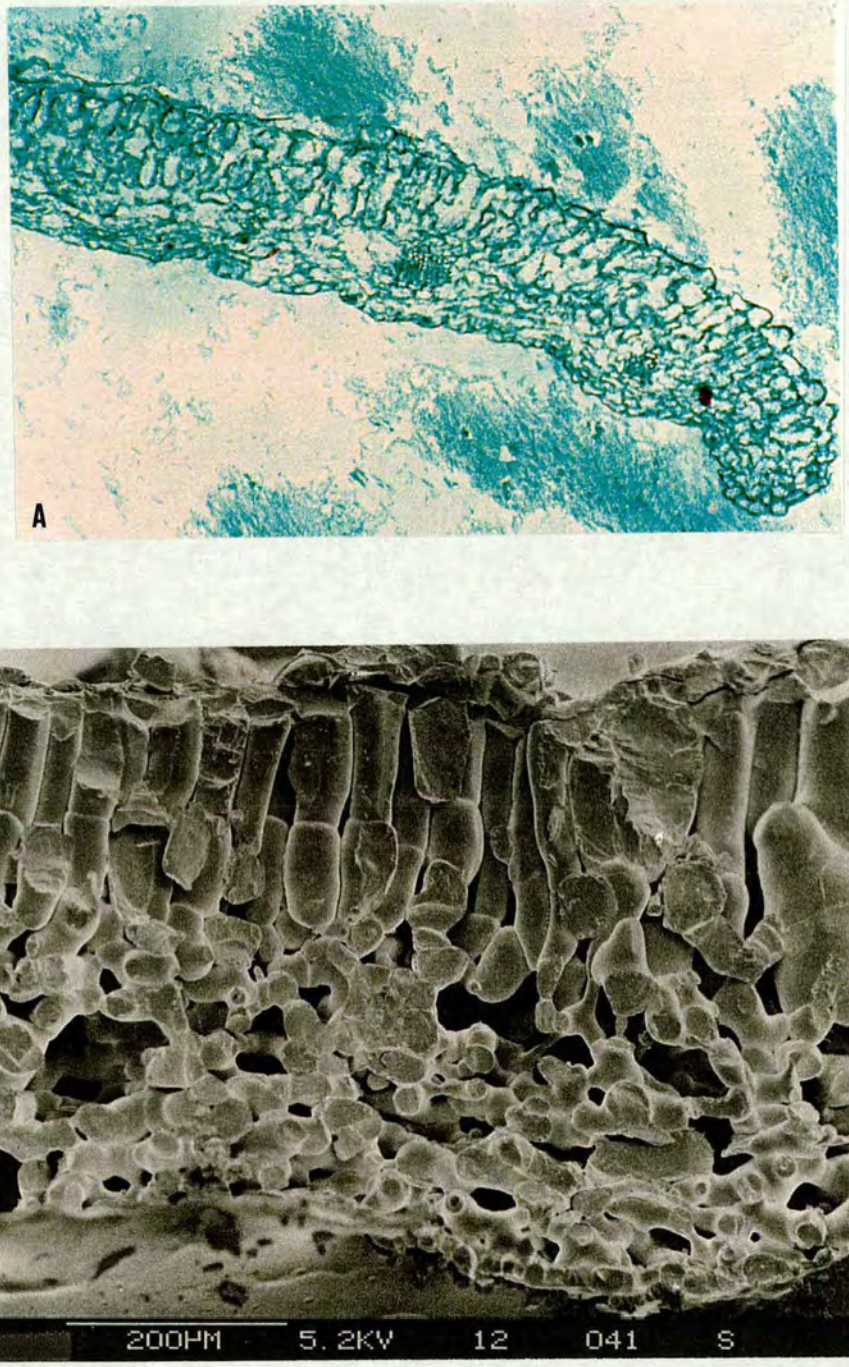

Figure 42: (A) Transverse section of a *wavy* mutant leaf lamina. (X23) (Fast Green stain). (B) Cryo-SEM transverse section of a *wavy* mutant leaf lamina. (Scale bar 200 μm)

3.2.5: The *Falx* (ED 211) mutant

Falx was the second leaf-shape mutant with distorted outline. Its phenotype was characterised by a sickle-shaped lamina (Fig. 43).

Figure 43: Phenotype of *Falx* mutant leaves.

Clones of cells appeared to grow slowly, begin to differentiate, but then die. Thus part of the leaf could not develop leading to sickle-shaped leaves with necrotic margins. The same appeared to occur in the shoot meristem, because meristems occasionally died, and a lateral shoot emerged. The phyllotaxis was normal decussate. The flowers were split with distorted petals and the stamens frequently produced no pollen. The dorsal leaf surface was undulating and puckered, especially at the margin. The leaf was thicker than WT as confirmed by histological sectioning (data not shown).

Morphologically the overall shape of the midrib and lamina of *Falx* mutant leaf was similar to WT, with well expanded cells below the vascular tissue (data not shown).

One suggestion explaining the *Falx* phenotype came from a similar mutant characterised at the John Innes Institute in Norwich which appeared to carry a mitochondrial mutation (C. Martin, pers. comm.). To test whether this might also be the case for *Falx*, reciprocal crosses were made between *Falx* and the WT plants. The

progeny showed a *Falx* mutant phenotype only when the mutant had been used as a female parent. This result was compatible with *Falx* being a mitochondrial mutation.

3.2.6: The *Spissifolia* (ED 208) mutant

Although the outline of *Spissifolia* was not different to WT, the leaves showed some peculiarities not found in WT and in the other mutants. Phenotypically the leaf was a little smaller than WT; the texture of the dorsal surface was pitted, uneven and waxy, but the major characteristic was the thickness of the lamina and its rigidity (Fig. 44). Only when the leaf matured was it possible to see the venation pattern, since during development the thickness of the lamina obscured it.

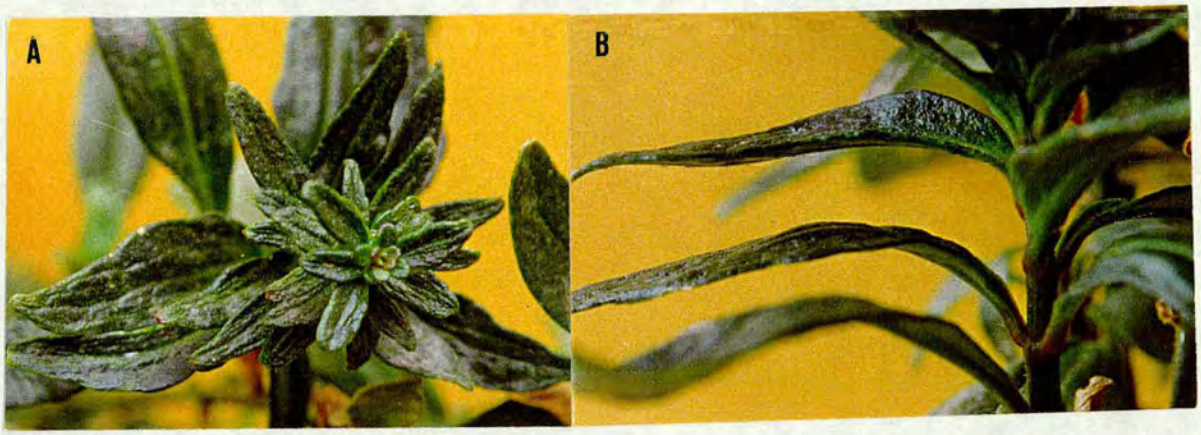

Figure 44: (A) Phenotype of *Spissifolia* mutant leaves. (B) A special feature of *Spissifolia* mutant leaves is their thickness.

After the plants underwent the transition to produce the inflorescence, the axis grew without producing axillary meristems (Fig. 45). Flowers were produced only sporadically, and these tended to be larger than those of WT.

From light microscopy, the dorsal surface of the midrib appeared not to curve away from the dorsal surface of the lamina. The vascular bundle was positioned quite high in the midrib towards the dorsal surface with much parenchymal tissue below (Fig. 46). The palisade cells in the lamina were not completely elongated. The spongy mesophyll had normal cells with large air-space (Fig. 47). Unlike the other mutants the height of the *Spissifolia* midrib was significantly different from WT, also the thickness of the lamina was statistically different from WT (Table 1 and 5). It appeared that the cells had undergone more periclinal division with new cell walls parallel to the leaf surface.

Spissifolia appeared to be semidominant. Heterozygous plants had a phenotype intermediate between those of the mutant and wild-type.

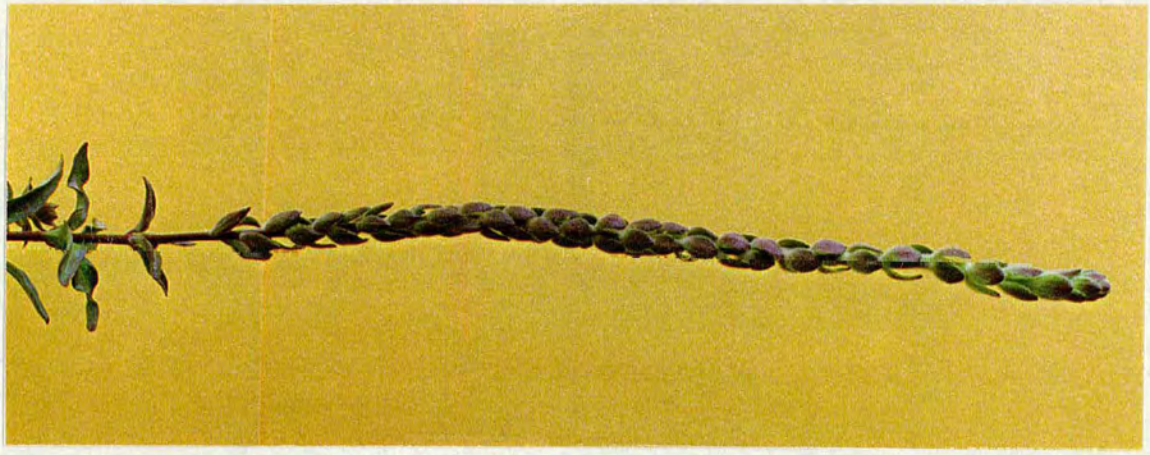

Figure 45: The inflorescence of a *Spissifolia* mutant plant.

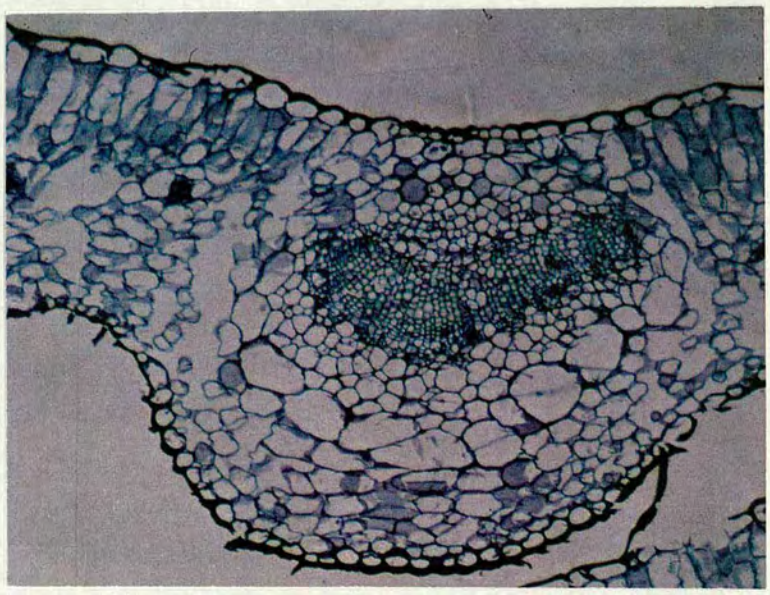

Figure 46: Transverse section of the midrib of a *Spissifolia* mutant leaf. (X23) (toluidine blue stain)

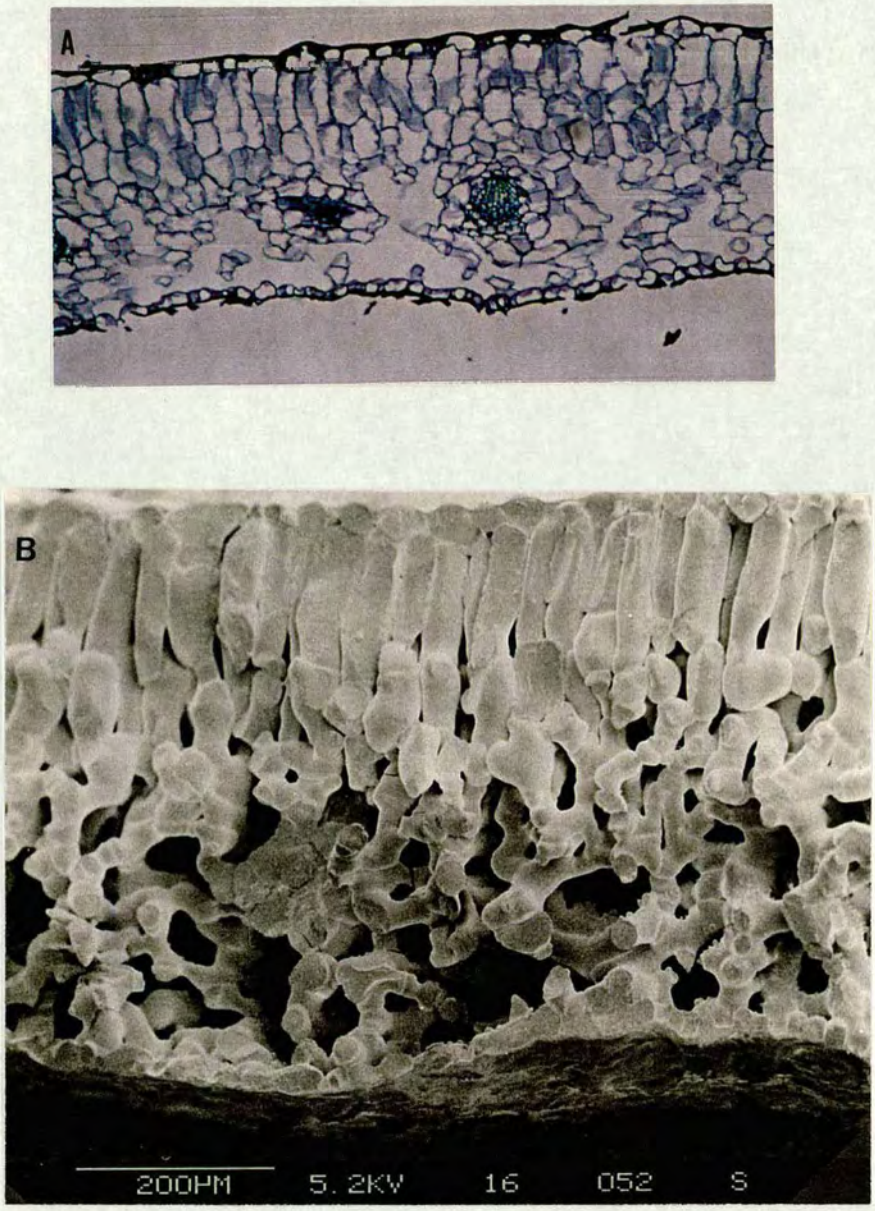

Figure 47: (A) Transverse section of a *Spissifolia* mutant leaf lamina. (X23) (toluidine blue). (B) Cryo-SEM transverse section of a *Spissifolia* mutant leaf lamina. (Scale bar 200 μm)

3.2.7: The *finifolia* (ED 712) mutant

finifolia was the narrowest leaf mutant recovered from the screening of the families that came from Norwich.

Figure 48: Phenotype of *finifolia* mutant leaves.

Like *wavy* it was very slow to develop, and took a year to produce flowers. Unfortunately the flowers of *finifolia* did not carry pollen and thus it was not possible to self-pollinate this mutant and screen it for reversion. Consequently the mutation was maintained as a heterozygote (made by fertilising mutant plants with wild-type pollen). However, it was also propagated by cuttings in the hope that somatic reversion would occur, to produce WT branches which could be used in transposon tagging. Phenotypically *finifolia* had very narrow leaves, with very rough, stippled adaxial surfaces (Fig. 48). The midrib was more pronounced on the ventral surface. The flowers were smaller than wild-type with contracted petals.

The morphological analysis revealed a midrib bigger than WT, with a curvature that was more gradual (Fig. 49). The parenchymal cells of the midrib were large but did not show air-spaces. The number of epidermal cells in the lamina were not statistically different to wild-type (Table 3), whereas differences were seen in the midrib width and in the number of ventral epidermal cells of the midrib (Table 2 and 4).

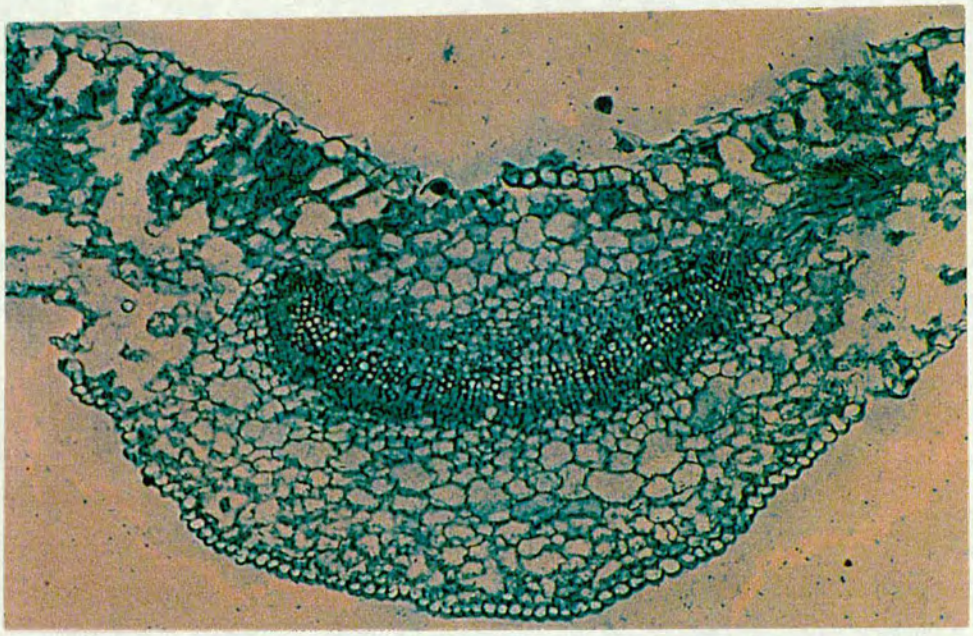

Figure 49: Transverse section of the midrib of a *finifolia* mutant leaf. (X23) (Fast Green stain)

For the next three leaf-shape mutants, genetic and statistical analysis was not performed.

3.2.8: The *asperfolia* (ED 706) mutant

The narrowness of this leaf mutant was less striking than *longilinea*, but nevertheless apparent. The margins of the lamina were curled towards the adaxial surface (Fig. 50). Although this feature was seen in the wild-type leaf during its development, subsequent leaf expansion flattens the lamina. This did not occur in *asperfolia* which retained the characteristic in mature leaves. The texture of the surface was also a remarkable characteristic of this leaf; it was very lumpy and very dimpled. The flowers were smaller than wild-type and the upper and lower lips curled towards the inner part of the flower.

Figure 50: Phenotype of *asperfolia* mutant leaves. Leaves show the characteristic curly and very lumpy appearance.

Morphologically the midrib was much smaller than wild-type, with a few layers making up the vascular tissue and the bundle (Fig. 51). However, the lamina was very thick and showed up to four layers of palisade cells. The spongy mesophyll had smaller cells than wild-type with large air-spaces (Fig. 52).

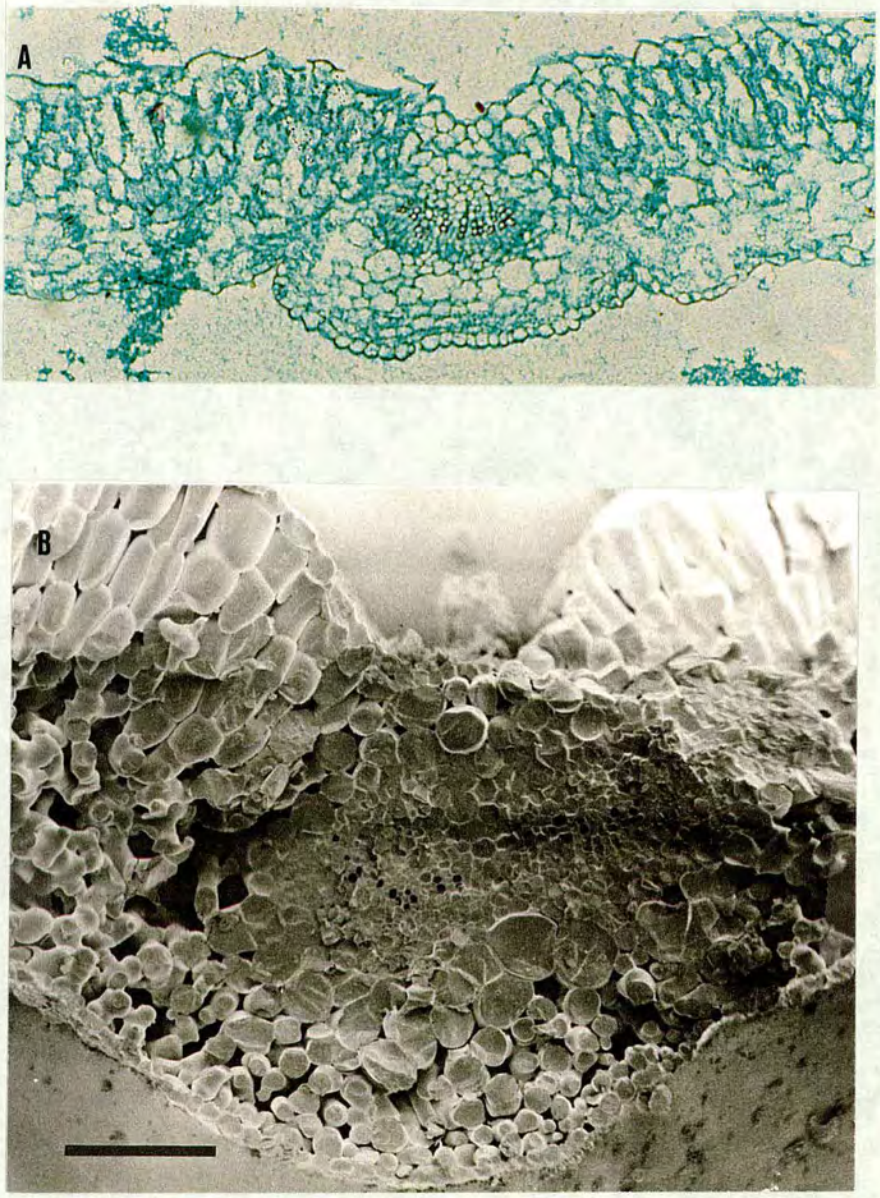

Figure 51: (A) Transverse section of the midrib of an *asperfolia* mutant leaf. (X23) (Fast Green stain). (B) Cryo-SEM transverse section of the midrib of an *asperfolia* mutant leaf. (Scale bar 200 μm)

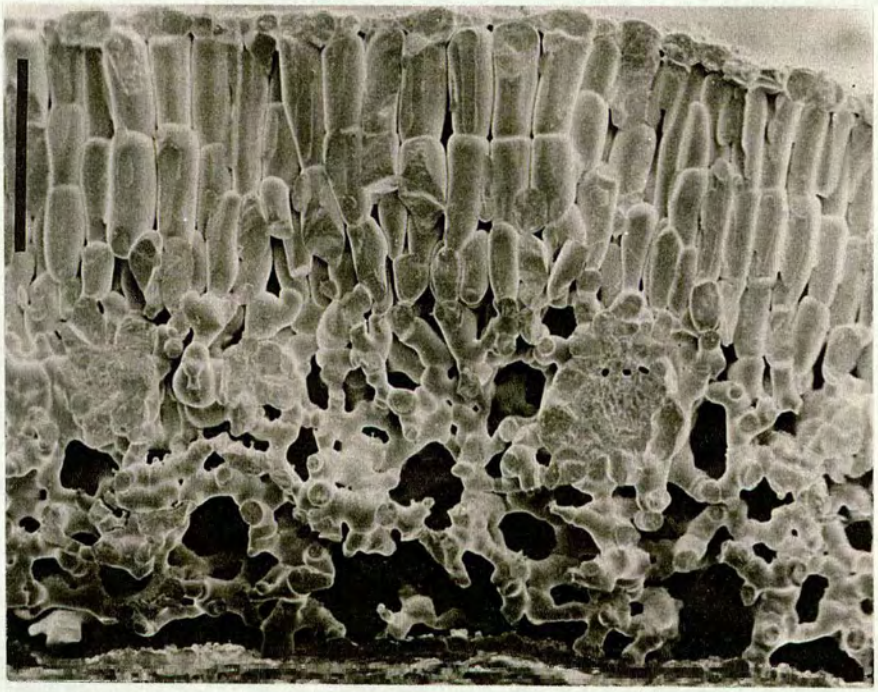

Figure 52: Cryo-SEM transverse section of an *asperfolia* mutant leaf lamina. Up to 4 files of palisade mesophyll cell are visible.

3.2.9: ED 727

This leaf-shape mutant showed very small leaves with occasionally distorted outlines. In the stage of elongation of the leaf axis, the edge of the leaf was curled towards the dorsal surface, but this feature was lost later in the development. The texture of the dorsal surface was rough and puckered. The flowers were normal in shape and produced pollen.

Morphologically the mid vein was very elongated with very few layers. The parenchymal cells forming the bundle sheath were not expanded. The lamina showed shorter palisade cells than wild-type, usually in triple layers. The spongy mesophyll was not very well expanded (Fig. 53).

3.2.10 ED 725

This leaf-shape mutant showed some analogy with *Falx*. Some leaves, as well as being distorted, showed areas of necrosis that occured at the margins of the lamina or in the inner part of it. Although there were similarities with *Falx*, only few leaves showed the sickle-like shape and the rest of the leaves were simply smaller than wild-type. In addition, the flowers of this mutant were normal, and they produced pollen.

The morphological analysis revealed a poorly developed midrib, with few cell layers of partially expanded parenchymal cells. The lamina had normal spongy mesophyll and palisade cells (Fig. 54).

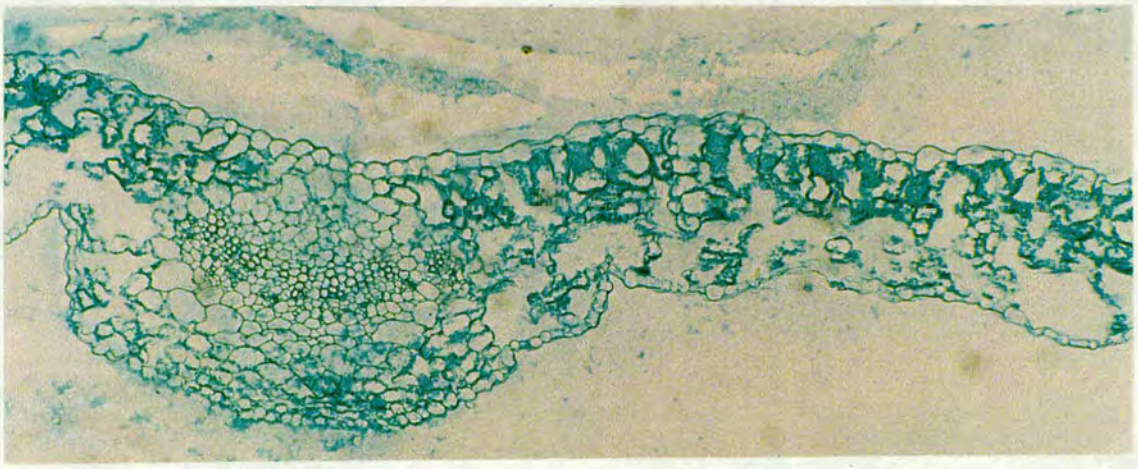

Figure 54: Transverse section of the midrib and part of the lamina of an ED 725 mutant leaf. (X23) (Fast Green stain).

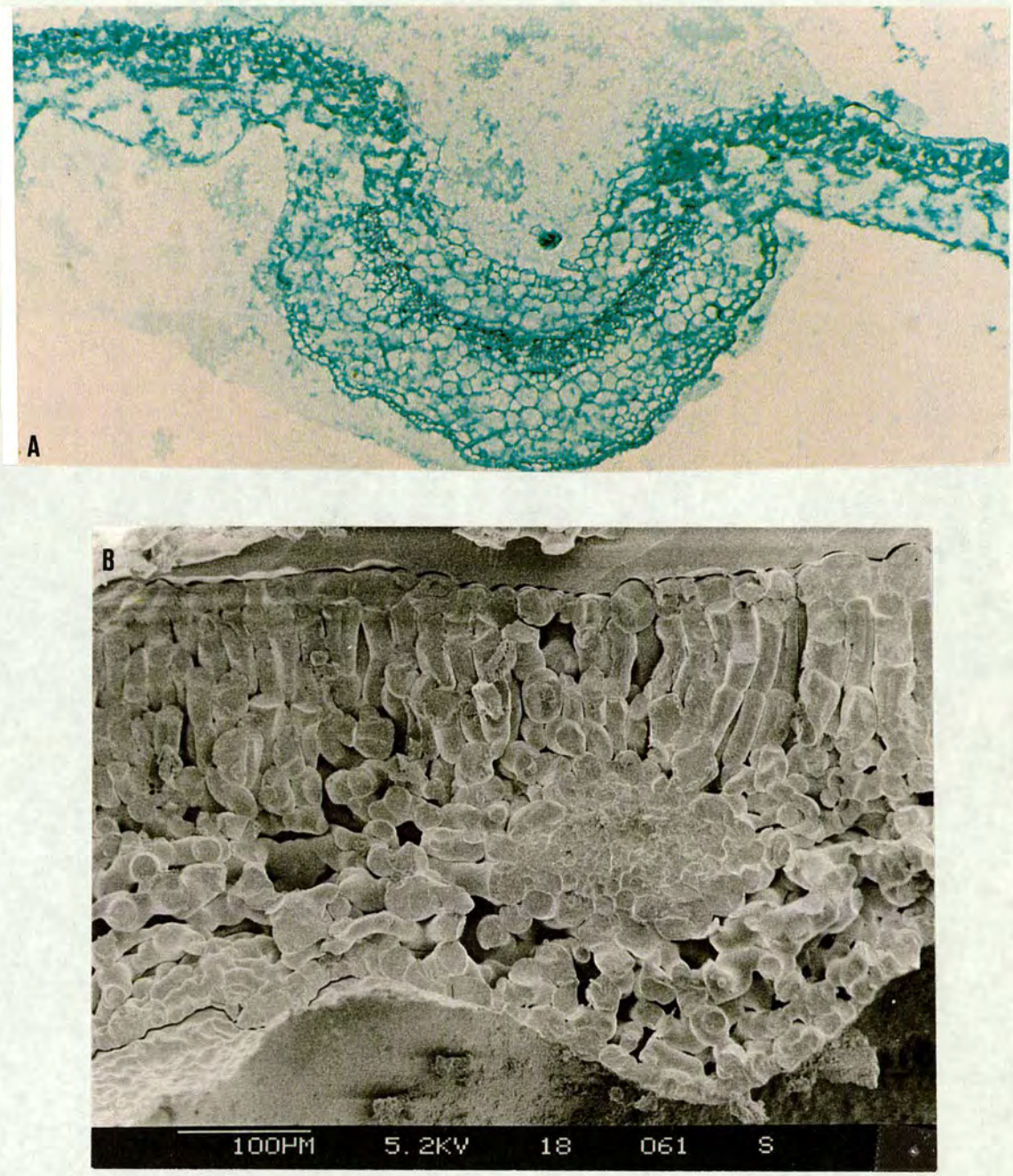

Figure 53: (A) Transverse section of the midrib of an ED 727 mutant leaf. (X23) (Fast Green stain). (B) Cryo-SEM transverse section of an ED 727 mutant leaf lamina and a lateral vein. (Scale bar 100 μm)

Tables of Variance Analysis

Table 1: Midrib height of each mutant and WT for the three different regions examined

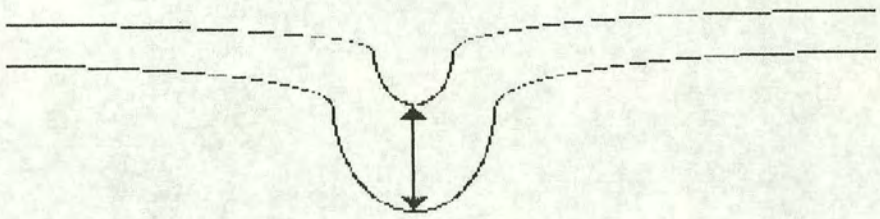

Tip region

Plant	longilinea	WT	spissifolia	graminifolia	wavy	finifolia	falx
Average (mm)	200.5	210.1	240.7	264.5	279.0	316.8	321.7
Grouping	a	a	b	c	d	e	e

Middle region

Plant	graminifolia	longilinea	wavy	WT	falx	finifolia	spissifolia
Average (mm)	258.1	324.2	406.6	410.6	453.3	541.8	1176.1
Grouping	a	a	a	a	a	a	b

Petiole region

Plant	graminifolia	wavy	falx	longilinea	spissifolia	finifolia	WT
Average (mm)	381.8	533.2	595.1	610.1	643.5	867.2	971.7
Grouping	a	b	c	c	d	e	f

Table 2: Midrib width of each mutant and WT for three different regions examined

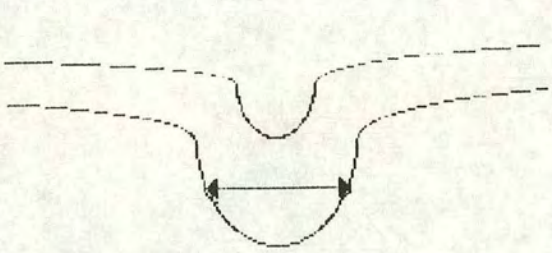

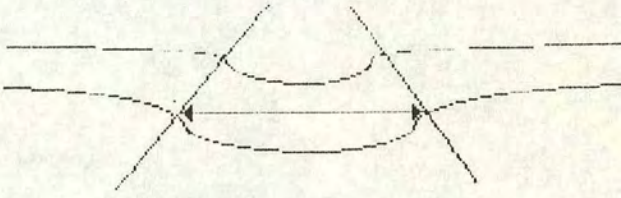

Tip region

Plant	spissifolia	falx	WT	finifolia	longilinea	graminifolia	wavy
Average (mm)	158.6	203.6	221.6	289.0	331.7	393.6	642.9
Grouping	a	b	c	b	e	f	g

Middle region

Plant	gram	WT	falx	longilinea	wavy	spissifolia	finifolia
Average (mm)	362.6	682.2	720.0	781.8	820.1	1036.1	1053.8
Grouping	a	b	c	d	e	f	g

Petiole region

Plant	gram	wavy	longilinea	WT	falx	spissifolia	finifolia
Average (mm)	501.0	892.1	972.8	1009.1	1082.2	1146.3	1333.3
Grouping	a	b	c	d	e	f	g

Table 3: Number ventral epidermal cells of half lamina of each mutant and WT, for the three different regions examined

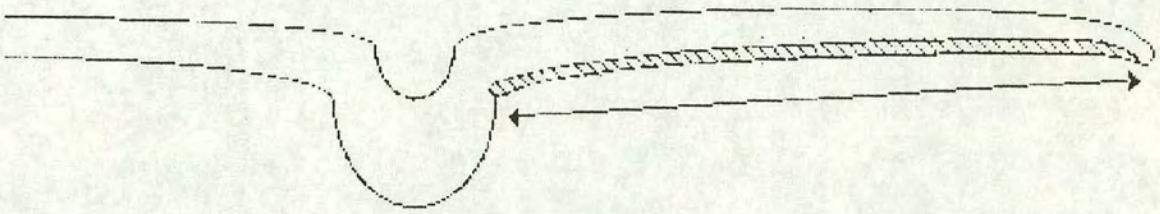

Tip region

Plant	finifolia	longilinea	graminifolia	WT
Average	62.4	72.9	80.3	106.7
Grouping	a	b	c	d

Middle region

Plant	graminifolia	wavy	longilinea	finifolia	WT
Average	104.2	126.6	182.0	291.7	301.9
Grouping	a	a	b	c	c

Petiole region

Plant	graminifolia	longilinea	WT	finifolia
Average	55.7	63.1	74.2	106.0
Grouping	a	b	c	d

Table 4: Number ventral epidermal cells of the midrib for each mutant and WT

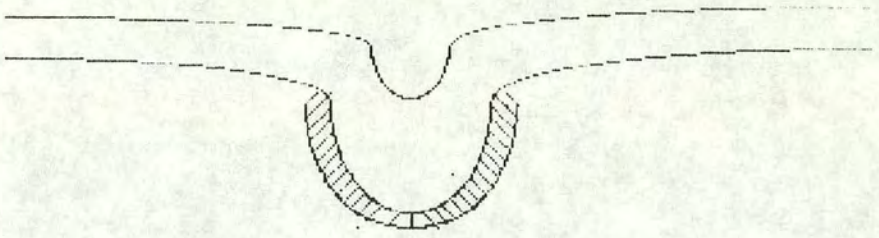

Tip region

Plant	falx	spissifolia	finifolia	gram	longilinea	WT	wavy
Average	10.6	14.6	18.3	20.2	22.6	28.6	39.5
Grouping	a	b	c	d	e	f	g

Middle region

Plant	graminifolia	falx	WT	longilinea	spissifolia	wavy	finifolia
Average	20.3	39.8	44.5	45.9	50.3	71.0	88.1
Grouping	a	b	c	c	d	e	f

Petiole Region

Plant	graminifolia	longilinea	wavy	WT	finifolia
Average	35.6	67.8	78.7	81.6	106.6
Grouping	a	b	c	d	e

Table 5: Lamina thickness at the distal point of each mutant and WT for the three different region examined

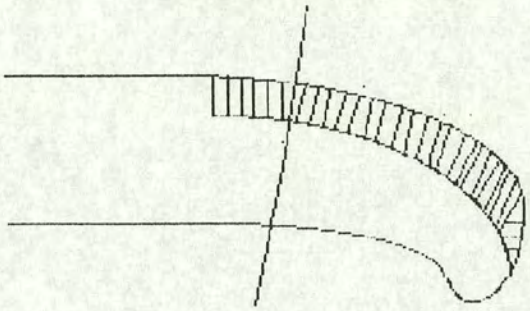

Tip region

Plant	longilinea	finifolia	graminifolia	spissifolia	wavy	WT	falx
Average (mm)	173.8	187.6	191.9	211.5	217.1	230.6	250.9
Grouping	a	b	b	c	c	d	e

Middle region

Plant	graminifolia	longilinea	finifolia	WT	wavy	spissifolia	falx
Average (mm)	189.9	204.8	211.2	221.6	226.1	232.9	250.9
Grouping	a	b	b	c	c	d	e

3.3: The choice of which leaf-shape mutants to tag

As shown in figure 55, the first step of transposon tagging is to grow the first generation (M_0) at 15°C, to increase the frequency of transposition. The next generation (M_1), produced by self-pollination of M_0 plants will carry mutant alleles in the heterozygous state. Selfed M_1 plants then provide the M_2 generation in which the homozygous mutants can be identified. At this stage, the mutants could be characterised morphologically and subjected to genetic analysis. In order to clone the mutated genes, further generations need to be grown. Self-pollination of the homozygous mutant plants produce the S1 generation which can be screened for reversion of the mutant phenotype.

The results of the morphogenetical characterisation indicated that *longilinea*, *Graminifolia* and *wavy* had interesting phenotypes for the following reasons. At least two of the mutants (*Falx* and ED 725) may have involved genes which were necessary for cell survival, and not for direct control of leaf development. This was supported by the observation that *Falx* was maternally inherited and therefore potentially a mitochondrial mutation. Of the remaining mutations, many seemed to have pleiotropic effects on leaf structure and on other parts of the plants (e.g. flowers). The most extreme example of this was *Spissifolia* which also affected the initiation of floral meristems (Fig. 45). It could be argued that these mutations affected genes with a general role in plant development, and that their effect on leaf structure was indirect; i.e. these genes did not directly control the patterns of cell division which result in leaf initiation and development. On the other hand, the possibility that genes involved in other developmental programmes might have a function in the determination of leaf-shape, can not be excluded.

In contrast, *longilinea* can be considered a true leaf shape mutant affecting only leaves. *longilinea* appeared to shift the pattern of cell growth in favour of those which contributed to the length of the leaf, and therefore the leaves of the mutant were both longer and narrower than WT.

Similarly, *Graminifolia* mutants showed a number of disruptions in leaf shape and pattern, which suggested that the *GRAM* gene had an important role in leaf morphogenesis. One way to explain the effect of this mutation on leaf development came from the model proposed to explain another leaf-shape mutation: *phantastica*. It was proposed that *phan* plays a role in establishing dorsoventrality in leaves (Waites and Hudson, 1995).

Figure 55: **TRANSPOSON-TAGGING : FLOW DIAGRAM**

M_0: $\underline{M^+}$ / M^+ — Grow lines with active transposon at low temperature (15^0C) to increase transposition.

Self-pollinate

M_1: $\underline{m::Tam}$ / M^+ — Self-pollinate M_1 plants to recover mutants homozygous for transposon insertion.

Self-pollinate

M_2: $\underline{M^+}$ / M^+ ; $\underline{m::Tam}$ / M^+ ; $\underline{m::Tam}$ / m::Tam — Test allelism and epistasis with other mutants. Characterise mutant phenotype morphogenetically

Self-pollinate

S_1: $\underline{m::Tam}$ / m::Tam $\quad \underline{M^+}$ / m::Tam — Screen progeny for revertants caused by excision of transposon

Self-pollinate

S_2: $\underline{M^+}$ / M^+ : $\underline{m:Tam}$ / ....M^+ : $\underline{m::Tam}$ / m::Tam

Identify copy of transposon which co-segregates with mutant allele by Southern hybridisation. Clone co-segregating transposon together with the DNA into which it is inserted. This flanking DNA can be used as a probe to isolate the wild-type gene.

Soon after primordium initiation occurs, cells near the boundary between dorsal and ventral domains are induced to change division pattern and so form the lamina by lateral proliferation. The dorsalising function (DF) attributed to *PHAN* gene, persists in the dorsal part of the lamina where it is necessary to specify the identity of dorsal cell types. The characteristic needle-like leaves of *phan* mutant lack the lamina and dorsal cell types, suggesting the complete loss of DF. The other intermediate leaf forms of *phan* mutant can be explained by reductions in the strength or position of DF expression. So if the boundary between dorsal and ventral domains moves towards more a dorsal position, the lamina will form in a more dorsal position and more of the leaf primordium will develop with ventral identity. The reduction in DF domain would result in fewer cells making a narrow leaf lamina.

The narrowed features of the *Gram* mutant leaf could be explained as a shift of the dorso/ventral boundary towards a more dorsal position. However, the *Gram* mutant lamina was not produced at a more dorsal position, and the ectopic dorsal epidermal cell type near the edge of the ventral side might be interpreted as a shift of the dorso/ventral boundary towards a more ventral position.

Another possible explanation of *Gram* phenotype and its pleiotropic effects is that *Graminifolia* is a mutation in *KNOTTED*-like gene. As it was described before, *Gram* mutants may form a shoot along the margin of the lamina. *KN1* driven by a constitutive promoter led to the formation of shoot meristems on the lamina of tobacco leaf (Sinha *et al.*, 1993).

The *Gram* mutant leaf had a long petiole, reminiscence of sheath/ligule displacement in *KN1* maize leaf. It could be hypothesised that the shift of lamina proliferation towards a more distal position caused by stem/petiole displacement, led to a narrower lamina. Moreover the presence of hairs and the alteration of the node/internode are all indications that *Gram* could be a mutation affecting a homeobox gene.

Finally, in the *wavy* mutant, the mid vein seemed to occupy a large part of the midrib (two symmetrical mid veins could be seen in the same histological sections). The reduced lamina in this mutant could be interpreted as reflecting an increase in the domain of the vascular tissue and the bundle sheath.

Since the leaf shape mutants came from WT lines carrying highly active transposons, it seemed likely that the mutations had been transposon induced, and might therefore be used to isolate the mutated genes by transposon-tagging. On the base of this assumption, and from the results of the morphological characterisation, three

homozygous leaf mutants, *longilinea, wavy* and *Graminifolia*, were self pollinated and the progeny screened for reversions to WT phenotypes.

3.4: Tagging of leaf-shape mutants

Reversion is a property of transposon-induced mutations and occurs when a transposon excises from the mutated locus. The revertants can be selfed to produce the S_2 generation (Fig. 55) which would segregate in the ratio of three wild-type plants to one of the mutant phenotype (3:1), and provide the material for molecular analysis. DNA from the plants can be examined by Southern hybridizations, and the transposon causing the mutation observed segregating with the mutant allele. The co-segregating transposon can then be cloned along with the sequences flanking it, and the flanking sequences used as a probe for the locus in isolation of the wild-type gene.

Plants for these three leaf-shape mutants were grown at 15°C and self pollinated to increase the frequency of transposon excision. At least 5,000 progeny plants for each mutant were scored for reversion of the phenotype. Only a single WT revertant was identified among the progeny of the *Graminifolia*$^{-202}$ mutant, suggesting that the others were not transposon induced.

One explanation for the instability of the mutant phenotype was that the *Gram*$^{-202}$ mutant allele carried a transposon, which could revert and restore wild-type gene function. Self pollination of the single WT revertant revealed that it was heterozygous: its progeny consisted of wild-type and *Gram* mutant plants in the ratio 3:1. It also suggested that the original revertant was not the result of accidental cross-pollination by a wild-type plant because the progeny had the same floral pigmentation phenotype as the *Gram* mutant progenitor (*Eluta*). Although *Gram* mutations are semidominant (i.e. heterozygotes have a phenotype intermediate between *Gram* homozygotes and WT) it was not possible to distinguish *GRAM/Gram* heterozygotes from *GRAM/GRAM* homozygotes unequivocally. This may have reflected the conditions under which the plants were grown. Therefore, homozygous *GRAM/GRAM* plants were identified by self-pollinating S_2 plants and growing a further generation.

3.5: Identification of a transposon linked to *Gram*$^{-202}$

To identify a transposon responsible for the *Gram* mutation, DNA was prepared from homozygous mutant and wild-type progeny of the original revertant. The DNA was digested with a number of restriction enzymes and subjected to Southern

hybridisation with probes from 10 different *Antirrhinum* transposons. A probe (the CACTA probe) derived from a sequence conserved between a number of transposons, detected a 6.9 kb band in *Bgl* II-digested DNA from mutant plants which was not present in homozygous wild-type plants (Fig. 56). *Bgl* II-*Sca* I double digestion gave a more clear band of the same size. The 6.9 kb band was present in 12 *Gram* mutant plants and absent in 12 WT progeny, indicating that it was closely linked to *Gram* locus. Although excision of this transposon appeared to have accompanied the reversion of *Gram*$^{-202}$ allele to WT, this may have been a coincidence. Ideally, excisions correlated with multiple independent reversion events are required as evidence that a particular transposon is responsible for the mutation. However, of all the transposons tested in Southern hybridisation experiments, this was the only copy which moved at the time of reversion. No other polymorphisms were detected using other transposons as probes, and the patterns generated by them was always the same between *Gram/Gram* and *GRAM/GRAM* progeny (data not shown).

To clone this fragment, a 6.9 kb size fraction of *Bgl* II-digested DNA was isolated from *Gram* mutants and ligated into λ Blue Star (Novagene, UK) at the *Bam HI* site. Positive phages were identified by hybridisation to the transposon probe and purified. Work to determine whether cloned sequences flanking the transposon represent the *GRAM* locus is continuing.

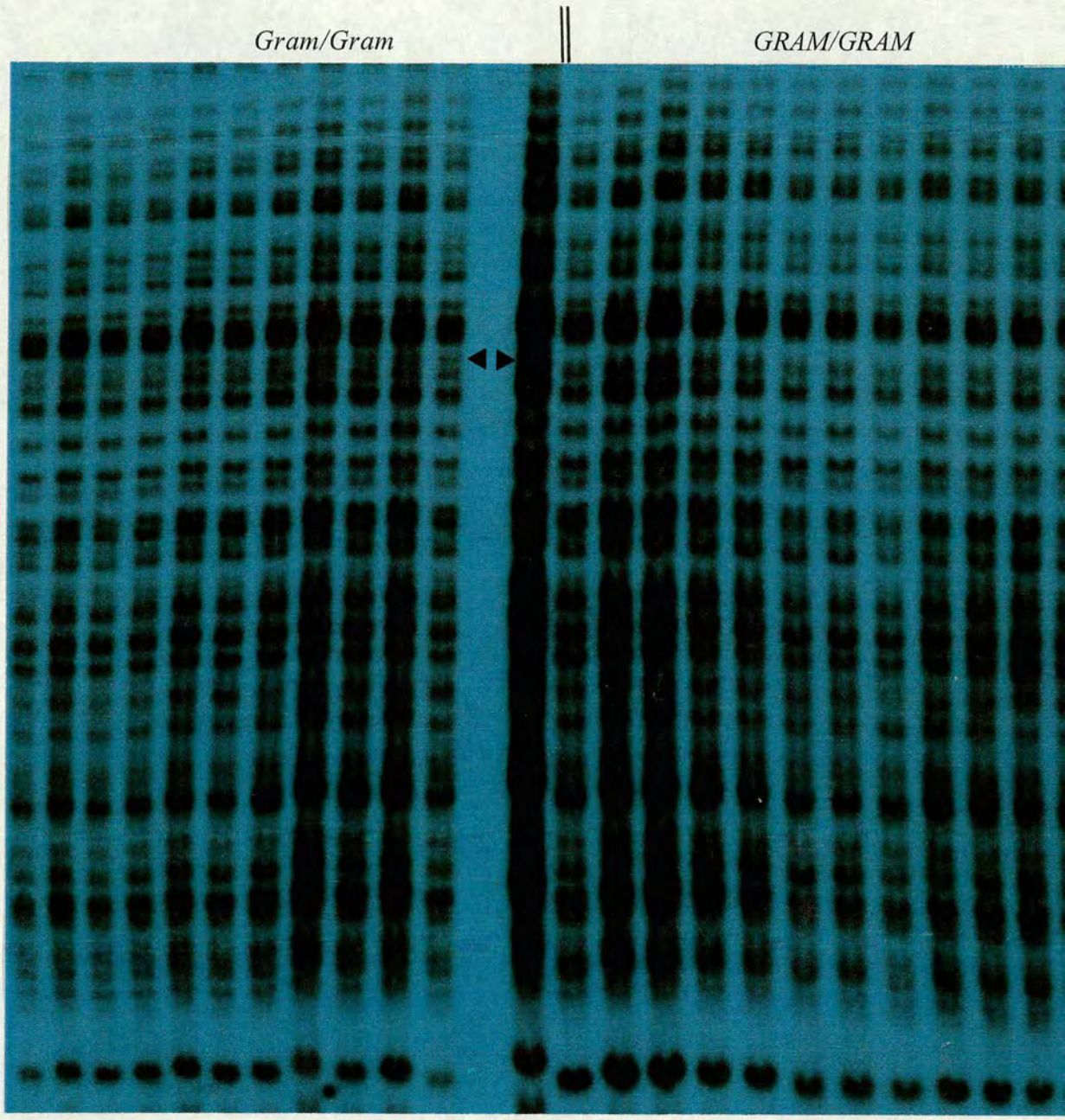

Figure 56: Southern hybridisation of the DNA from the progeny of a *GRAM/Gram*$^{-202}$ revertant. The revertant plant was self pollinated and DNA extracted from 12 homozygous *Gram* mutant progeny. A further self pollination of those progeny with WT phenotype allowed *GRAM/Gram* heterozygous and *GRAM/GRAM* homozygous plants to be distinguished. DNA was then extracted 12 plants homozygous for *GRAM* WT revertant allele. The DNA was cut with *Bgl* II and *Sca* I. A probe made from the right arm of Tam4 was used as a probe at low stringency to detecte a family of related transposons (CACTA family). A band of 6.9 kb was detected in the 12 *Gram/Gram* plants, but was absent from all homozygous *GRAM* revertants (triangles).

3.6: Isolation of *KNOTTED1* homologues

At the outset of this project, only one gene, *KNOTTED1*, was known to have a role in patterning the vegetative meristem. In WT maize plants, *KN1* is expressed in the apical meristem but down-regulated in leaf initials. Dominant gain-of-function mutations which allowed ectopic expression of *KN1* in the leaf primordia, caused abnormalities in leaves which could be interpreted as a gain of more proximal characteristics (Smith and Hake, 1992). These observations suggested that *KN1* had a role in distinguishing SAM cells from lateral organ initials, and that this distinction was established early in the meristem. Other *KN1*-like genes had been found to show patterned meristematic expression in maize (Freeling 1992), suggesting further roles in determining fate in the SAM. Because at least one of the leaf shape mutants, *Gram*, showed disruption in pattern reminiscent of gain of *KN1*-like functions, *KN1*-like genes were isolated from *Antirrhinum* as a first step in investigating their potential roles in leaf development and determination of shape.

In addition, due to the relatively larger size of *Antirrhinum* SAM, the isolation of homologues of *KN1* might give a better understanding of the domain of expression of homeobox genes in dicot plants. *A. majus* has been very well exploited in the expression studies of homeotic genes involved in flower morphogenesis (e. g. Bradley *at al.*, 1996). These studies led to a clear picture of temporal and spatial pattern of expressions in floral primordia or in the inflorescence meristem.

3.6.1: To isolate *KN1* homologues from *A. majus*

Over 250,000 plaques from a cDNA library cloned in *Eco* RI site λNM1149 derived from young inflorescence tissue (gift of R. Simon), were screened using the *KNOTTED1* cDNA (gift from S. Hake) as probe at low stringency (57°C, 4.5X SSC). 29 plaques were initially found to hybridise to *KN1* probe in a range of autoradiography signals from weak to very strong. These plaques were purified by a further round of hybridisation, and DNA extracted from liquid cultures using a Qiagen kit. Inserts were released by digestion with *Eco* RI, and their sizes determined by Southern hybridisation. Those selected for further analysis were ligated into the *Eco* RI site of pBluescript (Stratagene) and transformed by electroporation into the *E. coli* strain JM101. The cDNAs were analysed by restriction mapping and three clones (representing *SNAP1, SNAP2, SNAP3*) were selected for further studies. A further clone named *R* showed a

very strong hybridisation signal. Digestion of *R* with *Eco* RI gave four insert bands of approximately 850 bp, 1400 bp and 2300 bp and 2900 bp respectively.
On the basis of their sizes they were named *R1*, *R2, R3*, and *R4*, with *R1* being the smallest and *R4* the largest inserts respectively. *R1* and *R2* were extracted from agarose gel, purified and subcloned in pBluescript (Stratagene). Sets of deletions into the cDNA for *SNAP1*, *SNAP2*, *SNAP3* and *R1* were produced using Exonuclease III and sequenced using a Pharmacia T7 polymerase sequencing kit. Sequences were assembled and analysed using UWGCG and Staden programmes.

3.6.2: SNAP1 structure

The *SNAP1* cDNA is 1528 bp in length and has the ability to encode a protein, SNAP1 of 359 amino acids (Fig. 57). SNAP1 shows all the features of a KN1-like protein. *SNAP1* contains a 192 bp highly conserved DNA sequence, the homeobox (HB), which encodes for an equally conserved stretch of 64 amino acids, the homeodomain (HD) (Fig. 57 and 62) (Vollbrecht *et al.*, 1991). In *Drosophila melanogaster* as well as in other animals, the HD is responsible for sequence specific DNA binding (McGinnis *et al.*, 1984; Scott and Weiner, 1984). The homeodomain consists of 3 α-helices (Qian *et al.*, 1989; Kissinger *et al.*, 1990) with helix 2 and 3 forming a helix-turn-helix (HTH) motif similar to that found in prokaryotic DNA binding proteins (Shepherd *et al.*, 1984; Pabo and Sauer, 1984). It is helix 3 that makes direct contact with the DNA.

The amino acid sequence of SNAP1 showed an overall identity of 60.3% (UWGCG programme) with KN1. The identity increased up to 89.1% when the comparison was made between the two homeodomains, with 53 amino acids conserved out of 64 that form the HD (Fig. 62) (Table 6). SNAP1 shows even higher overall identity with two other plant homeodomain proteins, KNAT1 (Lincoln *et al.*, 1994) and TKN1 (Hareven *et al.*, 1996), isolated from *A. thaliana* and *Lycopersicum esculentum* respectively (Table 6). In addition, SNAP1 and TKN1 revealed two homologous motifs in the N-terminus (from amino acid 59 to 64, and from 72 to 81) (Fig. 58)

The other feature that SNAP1 shares with KN1 is the ELK region. It is located upstream of the HD from amino acid 241 to 261 (Fig. 57). The ELK region consists of leucine and other hydrophobic residues which occur with the same periodicity as in KN1. This region has been proposed to form a helix with a hydrophobic face which could stabilise a protein-DNA complex (Vollbrecht *et al.*, 1993). The position of the leucine residues is distinct from those of the *Arabidopsis Antennapedia*-like gene

products ATHD1 and ATHD2, in which the HD has an adjacent leucine zipper motif located at the C-terminus (Ruberti *et al.*, 1991).

SNAP1 contains a putative nuclear localisation signal (SKKKKKGK) located in the basic region preceding helix 1 of the HD (Fig. 57).

SNAP1 also shows similarities to KN1 outside these two highly conserved regions. The presence of the motif V/MMD(X)7-8YMD/E downstream to the HD differentiates SNAP1 from SNAP2 and SNAP3 *Antirrhinum* homeodomain proteins. This motif is common only to class 1 KNOTTED1-like proteins (Kerstetter *et al.*, 1994; D. Jackson pers. comm.).

Upstream to the ELK region negatively charged amino acids are present between amino acids 209 and 239 (Fig. 57). Acidic regions are common in other plant homeodomain proteins (Carbelli *et al.*, 1993; Schindler *et al.*, 1993; Ma *et al.*, 1994; Rerie *et al.*, 1994), and plant KN1-like proteins (Vollbrecht *et al.*, 1991). Acidic domains present in many other transcription factors (i.e. GAL4) (Ptashne and Gann, 1990), are involved in protein-protein interactions and work as transcriptional activation domains. Near the N-terminus of SNAP1 there are four short regions rich in serine (S), histidine (H) and glutamine (G). Amino acid homopolymers are common in many transcription factors (Laughon *et al.*, 1985). Experiments where single homopolymeric stretches of proline or glutamine were fused to the DNA binding domain of GAL4, could, in vitro, activate transcription (Gerber *et al.*, 1994).

However, different results have been obtained for the rice homeobox gene *OSH45* (see later *SNAP2* and *SNAP3*). The *OSH45* product contains stretches of polyalanine and polyglutamine at the N-terminus. This region together with the acidic region of the same protein was fused to the GAL4 binding domain. The construct was tested for its ability to activate a GUS reporter gene containing the binding site for GAL4 in rice protoplasts. It resulted in a suppression of the activation shown by the acidic region alone (Tamaoki *et al.*, 1995).

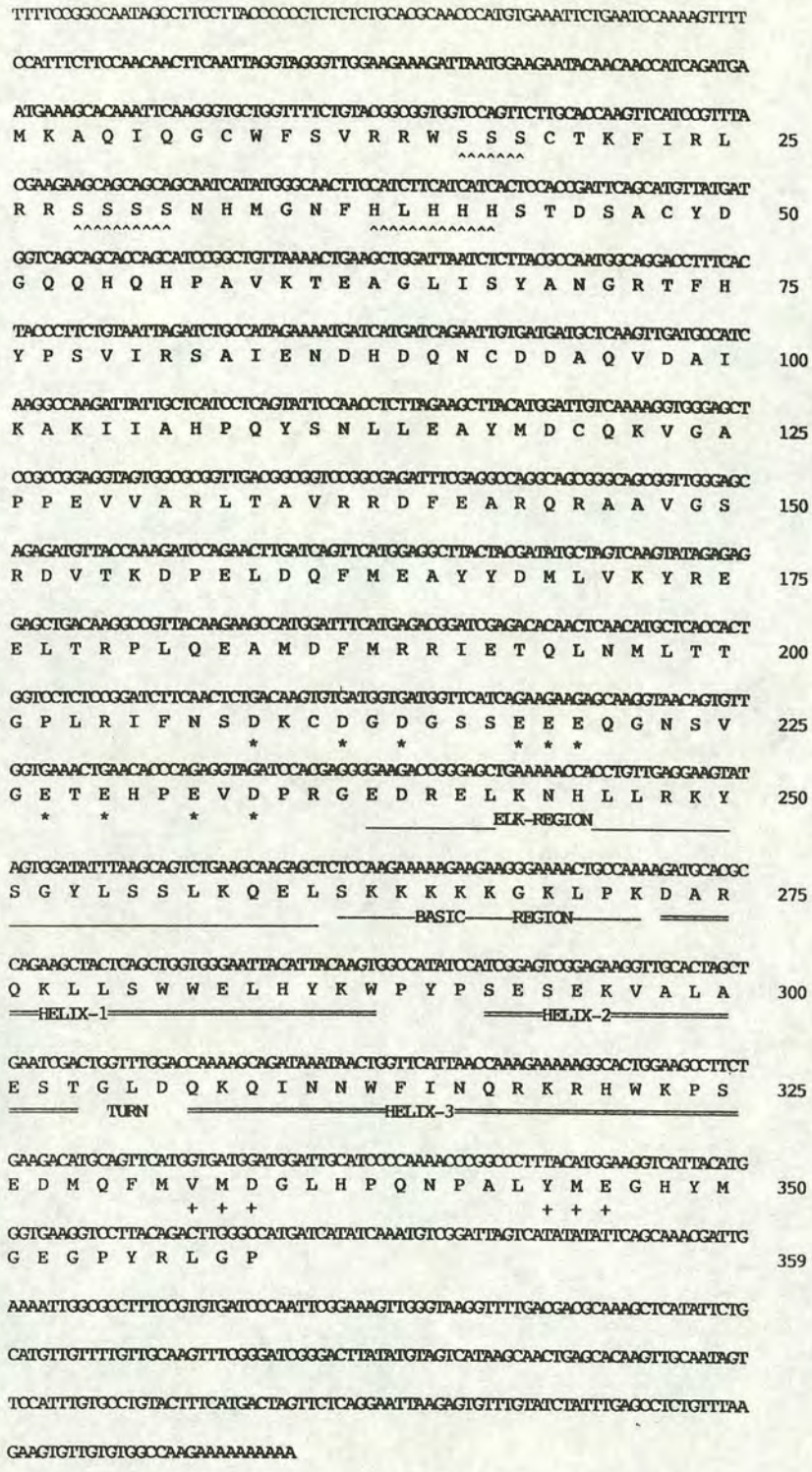

Figure 57: Nucleotide sequece of *SNAP1* cDNA and amino acid sequence of its protein product. The homeodomain with its three helices is indicated as are the ELK region and the basic region. Within the basic region lies the putative nuclear targeting signal (SKKKKKGK). Stretches of amino acids homopolymers are indicated by (^). Asterisks denote negatively charged amino acids. The amino acids of the motif V/MMD(X)7-8YMD/E are indicated with (+).

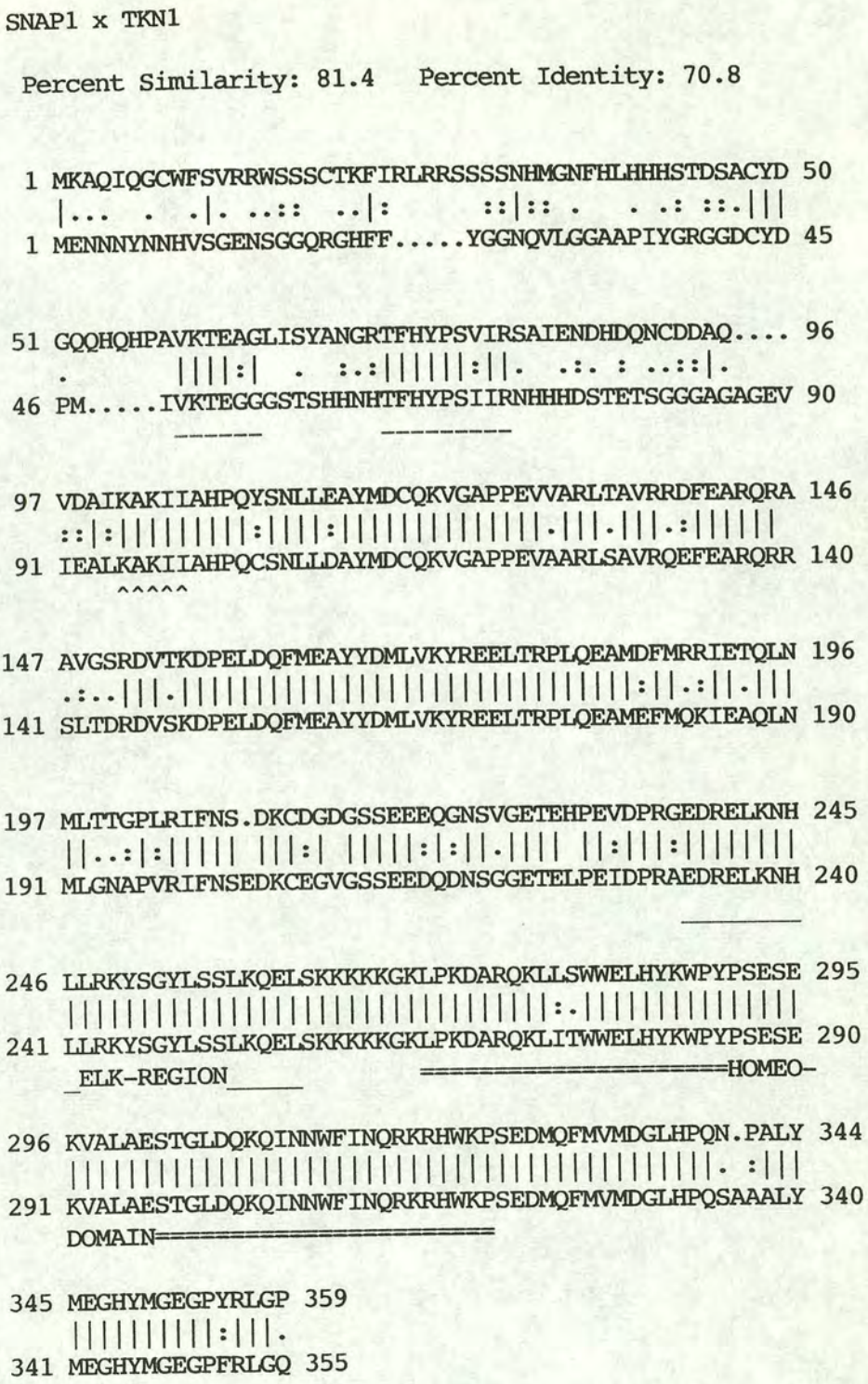

Figure 58: Pileup of SNAP1 versus TKN1. The two motifs near the N-teminus are indicated by dashes line.

3.6.3: SNAP2 structure

The *SNAP2* cDNA is 1844 bp long and encodes for a protein of 433 amino acids (Fig. 59). SNAP2 showed a low overall sequence homology when compared to SNAP1 or KN1, 28.4% and 31.2% identity respectively. The HD, including the basic region, shows 54% homology to SNAP1 or KN1 HDs (Table 7). In helix 3 of the HD, 13 amino acids are completely conserved. The main differences in amino acid sequence of the HD are localised in helix 1 and 2 (Fig. 62). SNAP2 contains the ELK motif, but has only one leucine residue, whereas three of the remaining four leucine residues found in SNAP1 are replaced by isoleucine (a similar amino acid). A cluster of negatively charged amino acids are found next to the ELK motif (Fig. 59). No clear stretches of homopolymers are found in SNAP2.

SNAP2 is found to show a high degree of sequence identity with the products of a number of HD proteins from maize (D. Jackson pers. comm.), and with *A. thaliana* (Zambryski *et al.*, in press), *Brassica napus* (Boivin *et al.*, 1994) and rice (Tamaoki *et al.*, 1995) (Table 7). Except from that of *Brassica napus*, the other homeodomain proteins contain stretches of conserved amino acids at the N-terminus.
The overall identity varies from 63.4% (SNAP2 vs BNHD1) to 71% (SNAP2 vs KNAT3 or KNAT4). From the KAEI motif (amino acid 149) towards the C-terminus, the proteins show very high sequence similarity. In the HD (excluding the basic region) the sequence homology reaches 94.5% in the case of SNAP2 HD versus the OSH45 HD from rice. As in the case of the *SNAP1* gene product, homology at the N-terminus of SNAP2 is limited to a motif of seven amino acids (NFLNLHT), conserved among these homeobox gene products (Fig. 59).

Following the classification proposed by Kerstetter and co-worker (1994), SNAP2 is a class 2 KN1-like protein. Class 2 proteins have an additional feature downstream of helix 3 of the HD: a region rich in serine (S) and/or in threonine (T). This feature is also present in SNAP2 (Fig. 59). No function has been assigned to this region.

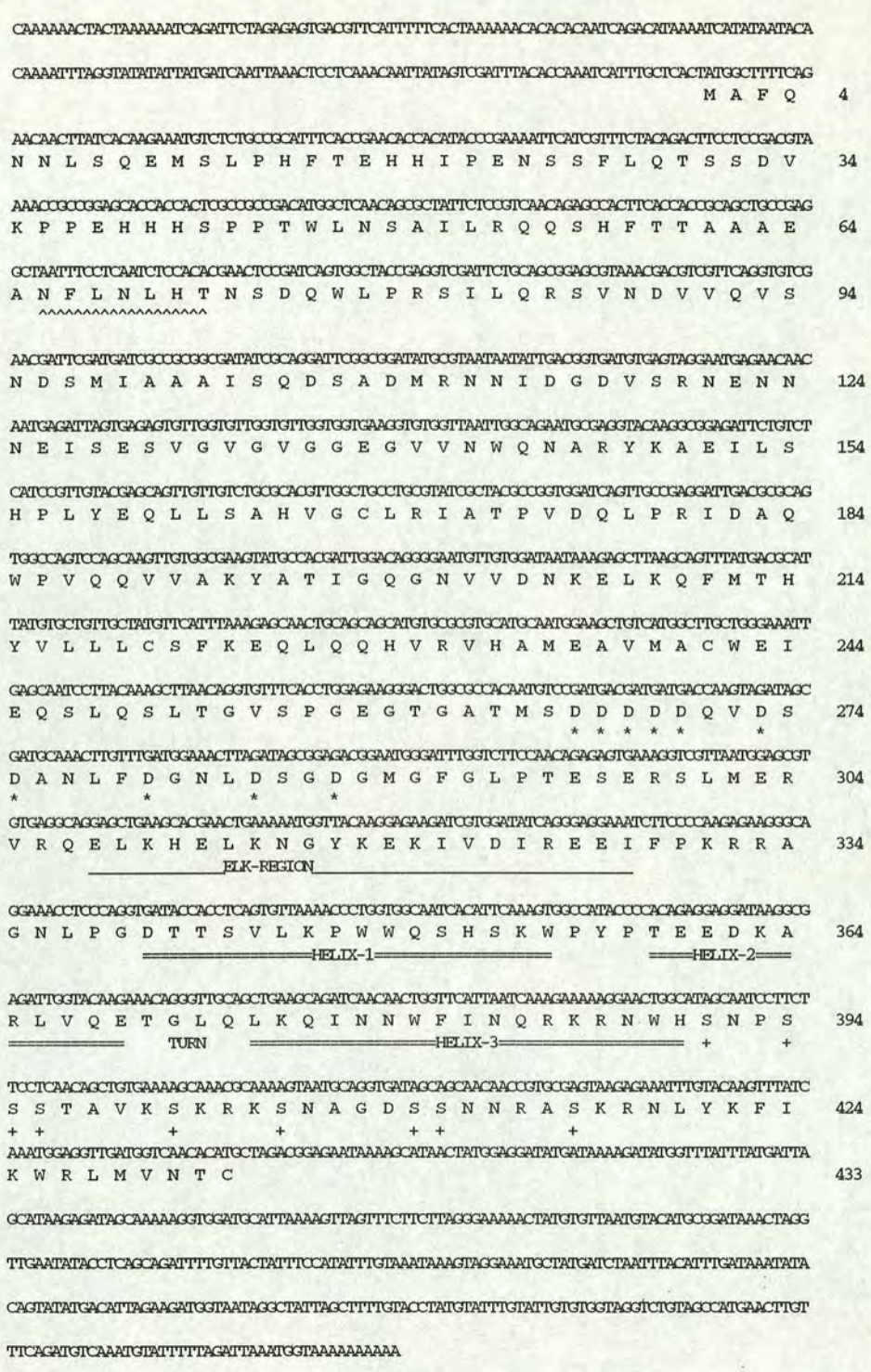

Figure 59: Nucleotide sequence of *SNAP2* cDNA and amino acid sequence of its protein product. Homeodomain, ELK region and a region rich in serine (+) are indicated. The amino acids of the motif NFLNLHT at the N-terminus of SNAP2 common to KNAT3, KNAT4, and OSH45, is indicated with the (^). Asterisks denote negatively charged amino acids.

3.6.4: SNAP3 structure

SNAP3 was the third homeobox gene isolated and characterised. Its cDNA is 1385 bp long and encodes a protein of 284 amino acids (Fig. 60). Sequence comparisons of the complete SNAP3 protein and of its homeodomain are shown in table 8. From these comparisons, SNAP3 appears to be a class 2 homeodomain protein, and results to be most similar to the product of *Brassica napus BNHD1* gene (Boivin *et al.*, 1994) (75.7% overall similarity and 87.1% in the HD) (Table 8). SNAP3 contains all the features of a homeodomain protein: the ELK region, an acidic region and short stretches of homopolymers (S, Q and G). In addition, it contains a region rich in serine (S) downstream to the HD, a feature of class 2.

3.6.5: Structure of the *R1* clone

The *R1* subclone was part of a bigger clone *R*. It was 859 bp long and showed two open reading frames interrupted by a non-coding region of 347 bp. Comparisons between *R1* and *KN1* indicated that the first open reading frame represented the putative nuclear localisation signal and helix 1, whereas the second represented helix 2, helix 3 and the C-terminus of the protein (Fig. 61). A clue to the possible identity of the 347 bp that interrupted the HD of *R1* came from the exson/intron structure of the maize *KN1*-like homeobox genes (*KNOX*). All the *KNOX* genes isolated so far have an intron in an absolutely conserved position in the homeobox near the region encoding for the N-terminal end of helix 2. The presence of an intron within the *R* subclone, together with the absence of a polyA tail and the large size of the insert in the positive phage, suggested that this consisted of a contaminating genomic fragment.

At the protein level, R1 showed 70.0% of identity to the KN1 homeodomain including the putative nuclear localisation signal and the C-terminus after the HD. The percent of identity of SNAP1 versus KN1 for the same regions was 77.0%. As a consequence it was thought that *SNAP1* was more similar to *KN1* than *R1*. At the time of the isolation of *R* clone, *STM* (Long *et al.*, 1996) had not yet been isolated. When the amino acid sequence of *STM* became available in the database, a comparison between R1 and STM revealed 88% percent of identity. This finding suggested that *R1* could be the orthologue of *STM* in *Antirrhinum majus*. However, a further characterisation of the R clone is required to prove if this is the case.

Figure 60: Nucleotide and deduced amino acid sequences of *SNAP3*. Symbols as in Figure 59.

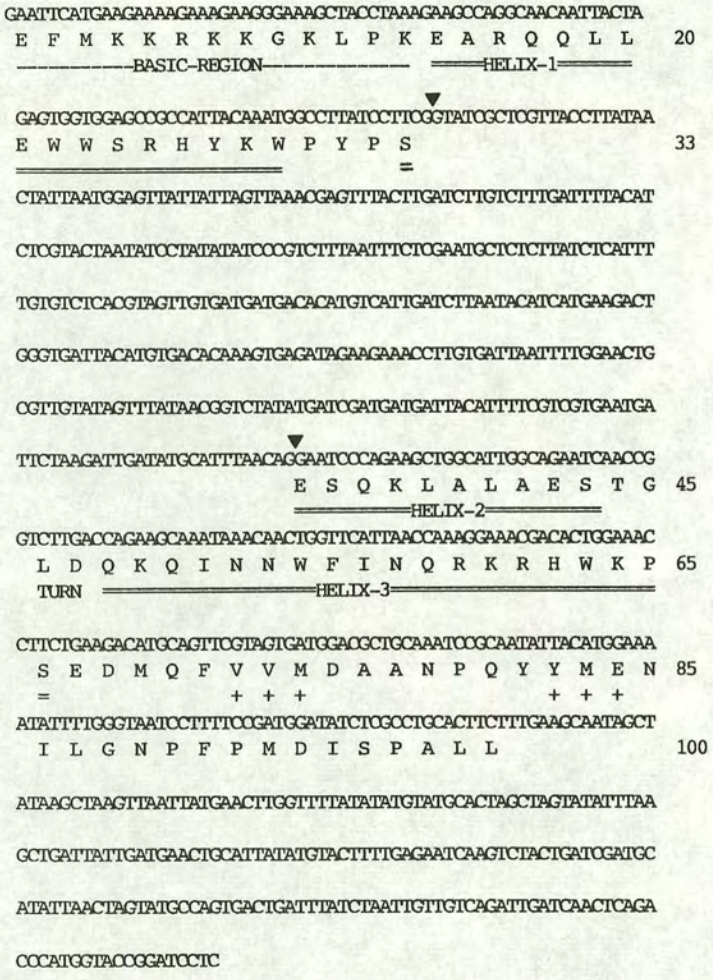

Figure 61: Nucleotide and deduced amino acid sequences of the *R1* clone. The basic region as well as the homeodomain are indicated. Triangles indicate the putative donor and acceptor splice sites.

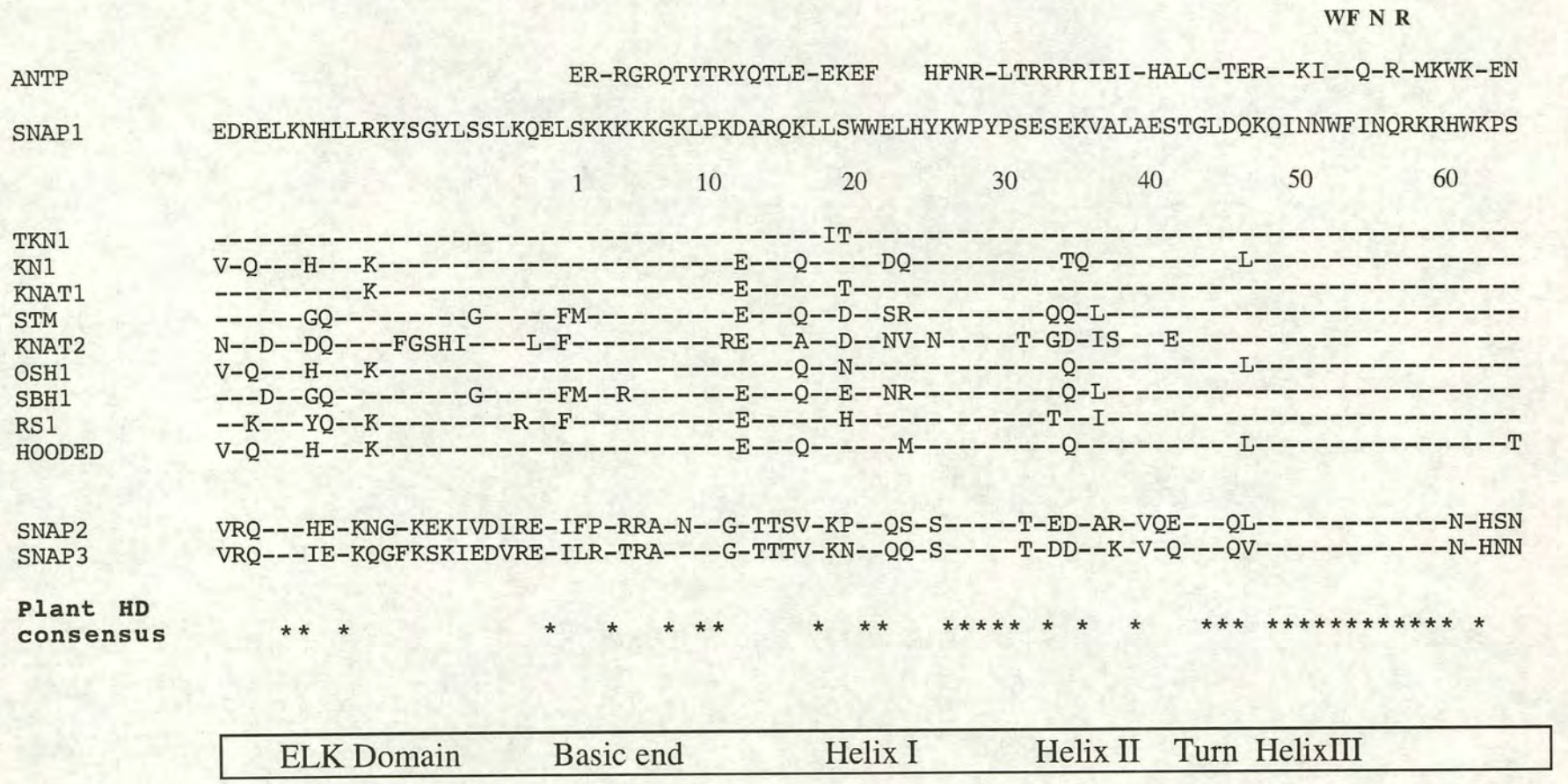

Figure 62: Pileup of several homeodomains from plants and ANTENNAPEDIA HD. The four invariant amino acids conserved among all known homeodomains are indicated. Dashed lines represent identical residues to those in SNAP1. Differences between SNAP1, 2 and 3 are mainly confined to the first two helices, whereas in helix 3 the thirteen conserved amino acids are still retained.

Table 6: Comparison of SNAP1 with other Plant Homeodomain Proteins

Organism	Protein	Class	%Overall Identity	%Identity HB
Z. mays	KN1	1	60.3	89.1
Z. mays	RS1	1	58.1	87.2
L. esculentum	TKN1	1	70.8	96.9
A. thaliana	STM	1	45.5	85.6
A. thaliana	KNAT1	1	62.8	96.9
A. thaliana	KNAT2	1	44.5	79.7
O. sativa	OSH1	1	58.5	93.7
G. max	SBH1	1	48.3	87.2
H. vulgare	HOODED	1	58.7	90.6
A. majus	R1 (clone)	1	------	87.2
A. majus	SNAP2	2	28.4	54.0
A. majus	SNAP3	2	34.5	61.3

Table 7: Comparison of SNAP2 with other Plant Homeodomain Proteins

Organism	Protein	Class	%Overall Identity	%Identity HB
A. thaliana	KNAT3	2	71.0	93.7
A. thaliana	KNAT4	2	71.0	93.7
A. thaliana	KNAT5	2	------	87.5
O. sativa	OSH45	2	64.9	94.5
B. napus	BNHD1	2	63.4	82.7
Z. mays	KNOX1	2	------	84.4
Z. mays	KNOX2	2	-------	87.5
Z. mays	KNOX6	2	-------	89.1
A. majus	SNAP3	2	61.0	79.0
A. majus	SNAP1	1	28.4	54.0
Z. mays	KN1	1	31.2	54.0

Table 8: Comparison of SNAP3 with other Plant Homeodomain Proteins

Organism	Protein	Class	%Overall Identity	%Identity HB
A. thaliana	KNAT3	2	65.9	80.5
A. thaliana	KNAT4	2	63.5	80.5
A. thaliana	KNAT5	2	-----	83.5
O. sativa	OSH45	2	63.0	75.0
B. napus	BNHD1	2	75.7	87.1
Z. mays	KNOX1	2	-----	82.2
Z. mays	KNOX2	2	-----	75.8
Z. mays	KNOX6	2	-----	80.5
A. majus	SNAP2	2	61.0	79.0
A. majus	SNAP1	1	34.5	61.3

3.7: Expression patterns of the *Antirrhinum* homeobox genes *SNAP1*, *SNAP2* and *SNAP3*

3.7.1: *SNAP1* Expression

The expression pattern of *SNAP1* mRNA was determined by in situ hybridisation to fixed tissues using a RNA probe. When the mutant phenotype is known, in situ hybridisation allows the function of the gene to be correlated to its pattern of mRNA expression. If the mutant phenotype is unknown, this technique can still contribute to understanding the function of the gene and its involvement in a biological process in WT plants.

For *SNAP1* the antisense and sense probes were synthesised from 392 bp of the 5' transcribed region. This represented the most variable part of plant *KN1*-like genes, and was therefore most likely to be an unique sequence which would avoid the possibility of cross hybridisation. The 392 bp *SNAP1* probe showed no significant homology to the corresponding region of *SNAP2* and *SNAP3*. Sense and antisense riboprobes were produced from *SNAP1* sequence cloned in opposite orientation with respect to the T7 promoter of pBluescript.

The expression pattern of *SNAP1* was analysed in median longitudinal sections of young WT vegetative meristems, axillary meristems, inflorescence meristems, and in flowers.

SNAP1 transcript was detected, using the antisense probe, in the peripheral zone of the WT vegetative SAM, in the site of initiation of a new leaf primordium (P0), and along the developing provascular tissue. Expression was also detected in provascular tissue from which the leaf trace would subsequently have been formed (Fig. 63). In contrast, the sense probe did not detect any signal in the provascular tissue or in the sides of the SAM (Fig. 63C).

If sections hybridised with the antisense probe were not perfectly median, the signal appeared to be localised throughout the SAM (66). Depending on conditions of the hybridisation (temperature, time of washing after hybridisation, salt concentration), sections hybridised with the sense probe sometimes gave a non-specific signal in the tip of the leaf or in more mature vascular tissue. To rule out the possibility that this signal represented antisense transcripts in planta, rather than background, Northern blots were performed using total RNA extracted from vegetative meristems including very young leaves. The RNA was hybridised with the same sense and antisense probes used for in situ hybridisation. The antisense probe was found to hybridise, giving an unique band,

whereas no signal was detected with the sense probe. This result indicated that the signal detected in the tip of the leaf or in more mature vascular tissue with the sense probe in some sections of WT vegetative meristems, was therefore due to non-specific hybridisation or binding of antibodies used to detect the riboprobe (Fig 63C and 65).

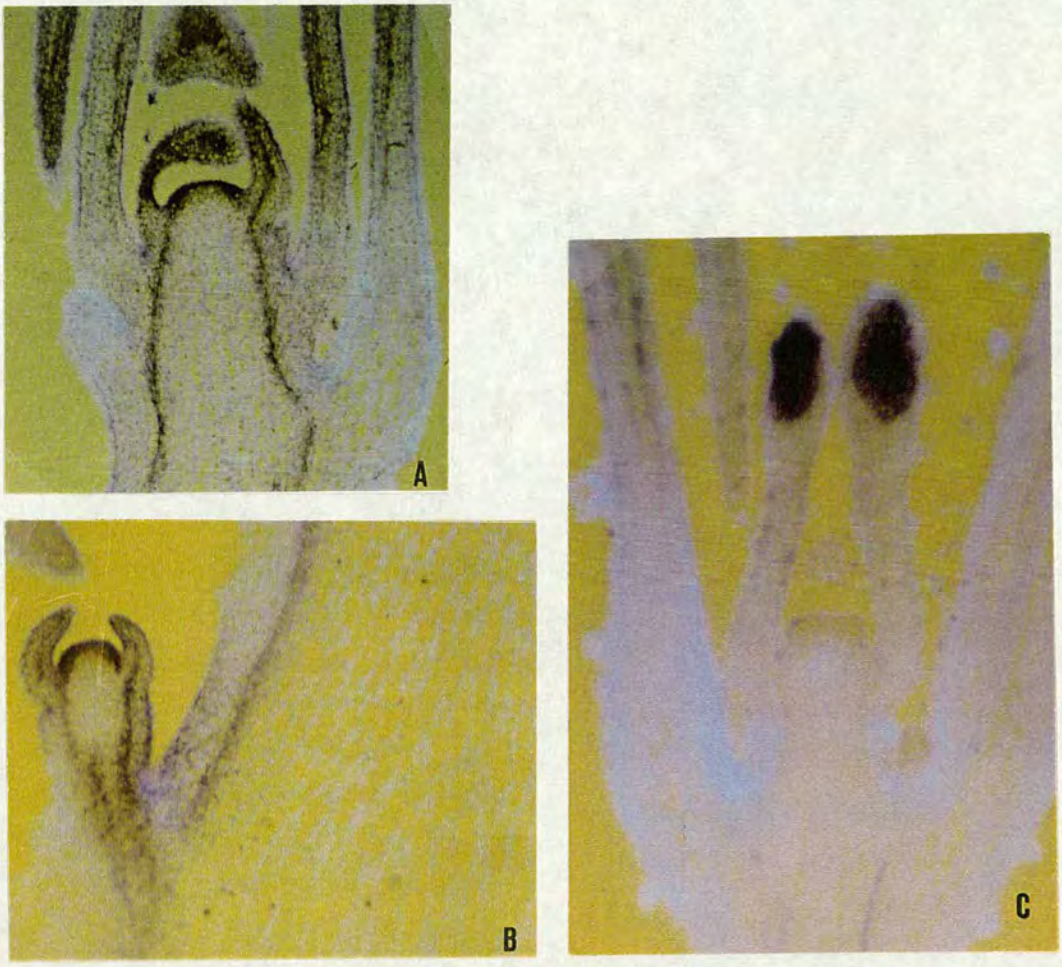

Figure 63: Expression pattern of *SNAP1* determined by in situ hybridisation, in a longitudinal section of an *A. majus* vegetative apex (A) and an axillary meristem (B).
A: *SNAP1* antisense riboprobe; expression was found to be localised in the site of initiation of new leaf primordia, along the developing provascular tissue and in the leaf trace. *SNAP1* expression was maintained until P4. B: the expression pattern in the axillary meristem is identical to that found in the vegetative apex (X23). No expression was detected in the central and rib zones of the SAM or in the cortex. C: using a *SNAP1* sense riboprobe no signal was detected in any part of an *Antirrhinum* vegetative apex. The signal at the tip of the two leaf primordia must be considered non-specific (X23) (see text).

In the inflorescence meristem, expression of *SNAP1* was similar to that in the vegetative meristem. *SNAP1* expression was confined to the peripheral zone of the inflorescence apex, where floral primordia would arise, and along the provascular tissue. The expression is maintained quite late until plastochron 4-6 (Fig. 64). The central and rib zones of the inflorescence meristem showed no expression of *SNAP1*. Similarly, no expression was found in the pith region of the stem and in the protoderm layer. *SNAP1* mRNA was also localised in the provascular tissue of the developing first two floral organs (Fig. 64). It was not possible to establish whether signal was also detected in the other two whorls of the flower.

The expression pattern of *SNAP1* was similar to the expression pattern found for *TKN1* in tomato (Hareven *et al.*, 1996). *TKN1* appeared to be strongly expressed in provascular tissue as is *SNAP1*. However, *TKN1* was also detected in all layers of the apical meristem whereas *SNAP1* was not expressed in the central and rib zones of the SAM. Clearly *SNAP1* had an expression pattern different from those of *KN1* and related maize homeobox genes and from *KNAT1* and *STM* of *A. thaliana*. These hox genes are preferentially expressed in the meristems of the plant, and no expression was detected in leaf or floral organ primordia or in provascular tissue (Jackson *et al.*, 1994; Long *et al.*, 1996; Lincoln *et al.*, 1994). Whether *SNAP1* was expressed in embryos or roots was not tested..

Expression of other homeobox genes in plant vascular tissue has been reported. *ATHB8* belonging to the family of HD-Zip transcription factors from *A. thaliana* (Baima *et al.*, 1995), has an expression pattern restricted to provascular cells. Another HD-Zip gene isolated from *Lycopersicum esculentum*, (*VAHOX1*) is specifically expressed in phloem during phases of secondary growth (Tornero *et al.*, 1996).

Figure 64: Expression pattern of *SNAP1* in a longitudinal section of an inflorescence apex detected with *SNAP1* antisense riboprobe. A: expression is seen to be localised in the flanks of the inflorescence meristem, along the developing provascular tissue as well as in the provascular tissues at early and late stages of flower development. Although the level of background is quite high (B), strong signal is seen at the flanks of the inflorescence meristem, predicting the site of lateral organ initiation (X23).

3.7.2: *SNAP2* and *SNAP3* expression.

For *SNAP2*, two RNA probes were made, one consisting of the first 670 bp of the cDNA clone (encoding part of the non-conserved N-terminus), and the other from positions 649-915. Alignment of the two *SNAP2* in situ probes with *SNAP1* did not reveal any significant and extended homologies likely to result in cross hybridisation.

The *SNAP3* probe consisted of the first 350 bp of the cDNA, and again it did not show any significant homology with the other *SNAP* sequences which would have allowed cross hybridisation. Sense and antisense RNA probes for *SNAP2* and *SNAP3* were prepared as described previously for *SNAP1*. For both *SNAP2* and *SNAP3* the expression patterns were determined using median longitudinal sections of vegetative and inflorescence meristems.

Remarkably the expression of *SNAP2* and *SNAP3* mRNA appeared to be the same as that of *SNAP1*. Signals were detected in the sites of initiation of new lateral primordia and along the provascular tissue (Fig. 66, 67, 69 and 70). These results were obtained consistently, using different tissue samples and independently produced probes. It appears unlikely that even restricted sequence homologies between the probe regions in the three genes could allow cross hybridisation. However, it was not possible to investigate further this pattern of expression using other regions of these three *Antirrhinum* hox genes. The sense probes for SNAP2 and SNAP3 did not detect any signal in the provascular tissue or in the sides of the SAM (Fig. 66B, 68 and 71).

Figure 69: Expression pattern of *SNAP3* detected using an antisense riboprobe in a longitudinal section of the vegetative apex. The expression pattern is identical to those observed for *SNAP1* and *SNAP2*.

Figure 65: Control hybridisation of inflorescence apex with a *SNAP1* sense riboprobe. Signal in tracheary elements must be considered non-specific (see text)

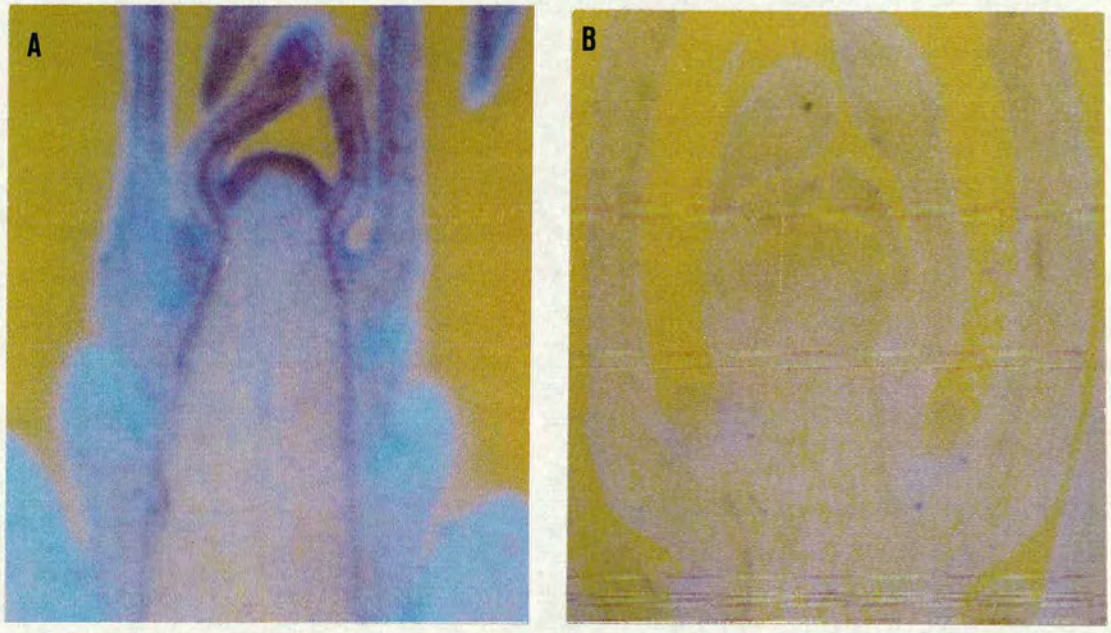

Figure 66: Expression pattern of *SNAP2* detected with an antisense riboprobe in a not perfectly median section of a vegetative apex (A). Signal appears localised throughout the SAM due to the section being non median. Signal is also visible in the leaf trace and in the provascular tissue. B: Control hybridisation of a vegetative apex with a *SNAP2* sense riboprobe.

Figure 67: Expression pattern of *SNAP2* detected with an antisense riboprobe in a longitudinal section of the inflorescence apex. The signal shows the same expression pattern as *SNAP1*.

Figure 68: Control hybridisation of the inflorescence apex with a *SNAP2* sense riboprobe.

Figure 70: Expression pattern of *SNAP3* in a longitudinal section of the inflorescence apex detected with an antisense riboprobe.

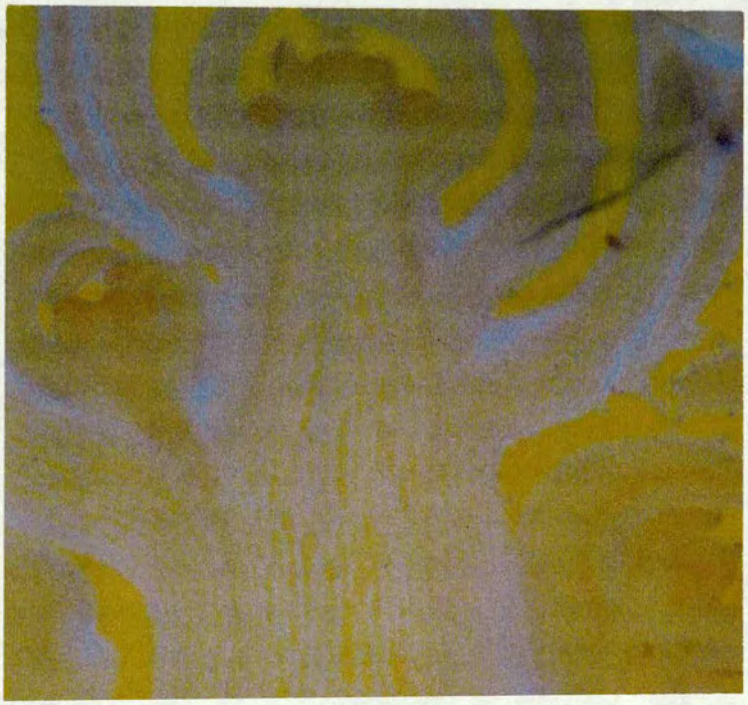

Figure 71: Control hybridisation of an inflorescence apex with a *SNAP3* sense riboprobe.

CHAPTER 4

Discussion & Conclusion

Discussion

4.1: *Antirrhinum majus*: a suitable system to study leaf development

Antirrhinum majus can be considered one of the best systems to study the development of lateral organs in dicot plants. A large number of genetic and molecular studies have been conducted using *Antirrhinum* as a model system (Coen *et al.*, 1986; Sommer *et al.*, 1988; Coen *et al.*, 1989). Mutations affecting the morphogenesis of lateral organs have been identified (Carpenter and Coen, 1990; Sommer *et al.*, 1990), and in many cases the corresponding genes responsible for these mutations have been cloned (Coen and Meyerowitz, 1991; Schwarz-Sommer *et al.*, 1992; Bradley *et al.*, 1993; Luo *et al.,* 1996). Several mutagenesis programmes conducted at the John Innes Institute in Norwich have led to the identification of new mutants with altered developmental patterns. In addition, a vast collection of leaf-shape mutants already exists which allows research on fundamental questions about the control of leaf morphogenesis. For these and other reasons mentioned earlier in this thesis, *Antirrhinum* appears to be a suitable system to study the morphogenesis of leaves and lateral organs.

4.2: The characterised leaf-shape mutants help to dissect leaf development.

In this project, nine new leaf-shape mutants were recovered by screening a plant population carrying active transposons. A further five mutants, *Gram*^{const}, *Gram*^{mut}, *hirzina*, *latifolia* and *phantastica*, came from the mutant collection maintained in Gatersleben, Germany. *hirzina*, *latifolia* and *phantastica* were the object of other studies whereas the remaining mutants were in part characterised in this thesis.

With the exclusion of *longilinea*, the other mutants cannot be considered true leaf-shape mutants in that they do not affect only the leaf. Pleiotropic effects were seen in almost all the mutants examined. Assuming that leaves and floral organs are homologous structures, mutations affecting the leaf might be expected to alter the shape of other lateral organs of the plant. For instance, in *Antirrhinum* plants carrying the *phan* mutation, the corolla of the flower was affected. Petal lobes were reduced to needles with cell types characteristic of the ventral part of WT petals (Waites and Hudson, 1995). On the contrary, *leunig*, a homeotic mutant of *Arabidopsis* that seems to negatively regulate *AGAMOUS* expression in the first two whorls of *Arabidopsis* flower, affected the margin of the leaf (Liu and Meyerowitz, 1995).

The final shape of a leaf is thought to be achieved through coordinated changes in the polarity and the rate of cell divisions in a group of initial cells located in the flanks of the SAM. Morphogenetical analysis of leaf-shape mutants provides a useful opportunity to study patterns of form. Many leaf-shape mutants showing alterations in the shape of the leaf have been characterised. For instance, the two tobacco leaf-shape mutants *lam1* and *fat1* (McHale, 1993) showed alterations in the length/width ratio and thickness of the lamina respectively. These alterations are thought to be caused by changes in the polarity of cell division during leaf development (McHale, 1993). In the *angustifolia* (*an*) mutant of *Arabidopsis*, the narrow feature of the leaf lamina is due to a defect in the polarity of cell elongation along the width of the lamina (Tsuge *et al.*, 1996). Similarly, the reduction in the length of the leaf observed in *rotundifolia* (*rot*) mutant of *Arabidopsis*, is thought to be a polar defect in cell elongation along the proximal/distal axis of the leaf (Tsuge *et al.*, 1996).

One of the leaf shape mutants characterised in this project, *longilinea*, appeared to shift the pattern of leaf growth in favour of that which contributed to the length of the leaf. The only pleiotropic effect of the *longilinea* mutation was on the spongy mesophyll, which appeared to be missing from areas of the lamina. A tentative explanation for this can be proposed. In WT leaves, division of spongy mesophyll cells stops before that of the other cell layers (Steven and Sussex, 1989) and this results in spongy mesophyll cells being pulled apart. The *longilinea* mutants also grew for a longer period than WT. If the increased period of growth affected only the epidermis and the palisade layers, the disruptive effect on the spongy mesophyll would be exaggerated and could perhaps account for the gaps found in this part of the mutant leaf. The higher density of palisade chloroplasts in the regions that lacked spongy mesophyll might be a reaction to compensate for the loss of photosynthetic potential in these regions.

In the *Spissifolia* mutant, the lamina and midrib were significantly thicker than in the WT. In addition the palisade cells in the lamina were not completely elongated along the dorsal/ventral axis. These findings suggest that in the *Spissifolia* mutant, cells of the developing lamina might have undergone more periclinal cell divisions. Similarly in the *asperfolia* mutant leaf, up to 4 files of palisade mesophyll cells were seen in transverse sections, indicating an alteration in the polarity of cellular divisions.

Leaf-shape mutants with these types of alterations strongly suggest that oriented division and polarity of cell expansion are critical processes for the generation of the leaf shape, where cells are considered the building blocks on which the shape of

the leaf depends. However, Sinott (1958) suggested that in the case of the shape of fruits of members of *Cucurbitaceae*, there existed genes that determined the shape directly, and that did not act by controlling polarity of cell division and expansion.

In the case of leaves, this view is supported by the characterisation of the *tangled1* (*tan1*) mutant of maize (Smith *et al.*, 1996). In the leaf of *tan1* mutants, longitudinal cell divisions that would contribute to the widening of the blade are substituted by aberrantly oriented cell divisions. Nevertheless, the length/width ratio of the blade in *tan1* mutants is the same as the WT at the same developmental stage, and a mature *tan1* leaf has virtually the same shape as the WT leaf. These observations demonstrate that the generation of the final shape, at least in the maize leaf, does not strictly depend on the polarity of cell division. Moreover they imply that the final shape of a lateral organ is established by means of spatial control of growth at the regional level independent of the polarity of cell divisions. In other words, cells in a developing leaf might respond to a morphogenetic field which dictates the final shape regardless of their division orientations (Smith *et al.*, 1996).

Although the nature of the morphogenetic signals that determine the shape of a leaf is still unknown, regional identities or domains within the leaf exist, as demonstrated by mutations which disrupt these domains (Freeling, 1992; Smith and Hake, 1993; Waites and Hudson 1995; Scalon *et al.*, 1996). Such a disruptive function may be ascribed to the *Graminifolia* (*Gram*) mutation.

4.3: *Gram* mutation alters regional identities within the phytomer unit

In the leaf of *Gram* mutant plants, the reduced number of ventral epidermal cells across the lamina appeared to indicate reduced cellular divisions along the lateral axis, which would account for the narrowness of the leaf. However, the morphological alterations observed within the phytomer of *Gram* mutant plants, suggest that the *Gram* mutation altered developmental patterns. These alterations are:

1. a stripe of dorsal epidermal cells along the ventral margin;
2. an alteration of the node-internode, with consequent alteration of the phyllotaxis;
3. hairs along the margins of the mutant leaf;
4. the formation of ectopic shoots at the margin of the leaf lamina.

It is difficult to explain these morphological alterations without knowing the nature of the *GRAM* gene. However, an attempt is made here which can account for at least some of the alterations seen in *Gram* mutant plants.

One of the major features of *Gram* mutant leaf is its narrowness. In mutants of other species, narrowness may result from loss of lateral cell proliferation (e.g. in the *lam* mutant of tobacco, McHale, 1993), which may correspond to loss of a lateral domain of the leaf. For example, leaves of maize plants homozygous for the recessive mutation at the *narrow sheath* (*ns*) locus have a narrow blade and sheath. The narrow feature of the *ns* leaf is due to loss of the marginal leaf domain (Scalon *et al.*, 1996). Similarly, *Gram* mutant phenotype could be interpreted as suggesting that *GRAM* is required for laminal lateral proliferation. However, another possibility consistent with the semi-dominant behaviour of *Gram* mutant alleles, is that the mutation involves gains-of-function which alters developmental pattern early in leaf development and hence gives rise to narrow leaves. A number of dominant gain-of-function mutations at maize loci, *KN1*, *RS1* and *LG3* give rise to ectopic expression of the genes in developing leaves and result in the distal displacement of proximal characteristics (e.g. transformation of blade into sheath tissue). In the case of the *Gram* mutant alleles, many of the aspects of the mutant phenotype can be interpreted as a shift in the positional identity. The production of ectopic shoots from the margins of the mutant leaves is a characteristic of the nodes of wild-type plants and compatible with a proximal to distal shift of identity. Similar phenotype is produced by the expression of *KN1*, which is usually confined to the meristem, in leaves of transgenic tobacco plants (Sinha *et al.*, 1993). Similarly, production of hairs from the margin of *Gram* mutant leaves can be considered stem hair misexpression. The narrowness of *Gram* mutant leaves is also compatible with a shift of the petiole-like character more distally. However, one aspect of the *Gram* mutant phenotype - the stripe of dorsal cells in the ventral margins of the leaf - is more difficult to explain because it suggests a dorso-ventral shift in identity. It has been postulated that the *PHANTASTICA* gene is required for dorsal cell identity and that interaction between cells with dorsal and ventral identities leads to lateral proliferation of the lamina at the boundary. In *phan* mutant leaves, as in wild-type, the boundary between dorsal and ventral cell types corresponds to the edge of a leaf blade. This is not the case in the *Gram* mutants, where the boundary between dorsal and ventral cells is shifted from the leaf edge, and identity therefore appears to have been uncoupled from proliferation. This would be consistent with a role of *GRAM* downstream of *PHAN* in the determination of dorso-ventral cell types, but not lateral proliferation. However, *Gram/phan* double mutants show a novel

phenotype, in which *phan* is not epistatic to *Gram*, suggesting that *PHAN* does not regulate *GRAM*, but that the two genes function independently.

On the base of these observations, it could be hypothesised that *Gram* is a gain-of-function mutation in a *KNOTTED1*-like gene.

However, a further possible explanation can be given for the phenotype of *Gram* mutation. One could be that the *GRAM* gene is responsible for setting a boundary between the SAM and the founder cells of a lateral primordium. Loss of *GRAM* function may lead to the alteration of this hypothetical boundary with the consequent misexpression of meristem-specific genes in domains of leaf primordia. Similarly to *no apical meristem* mutation of petunia (Souer *et al.*, 1996), in *Gram/phan* double mutant the primary SAM fails to develop. *NAM* mRNA accumulates in a stripe forming a ring which surrounds the site of initiation of lateral organs.

Of course, the future cloning of *GRAM* gene will be of great help in the understanding its function.

4.4: Homeobox genes

The homeobox (HB), a 180 bp DNA sequence, was first identified as a region of similarity in sequence of genes involved in the control of *Drosophila* development (McGinnis *et al.*, 1984; Scott and Weiner, 1984). The homeobox (HB) constitutes a highly conserved part of the protein coding region of this family of genes, and the corresponding 60 amino acids have been named the homeodomain (HD).

The homeobox genes of *Drosophila* include homeotic genes that control segmental differentiation (McGinnis *et al.*, 1984), segmentation genes that control the division of the embryo into segments and in some cases control other homeotic genes (Laughon and Scott, 1984), genes that control dorsal/ventral differentiation (Rushlow *et al.*, 1987), genes that act maternally to control anterior-posterior polarity of the embryo (Struhl *et al.*, 1989), and many other genes involved in other developmental mechanisms (Scott *et al.*, 1989).

Following the identification of *Drosophila* homeobox genes, closely related hox-genes were found in many higher eukaryotic organisms in the animal kingdom including humans (Boncinelli *et al.*, 1988), and in the plant kingdom (Ruberti *et al.*, 1991; Vollbrecht *et al.*, 1991).

Molecular analysis of the *Drosophila* homeodomain proteins based on sequence similarities with prokaryotic DNA-binding proteins (Pabo and Sauer, 1984), and with the two yeast mating-type proteins *MAT a1* and *MAT α2* (Shepherd *et al.*, 1984),

suggested that the structure of the HD includes a helix-turn-helix motif involved in sequence-specific DNA binding. This hypothesis was directly confirmed by the determination of the three dimensional structure of ANTENNAPEDIA (ANTP) protein by nuclear magnetic resonance (Qian *et al.*, 1989). The HD of ANTP contains four α-helices. The crucial helix-turn-helix motif is located in helices two and three. It is the third helix which makes a direct contact with the DNA, fitting in the major groove (Otting *et al.*, 1990; Kissinger *et al.*, 1990).

4.5: Considerations of the amino acid structure of SNAP1

The SNAP1 homeodomain protein has high sequence homology with a number of class 1 plant homeodomain proteins. The SNAP1 HD contains the four invariant amino acids (WF-N-R). Within the SNAP1 helix 3 ("the recognition helix"), 13 consecutive amino acids are completely conserved among SNAP1 and many of KN1-like proteins isolated so far (Fig. 61). Structural studies conducted with ANTENNAPEDIA and ENGRAILED HDs have identified the key residues (Q50, R53 and M54) in helix 3 that contact specific bases in the major groove of the binding site (Gehring *et al.*, 1990; Krumlauf and Gould, 1992). Moreover, swap studies have indicated that the change of amino acid 9 in helix 3 (corresponding to position 54 in plant HDs or position 50 in animal HDs) results in altered specificity of the HD proteins for the DNA binding sequence (Treisman *et al.*, 1989). All the homeobox genes isolated from plants using *KN1* as a heterologous probe, have in their corresponding proteins not only the same amino acid in position 9 of helix 3, but also 13 residues completely conserved in the same helix. It could be thought that due to the high conservation of amino acid sequence within the HD, all these proteins may bind to a common sequence motif present in their target genes.

However, the temporal and spatial expression patterns of *KN1* and related plant homeobox genes distinguish between them. In addition, gain-of-function mutations in hox genes which lead to their ectopic expression [*HOODED* from barley (Muller *et al.*, 1995), *KN1* (Vollbrecht *et al.*, 1991) and *RS1* (Schneeberger *et al.*, 1995) from maize], have different effects on the development of the plant.

Thus similarities or differences in the amino acid sequences of the HD are not sufficient to account for the specificity of action of plant homeobox genes.

KN1 has been shown to be localised in the nucleus, characteristic of a gene which is likely to be a transcription factor. Recently, transformation experiments in tobacco and transfection of onion epidermal cells with part of KN1 including the

homeobox fused to the GUS reporter gene driven by the 35-S promoter, have shown that this region is sufficient for nuclear localisation. In addition, deletion analysis revealed that the HD including the three α-helices, or the ELK region alone, can work independently as nuclear localisation signals (Meizel and Lam, 1996).

Although the N-termini of plant homeodomain proteins show common features (e.g. a stretch of homopolymers and acidic regions) they are the most variable regions of the HD proteins. For instance, the ortholog of KN1 in rice, OSH1, has an overall identity of 78.4% with KN1 (Matsouka *et al.*, 1993). OSH1 shows homology of sequence with KN1, which extends to the N-terminus region, whereas KNAT1 from *Arabidopsis* or the tomato ortholog TKN1, do not show the same extended homology. On the contrary, amino acid sequence comparison between SNAP1 and TKN1 reveals two homologous motifs in the N-terminus (from amino acid 59 to 64, and from 72 to 81) (Fig. 58). The significance of these new sequence homologies and their role in the HD proteins function and specificity is unknown.

It is only downstream of the motif KAKII (amino acid position 101 in SNAP1) (Fig. 58) common to all the plant HD proteins, that the observed sequence homologies are significant. Stretches of homopolymers are found in KN1-like proteins, although the amino acid making up the stretch and the position of the stretch within the N-terminus is variable. However, three HD proteins KN1, OSH1 and HOODED represent one class where the homology extends upstream of the KAKII motif into the most variable region (data not shown). The stretches of homopolymers are in the same position having almost identical amino acid composition. An additional similarity is seen in parts of the N-terminus which have unknown function. The HD proteins STM (Long *et al.*, 1996) and SBH1 (*Glycine max*) (Ma *et al.*, 1994) are exceptional in showing similarity to the very end of the N-terminus. It will be interesting to see if R1 will also show a similar feature. SNAP1 and TKN1 have sequence homologies at the N-terminus, between amino acids 59 and 82 (Fig. 58). A database search using the consensus similarity for this part of SNAP1 and TKN1 was performed. No plausible homology was found with any protein in the database.

The function of the N-terminus of HD proteins remains obscure. The N-terminus may be responsible for the movement of the HD proteins from cell to cell, or contribute to the specificity of the HD by interaction with specific accessory proteins. Lucas and co-workers (1995) have shown that KN1 can move from one cell to another via plasmodesmata, but no clear result has yet been obtained as to which part of the KN1 protein is responsible for the apparent increase of plasmodesmal size exclusion limit.

From studies carried out in yeast and *Drosophila*, a continuous flux of data indicates that proteins containing a homeodomain can act in a cooperative manner through interaction either with the same HD protein or with other accessory factors (Baxter *et al.*, 1994; Ho *et al.*, 1994; Bertuccioli *et al.*, 1996; Jun and Desplan, 1996; Ma *et al.*, 1996; Mann and Chan, 1996: Mead *et al.*, 1996). Recently it has been shown that another important class of transcription factor, the *MADS-box* genes, involved in the specification of floral organ identity, act in a cooperative manner through the formation of heterodimers (Davies *et al.*, 1996). Thus protein-protein interaction appears necessary to create protein/DNA complexes of high binding specificity required for transcription factors to exert their action.

Similar considerations apply to SNAP2 and SNAP3 proteins. SNAP2 and 3 show similarities to several class 2 KN1-like proteins and helix-1 and 2 of their HDs show the main difference in amino acids sequence compared to class 1 of the plant homeodomain protein.

4.6: Expression pattern of *Antirrhinum* homeobox genes: a novel pattern of expression

The absence of mutant phenotypes for the three new homeobox genes isolated from *Antirrhinum*, makes it difficult to understand their roles in development. In general it is possible to say that the domains of function of plant transcription factors are contained within their domains of expression. For instance *DEFICIENS* and *GLOBOSA* mRNA are expressed in the second and third whorls of the *Antirrhinum* flower, where they exert their function (Schwarz-Sommer *et al.*, 1992; Trobner *et al.*, 1992), or *APETALA1* of *A. thaliana* which is expressed in all four flower whorls but is functional only in the first and second whorls (Mandel *et al.*, 1992; Bowman *et al.*, 1993). Thus, indications of the function of the three hox genes from *Antirrhinum* could be extrapolated from mRNA expression data. However, *KN1* represents an exception because although its mRNA is not expressed in the L1 layer, its protein is present in it. Therefore mRNA expression data for hox genes must be treated with caution when interpreting possible functions.

In order to facilitate the data interpretation and hypothesise a possible role of the *SNAP* genes, descriptions of the domains of expression of some of the best characterised plant homeobox genes will be given briefly.

KN1 was the first hox gene isolated from plants (Hake *et al.*, 1989). The *KN1* maize mutants show abnormalities in the leaf. Proliferation of epidermal cells of the leaf form knots located along lateral veins. Ectopic ligule fringes are also formed (Freeling and Hake, 1985; Sinha and Hake, 1990). *KN1* is a dominant mutation which leads to a gain-of-function, and the lack of a recessive phenotype has made it difficult to establish the function of the wild-type *KN1* gene. On the basis of the expression of KN1, which is confined to the SAM of wild-type plants (Smith *et al.*, 1992; Jackson *et al.*, 1994), and the transformation experiment in tobacco plants (Sinha *et al.*, 1993), it was postulated that *KN1* has a role in maintaining the cells in the SAM in an undifferentiated state. Interestingly, *KN1* and its protein were not expressed in the site of initiation of an incipient leaf primordium, leading to the hypothesis that the down regulation of *KN1* in the flanks of the SAM is a signal for the formation of a new lateral organ (Fig.). *KN1* mRNA is not expressed in provascular cells associated with developing lateral vein traces in the shoot apex (Fig. 72) (Jackson *et al.*, 1994). The initiation of these lateral veins within the meristem was accompanied by the down regulation of *KN1* until plastochron 4. However, as lateral veins developed, a ring of cells encircling the lateral veins expressing *KN1* becomes discernible, just below the 9th leaf (Smith *et al.*, 1992). Mature vascular bundles did not express *KN1*.

More recently a similar hox gene, *SHOOT MERISTEMLESS* (*STM*), has been cloned from *A. thaliana*. Plants homozygous for a recessive mutation at the *STM* locus, failed to develop a SAM (Barton and Poethig, 1993). Since gain-of-function and loss-of-function often result in opposite phenotype, it was hypothesised that *STM* mutation was a result of loss-of-function in an *Arabidopsis KN1*-like gene. The cloning confirmed that this was the case (Long *et al.*, 1996). The *STM* mRNA expression pattern was found to be very similar to that of *KN1* with only one difference. *STM* mRNA was detected in the L1 layer of the *Arabidopsis* SAM (Fig. 72) (Long *et al.*, 1996).

Other hox genes have been well characterised but their mutant phenotypes are unknown. *KNAT1* from *Arabidopsis* showed a different expression pattern to *STM*. Expression was concentrated in the peripheral and rib zones of the SAM. However, high levels of transcript were also seen below the meristem in the subapical region where widening takes place. Expression extended to the base of developing leaf primordia and was detected in the cortex. After the plant underwent the transition to inflorescence meristem, the expression of *KNAT1* transcript was restricted to the cortex of the primary inflorescence. *KNAT1* was not expressed in provascular tissue at any stage of *Arabidopsis* development (Fig. 73) (Lincoln *et al.*, 1994).

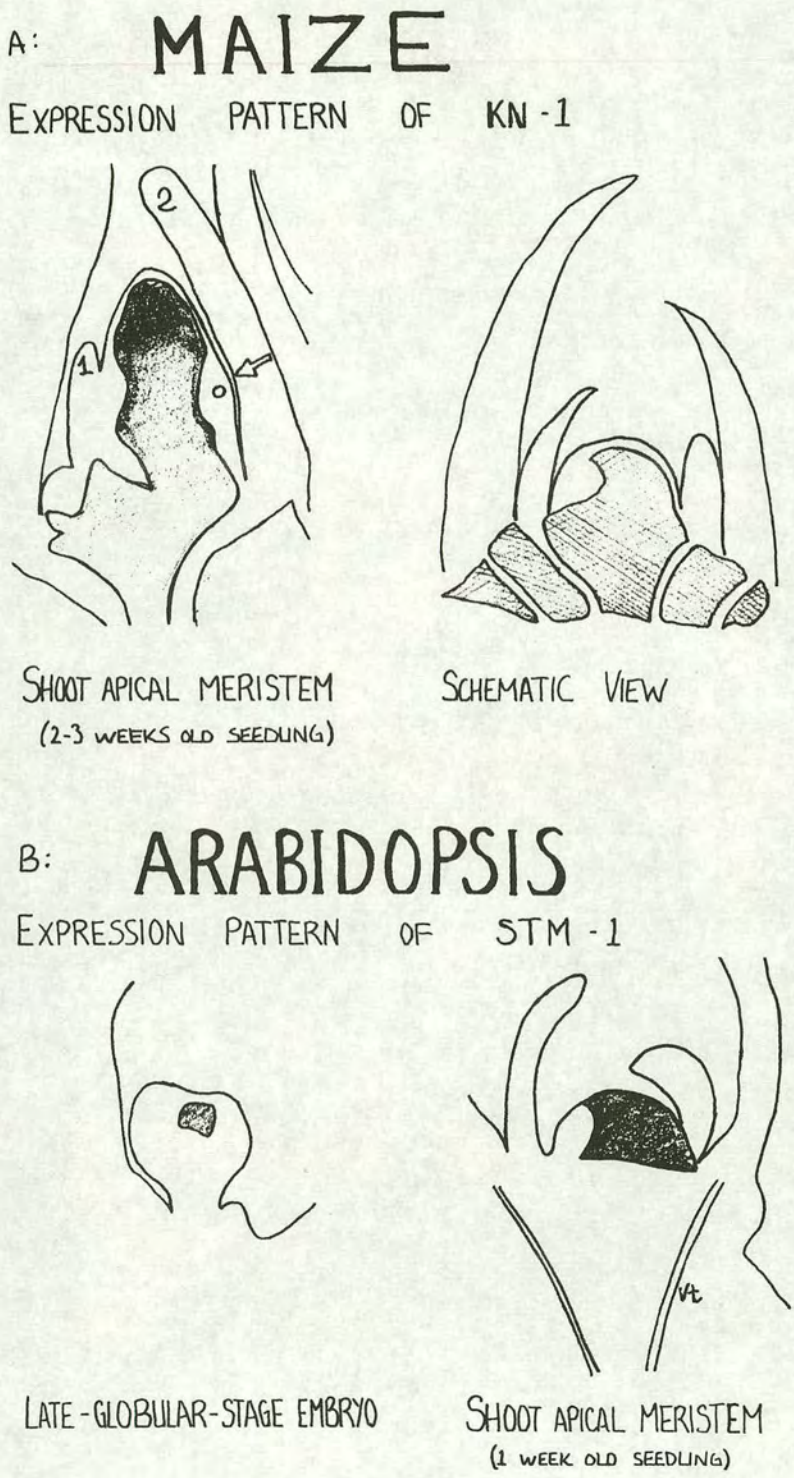

Figure 72: (A) The arrow indicates the site of initiation of a new maize leaf primordium. (B) vt indicates the vascular tissues. The shadowed areas in both (A) and (B) represent the regions of gene expression.

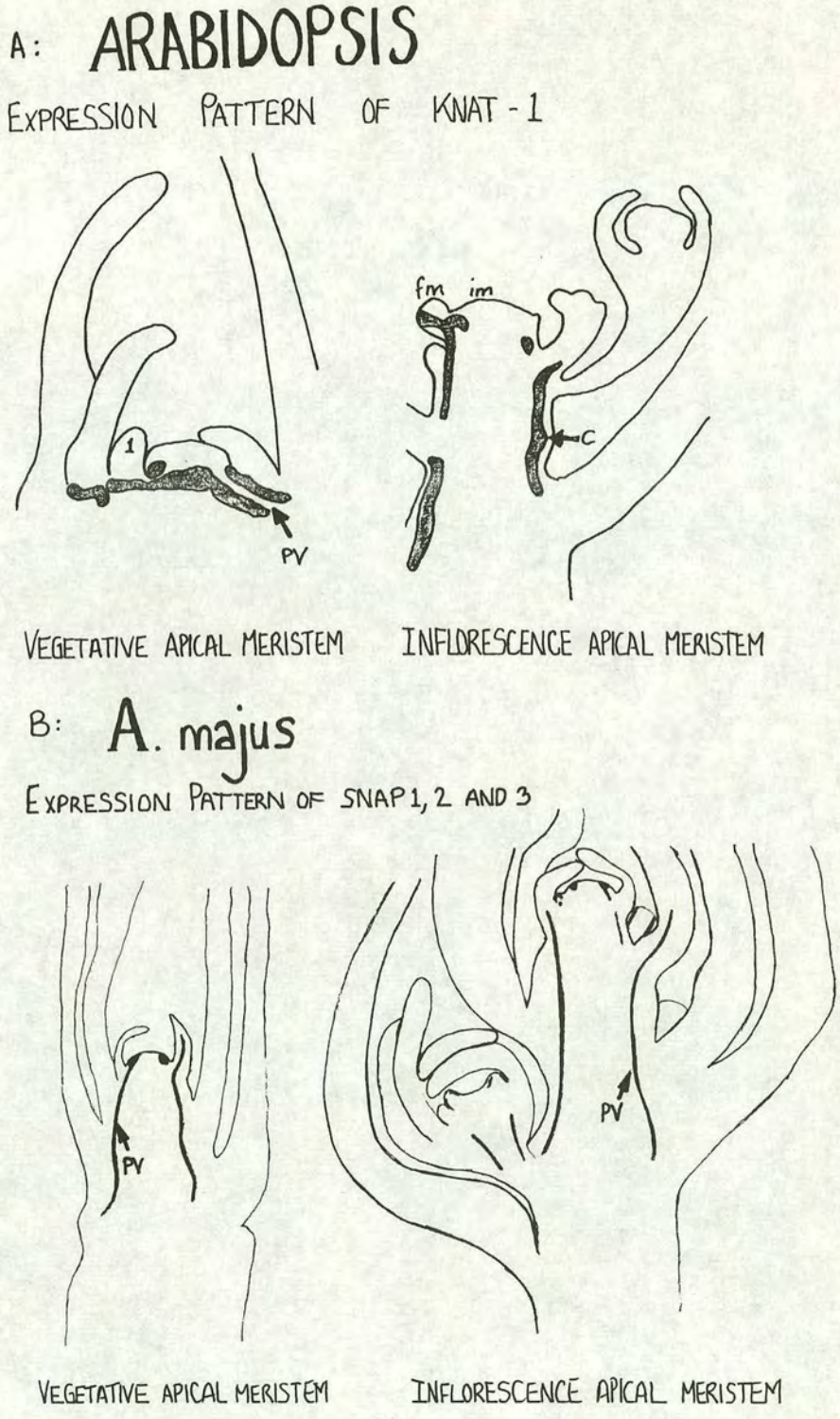

Figure 73: (A) c indicates the cortex, pv the provascular tissues, fm the floral meristem and im the inflorescence meristem. (B) pv indicates the provascular tissues. The shaded areas in both (A) and (B) represent the regions of gene expression.

KN1, *STM* and *KNAT1* define different domains of the SAM. Other *KN1*-like genes in maize, *RS1*, *KNOX3* and *KNOX8*, define domains within the zones of the meristem which give rise to the different parts of the phytomer unit (Jackson *et al.*, 1994).

The three homeobox genes from *Antirrhinum* clearly define a new domain of expression, distinct from that of the other plant HB genes. *SNAP1*, *2* and *3* mRNAs are expressed along the developing provascular tissue. Class 1 plant HB genes are generally characterised by the absence of expression in lateral organs, and they define genes with meristematic function. Based on sequence similarities, *SNAP1* can be assigned to class 1. However, *SNAP1* mRNA was found to be expressed in the site of initiation of primordia. A similar pattern of expression was reported for the class 1 HB gene *TKN1,* from tomato (Hareven *et al.*, 1996). *TKN1* was found to be expressed throughout the SAM of tomato plants (Hareven *et al.*, 1996), whereas *SNAP1* expression is absent in the rib and central zones of *Antirrhinum* SAM. *TKN1* and *SNAP1* therefore show expression patterns distinct from other class 1 genes.

Hareven and co-workers (1996) have hypothesised that the expression of *TKN1* reflects the compound architecture of tomato leaves compared with the simple leaves of *Antirrhinum*, *Arabidopsis* or maize. They overexpressed *KN1* in WT tomato plant, and found an increase of compoundness of the leaf. In other experiments, the same authors overexpressed *KN1* in several tomato leaf-shape mutants which have simple leaves with entire margins or leaves with reduced numbers of lateral leaflets (Mathan and Cole, 1964; Caruso, 1968). They found that *KN1* misexpression did not induce the compoundness of leaves observed for the WT tomato plant or in *petroselinum* mutant plants which show a similar phenotype to that produced by *KN1* overexpression (Hareven *et al.*, 1996). From these results they suggested that differences between compound and simple leaves are the result of differential meristematic activities within the leaf primordium.

However, it could be argued that compound leaves and simple lobed leaves are not fundamentally different, and there is evidence to support this view. For instance, overexpression of *KN1* or *KN1*-like genes in *Arabidopsis* and tobacco induced formation of lobed leaves, which also had shoot-like characteristics (Sinha *et al.*, 1993; Jackson, 1996), or the formation of ectopic stipules in *Arabidopsis* leaves (Chuck *et al.*, 1996). Alternatively the overexpression of *KN1* in WT tomato plant might dramatically alter the steady-state levels of other homeobox genes expressed during tomato leaf development, leading to the super-compound leaf phenotype indirectly.

In the library screening performed in this project to identify *KN1*-like genes, 29 clones where found to hybridise with *KN1* cDNA probe. Although not all 29 clones represented different genes, from the restriction analysis of these 29 clones (data not shown) and from of RT-PCR experiment performed using mRNA from vegetative shoots (I. R. Oliver pers. comm.), at least a dozen different *KN1*-like genes are present in *Antirrhinum* majus genome. The *R1* clone is a class 1 hox gene with a very high amino acids sequence similarity to STM. This clearly indicates that other homeobox genes are present in the genome of *Antirrhinum majus* and they could define other domains of the phytomer, whereas *SNAP1*, *SNAP2* and *SNAP3* may be required for the determination of vascular tissue. Since a leaf always has a strand of vascular tissue associated with it, expression of *Antirrhinum SNAP* genes in the site of primordia initiation is consistent with this view.

Other *KN1*-like homeobox genes (*KNAT3*, *KNAT4*, and *KNAT5*) have been isolated from *Arabidopsis thaliana* by means of sequence similarity (Zambryski *et al.*, 1997 in press). All three genes belong to class 2, like *SNAP2* and *SNAP3*. The expression pattern of *KNAT3* suggests that it has a more general role in development than class 1 genes. *KNAT3* expression was detected in cotyledons, hypocotyl and root three days after germination. Six days after germination the expression of *KNAT3* took on a pattern which remained constant through the rest of the vegetative phase of development. *KNAT3* expression was excluded from the meristem and appeared in leaf primordia longer that 250 μm in the vascular tissue of the leaf lamina and of the petiole (A. M. Laborda pers. comm.).

If the number of events that must occur in the SAM in order to set the pattern for formation and differentiation of the vascular system is considered, it is not surprising that the three *Antirrhinum* homeobox genes have been found to have the same expression pattern. It has already been mentioned that one possible way for homeodomain proteins to achieve their specificity is by cooperation with other proteins of the same family, or with members of a different gene family (Mann and Chan 1996; Davies *et al.*, 1996). The similarity of expression patterns of the three *SNAP* genes suggest that they may encode interacting proteins.

Homeobox genes containing a leucine-zipper motif have been cloned from *A. thaliana* (Baima *et al.*, 1995) and tomato (Tornero *et al.*, 1996) and their transcripts seen to be localised in vascular tissue. *ATHB8* from *A. thaliana* is expressed in provascular tissue and its expression is modulated by auxin (Baima *et al.*, 1995). *VAHOX1* from tomato is expressed during the secondary phases of vascular development. Auxin is known to be an inducer of vascular development (Sach, 1991) and leaf primordia is a

source of auxin, suggesting that primordia might induce vascular cell fate via genes such as *ATHB8*. In the case of the SNAP genes, expression is detected in lateral organ initials prior to primordial emergence, and in vascular initials, suggesting that these genes may have similar roles in vascular cell fate. However, in absence of mutant phenotypes, it is difficult to determine whether the *SNAP* genes might act upstream or downstream of hormone signalling. Another *A. thaliana* homeobox gene *GLABRA* (*GL2*) involved in the specification of hairless root epidermal cell type, has been shown to act early, upstream of hormones (Masucci and Schiefelbein, 1996). On the other hand, a HB-leucine zipper gene from *Arabidopsis*, *ATHB7* has been shown to be induced by water deficit and by abscisic acid (ABA) (Soderman *et al.*, 1996). Therefore, no generalisation can be made about the relationships between homeobox genes and hormone signalling.

One important difference that emerges from the expression pattern of *Antirrhinum* HB genes, is that not necessarily all the homeobox genes are involved in processes which maintain cells in an undifferentiated state. This may be true for genes like *KN1* or *STM*, but in the case of HB genes like *GL2* (Rerie *et al.*, 1994) or *BELL* (*BEL1*) (Reiser *et al.*, 1995) different functions have been assigned. For instance, plants homozygous for *bell* mutation show loss of the ovule integument, which is replaced by disorganised collar tissue (Modrusan *et al.*, 1994). *BEL1* is expressed only in the ovules in a region that will give rise to the integument (Reiser *et el.*, 1995), and at least part of its function appears to be the repression of *AGAMOUS* expression in integuments and ovules (Ray *et al.*, 1994). Similarly, *SNAP1*, *SNAP2* and *SNAP3* could specify a region of the meristem which is determined to became a specialised tissue.

Vascular tissue or its precursor may have a role in organising subsequent development of the leaf. Sharman's studies on maize leaf development (1942) indicated that the midvein is specified first and thus could send signals which might promote leaf initiation. Cerioli and co-workers (1994), showed that epidermal cells between the veins of the maize leaf behave as clonal compartments, or modules. Although this idea that provascular strands may act as inducers is only a speculation, the isolation and characterisation of the expression pattern of *SNAP1*, *SNAP2* and *SNAP3* could be an important starting point to test this hypothesis. The isolation of plants carrying mutations for these three *Antirrhinum* HB genes, based on reverse PCR screening (Krysan *et al.*, 1996), will greatly help the understanding of the involvement of vascular tissue in the making of lateral organs such as leaves.

References

Almeida, J., Carpenter, R., Robbins, T. C., Martin, C. and Coen E. S. (1989). Genetic interactions underlying flower patterns in *Antirrhinum majus*. Genes and Dev. **3:** 1758-1767.

Amos, A. L. and Bradshaw Amos, W. (1991). Properties of tubulin. In Molecules of the Cytoskeleton. Eds. MacMillan New York. 117-141.

Avery, G. S. (1933). Structure and development of tobacco leaf. Am. J. Bot. **20:** 565-592.

Baima, S., Nobili, F., Sessa, G., Lucchetti, S., Ruberti, I. and Morelli, G. (1995). The expression of *Athb-8* homeobox gene is restricted to provascular cells in *Arabidopsis thaliana*. Development 121: 4171-4182.

Barton, M. K. and Poethig R. S. (1993). Formation of the shoot apical meristem in *Arabidopsis thaliana*: an analysis of development in the wild-type and *shoot meristemless*. Development **119:** 823-831.

Battey, N. H. and Lyndon, R. F. (1988). Determination and differentiation of leaf and petal primordia in *Impatiens balsamina*. Ann. Bot. **61:** 9-16.

Baxter, S. M., Gontrum, D. M., Phillips, C. L., Roth, A. F. and Dahlquist, F. W. (1994). Heterodimerization of the yeast homeodomain transcriptional regulators alpha 2 and a1: secondary structure determination of the a1 homeodomain and changes produced by alpha 2 interactions. Biochemistry **33:** 15309-20.

Becraft, P. W. and Freeling, M. (1994). Genetic analysis of *Rough sheath1* developmental mutants of maize. Genetics **136:** 295-311

Bernier, G., Havelange, A., Houssa, C., Petitjean, A. and Lejeune, P. (1993). Physiological signals that induce flowering. The Plant Cell **5:** 1147-1155.

Bertuccioli, C., Fasano, L., Jun, S., Wang, S., Sheng, G. and Desplan C. (1992). In vivo requirement for the paired domain and homeodomain of the *paired* segmentation gene product. Development **122:** 2673-2685.

Boivin, R., Hamel, F., Beauseigle, D. and Bellemare G. (1994). Stage-specific transcription of the homeobox gene *Bnhd1* in young tissues and flowers of *Brassica napus*. Biochim. Biophys. Acta **1219(1):** 201-204.

Boncinelli, E., Somma, R., Acampora, D., Pannese, M., D'Esposito, M., Faiella, A. and Simeone, A. (1988). Organisation of human homeobox genes. Hum. Reprod. **3:** 880-886.

Bowman, J. L., Alvarez. J., Weigel, D., Meyrowizt, E. M. and Smyth, D. R. (1993). Control of flower development in *Arabidopsis thaliana* by *APETALA1* and interacting genes. Development **199:** 721-743.

Bowman, J. L., Smyth, D. R. and Meyerowitz, E. M. (1991). Genetic interactions among floral homeotic genes of *Arabidopsis*. Development **112:** 1-20.

Bradley, D., Carpenter, R., Copsey, L., Vincent, C., Rothstein, S. and Coen E. S. (1996). Control of inflorescence architecture in *Antirrhinum*. Nature **379:** 791-7

Bradley, D., Carpenter, R., Sommer, H., Hartley, N. and Coen, E. S. (1993). Complementary floral homeotic phenotypes result from opposite orientations of a transposon at the *plena* locus of *Antirrhinum*. Cell **72:** 85-95

Brownlee, C. and Berger, F. (1995). Extracellular matrix and pattern in plant embryos: on the lookout for developmental information. Trends Genet. **11:** 344-8

Carbelli, M., Sessa, G., Baima, S., Morelli, G. and Ruberti I. (1993). The *Arabidopsis Athb-2* and *-4* genes are strongly induced by far-red-rich light. Plant J. **4:** 469-479.

Carpenter, R. and Coen, E. S. (1990). Floral homeotic mutations produced by transposon-mutagenesis in *Antirrhinum majus*. Genes Dev. **4:** 1483-93.

Caruso, J. L. (1968). Morphogenetic aspects of a leafless mutant in tomato. General pattern in development. Am. J. Bot. **55:** 1169-1179.

Cerioli, S., Marocco, A., Maddaloni, M., Motto, M. and Salamini F. (1994). Early event in maize leaf epidermis formation as revealed by cell lineage studies. Development **120:** 2113-2120.

Chuck, G., Lincoln, C. and Hake. S. (1996). *KNAT1* induces lobed leaves with ectopic meristem when overexpressed in *Arabidopsis*. Plant Cell 8: 1277-1289.

Clark, J. K. and Sheridan, W. F. (1986). Developmental profiles of the maize embryo-lethal mutants *dek22* and *dek23*. J. Hered. **77:** 83-92.

Coen, E. S. (1991). The role of the homeotic genes in flower development and evolution. Ann. Rev. Plant Physiol. Plant Mol. Biol. **42:** 42241-249.

Coen, E. S. and Meyerowitz, E. M. (1991). The war of the whorls: genetic interactions controlling flower development. Nature **353:** 31-7.

Coen, E. S., Carpenter, R. and Martin, C. (1986). Transposable elements generate novel spatial patterns of gene expression in Antirrhinum majus. Cell **47:** 285-296.

Coen, E. S., Robbins, T. P., Almeida, J., Hudson, A. and Carpenter R. (1989). Consequence and mechanisms of transposition in *Anthirrhinum majus*. In Mobile DNA. Eds. D. E. Berg and M. M. Howe. American Society for Microbiology. Washington, D. C. 413-435.

Cunninghame, M. E. and Lyndon, R. F. (1986). The relationship between distribution of periclinal cell division in the shoot apex and leaf initiation. Ann. Bot. **57:** 737-746.

Davies, B., Egea-Cortines, M., de Andrade Silva, E., Saedler, H. and Sommer, H. (1996). Multiple interactions amongst floral homeotic MADS box proteins. EMBO J **15:** 4330-4343

Dawe, R. K. and Freeling, M. (1991). Cell lineage and its consequences in higher plants. Plant J. **1 (1):** 3-8.

DiNardo, S. and Heemskerk, J. (1990). Molecular and cellular interactions responsible for intrasegmental patterning during Drosophila embryogenesis. Semin. Cell Biol. **1:** 173-183.

Dolan, L. and Poethig, R. S. (1991). Genetic analysis of leaf development in cotton. Development Supp. **1:** 39-46.

Erickson, R. O. and Michelini, F. J. (1957). The plastochron index. Am. J. Bot. **44:** 297-305.

Esau, K. (1942). Vascular differentiation in the vegetative shoot of *Linum*. I. The procambium. Am. J. Bot. **29:** 738-747.

Esau, K. (1971). Anatomy of seed plants. 2nd Ed. Wilyey New York.

Feinberg, A. P. and Vogelstein, B. (1983). A technique for radiolabeling DNA restriction endonuclease fragments to high specific activity. Anal. Biochem. **132:** 6.

Foard, D. E. (1971). The initial protrusion of a leaf primordium can form without concurrent periclinal cell division. Can. J. Bot. **49:** 1601-1603.

Foster, A. S. (1936). Leaf differentiation in angiosperms. Bot. Rev. **2:** 349-372.

Fowler J. E., Muehlbauer G. J. and Freeling M. (1996). Mosaic analysis of the *liguleless3* mutant phenotype in maize by coordinate suppression of mutator-insertion alleles. Genetics **143:** 489-503

Fowler, J. E. and Freeling, M. (1996). Genetic analysis of mutations that alter cell fates in maize leaves: dominant *Liguleless* mutations. Dev. Genet. **18:** 198-222

Freeling, M. (1992). A conceptual framework for maize leaf development. Dev. Biol. **153:** 44-58.

Freeling, M. and Hake, S. (1985). Developmental genetics of mutants that specify *Knotted* leaves in maize. Genetics **111:** 617-634.

Garcia-Bellido, A., Ripoll, P. and Morata, G. (1973). Development compartmentalisation of the wing disc of Drosophila. Nature New Biol. **245:** 251-253.

Gehring, W. J., Muller, M., Affolter, M., Percival-Smith, A., Billeter, M., Qian, Y. Q., Otting, G. and Wuthrich, K. (1990). The structure of the homeodomain and its functional implications. Trends Genet. **6:** 323-229.

Gerber, H.-P., Seipel, K., Georgiev, O., Hofferer, M., Hug, M., Rusconi, S. and Schaffener, W. (1994). Transcriptional activation modulated by homopolymeric glutamine and proline stretches. Science **263:** 808-811.

Goodrich, J., Carpertern, R. and Coen E. S. (1992). A common gene regulates pigmentation pattern in diverse plant species. Cell **68:** 955-964.

Green, P. B. and Lang, J. M. (1981). Toward a biophysical theory of organogenesis: Birifringence observations on regenerating leaves in the succulent, *Graptopetalum paraguayense*. E. Walther. Planta **15:** 413-426.

Green, P. B. and Linstead, P. (1990). A procedure for SEM of complex structures applied to the inflorescence of snapdragon (*Antirrhinum*). Protoplasma **158:** 33-38.

Green, P. B. (1992). Cellulose orientation in primary growth: an energy-level model for cytoskeletal alignment. Curr. Top. in Plant Bioch. and Physiol. **11:** 99-117.

Gunnig, B. E. S. and Hardham, A. R. (1982). Microtubules. Annu. Rev. Plant Physiol. **33:** 651-698.

Hake, S., Vollbrecht, E. and Freeling, M. (1989). Cloning *Knotted*, the dominant morphological mutant in maize using *Ds* as a transposon tag. EMBO J. **8**: 15-22.

Hardham, A. R., Green, P. B. and Lang, J. M. (1980). Reorganisation of cortical microtubules and cellulose deposition during leaf formation in *Graptopetalum paraguayense*. Planta **149:** 181- 195.

Hareven, D., Gutfinger, T., Parnis, A., Eshed, Y. and Lifschitz, E. (1996). The making of a compound leaf: genetic manipulation of leaf architecture in tomato. Cell **84:** 735-744.

Hudson, A., Carpenter, R. and Coen, E. S. (1993). Olive: a key gene required for chlorophyll synthesis in Antirrhinum majus. EMBO J. **12:** 3711-3719.

Jackson, D. (1996). Plant morphogenesis: Designing leaves. Curr. Biol. **6:** 917-919.

Jackson, D., Veit, B. and Hake, S. (1994). Expression of maize *KNOTTED-1* related homeobox genes in the shoot apical meristem predict patterns of morphogenesis in the vegetative shoot. Development **120 (2)**: 405-413.

Jesuthasan, S. and Green, P. B. (1989). On the mechanism of decussate phyllotaxis: Biophysical studies an the tunica layer of *Vinca major*. Am. J. Bot. **76:** 1152-1166.

Jun,. S. and Desplan, C. (1996). Cooperative interaction between paired domain and homeodomain. Development **122:** 2639-2650.

Kaplan, R. (1937). Ueber die Bildung der Stele aus dem Urmeristem von Pteridophyten und Spermatophyten. Planta **27:** 224-268.

Kerstetter R., Vollbrecht E., Lowe B., Veit B., Yamaguchi J. and Hake S (1994). Sequence analysis and expression patterns divide the maize *knotted1*-like homeobox genes into two classes. Plant Cell **6:** 1877-87

Kissinger, C. R., Liu, B., Martin-Blanco, E., Kornberg, T. B. and Pabo, C. O. (1990). Crystal structure of engrailed homeodomain-DNA complex at 2.8 A resolution: a framework for understanding homeodomain-DNA interactions. Cell **63:** 579-590.

Knox, J. P. (1993). The role of cell surface glycoproteins in differentiation and morphogenesis. In Battey, N. H., Dickinson, H. G. and Hetherington A. M. Eds. Society for Experimental Biology Seminar Series, Post-translational modification in plant. Cambridge University Press, 267-283.

Krumlauf, R. and Gould A. (1992). Homeobox cooperativity. Trends Genet. 8: 297-300.

Krysan, P. J., Young, J. C., Tax, F. and Sussman, M. R. (1996). Identification of transferred DNA insertions within *Arabidopsis* genes involved in signal transduction and ion transport. Proc. Natl. Acad. Sci. USA **93:** 8145-50.

Langdale, J. A., Lane, B., Freeling, M. and Nelson, T. (1989). Cell lineage analysis of maize bundle sheath and mesophyll cells. Dev. Biol. **133:** 128-139.

Laughon, A., Carrol, S. B., Storter, F. A., Riley, P. D. and Scott, M. P. (1985). Common properties of proteins encoded by *Antennapedia* complex genes of *Drosophila melanogaster*. Cold Spring Habor Symp. Quant. Biol. **50:** 253-262.

Lawrence, P. A. (1992). The Making of a Fly. The Genetics of Animal Design. Blackwell Scientific Publications. Oxford. 78-106

Lincoln, C., Long, J., Yamaguchi, J., Serikawa, K. and Hake, S. (1994). A *knotted1*-like homeobox gene in *Arabidopsis* is expressed in the vegetative meristem and dramatically alters leaf morphology when overexpressed in transgenic plants. Plant Cell **6:** 1859-76

Liu, Z. and Meyerowitz, E. M. (1995). *LEUNIG* regulates *AGAMOUS* expression in Arabidopsis flowers. Development **121:** 975-91

Long, J. A., Moan, E. I., Medford, J. I. and Barton M. K. (1996). A member of the *KNOTTED* class of homeodomain proteins encoded by the *SHOOT MERISTEMLESS* gene of *Arabidopsis*. Nature. 379: 405-413.

Lucas, W. J., Bouche-Pillon, S., Jackson, D. J., Nguyen, L., Baker, L., Ding, B. and Hake, S. (1995). Selective trafficking of KNOTTED1 homeodomain protein and its mRNA through plasmodesmata. Science **270:** 1980-1983.

Luo, D., Carpenter, R., Vincent, C., Copsey, L. and Coen, E. S. (1996). Origin of floral asymmetry in *Antirrhinum*. Nature **383:** 794-799

Luo, D., Coen, E. S., Doyle, S. and Carpenter R. (1991). Pigmentation mutants produced by transposon mutagenesis in *Antirrhinum majus*. Plant J. **1:** 59-69.

Lyndon, R. F. (1990). Meristem functioning: formation of bracts, leaves and floral organs. In Plant Development. Unwin Hyman London. 39-57.

Ma, H., McMullen, M. D. and Finer, J. J. (1994). Identification of a homeobox-containing gene with enhanced expression during soybean (*Glycine max* L.) somatic embryo development. Plant Mol. Biol. **24:** 465-473.

Ma, K., Yuan, D., Diepold, K., Scarborough, T. and Ma, J. (1996). The *Drosophila* morphogenetic protein Bicoid binds DNA cooperatively. Development **122:** 1195-1206.

Maksymowych, R. (1973). Analysis of leaf development. Cambridge University Press, UK.

Maksymowych, R. and Erickson, R. O. (1977). Phillotactic change induced by giberellic acid in *Xanthium* shoot apices. Am. J. Bot. **64:** 33-34.

Mandel, M. T., Gustafson-Brown, C., Savidge, B. and Yanofsky, M. F. (1992). Molecular characterisation of the *Arabidopsis* floral homeotic gene *APETALA1*. Nature **360:** 273-277.

Mann, R. S. and Chan S.-K. (1996). Extra specific from *extradenticle*: the partnership between HOX and PBX/EXD homeodomain proteins. Trends Genet. **12:** 258262.

Marc, R. and Hackett, W. P. (1991). Giberellic-induced reorganisation of spatial relationship of emerging leaf primordia at the shoot apical meristem in *Hedera helix*. Planta **185:** 171-178.

Marx, G. A. (1977). A genetic syndrome affecting leaf development in *Pisum* . Am. J. Bot. **64:** 273-277.

Marx, G. A. (1987). A suite of mutants that modify pattern formation in pea leaves. Plant Mol. Biol. Rep. **5:** 311-335.

Masucci, J. D. and Schiefelbein, J. W. (1996). Hormones act downstream of *TTG* and *GL2* to promote root hair outgrowth during epidermis development in the Arabidopsis root. Plant Cell **8:** 1505-1517

Mathan, D. S. and Cole, R. D. (1964). Comparative biochemical study of two allelic forms of a gene affecting leaf-shape in tomato. Am. J. Bot. **52:** 560-566.

Matsuoka, M., Ishikawa, H., Saito, A., Tada, Y., Fujimura, T. Kano-Murakani, Y. (1993). Expression of a rice homeobox gene causes altered morphology of transgenic plants. Plant Cell **5:** 1039-1048.

Mayer, U., Torres-Ruiz, R. A., Berleth, T., Misera, S. and Jurgens, G. (1991). Mutation affecting body organisation in the *Arabidopsis* embryo. Nature **353:** 402-407.

McArthur, I. C. S. and Steeves, T. A. (1972). An experimental study of vascular differentiation in *Geum chiloense* Balbis. Botan. Gaz. **133:** 276-287.

McGinnis, W., Levine, M., Hafen, E., Kuroiwa, A. and Gehring, W. J. (1984). A conserved DNA sequence in homeotic genes of *Drosophila* Antennapedia and bithorax complexes. Nature **308:** 428-433

McHale. N. A. (1993). *LAM-1* and *FAT* genes control development of the leaf blade in *Nicotiana sylvestris*, Plant Cell **5:** 1029-1038.

Mead, J., Zhong, H., Acton, T. B. and Vershon, A. K. (1996). The yeast alpha2 and MCM1 proteins interact through a region similar to a motif found in homeodomain proteins of higher eukaryotes. Mol Cell Biol **16:** 2135-43 .

Medford, J. I. (1992). Vegetative apical meristem. Plant Cell **4:** 1029-1039.

Meicenheimer, D. R. (1981). Changes in *Epilobium* phyllotaxis induced by N-1-naphthylphthalamic acid α-4-chlorophenoxyisobutyric acid. Am. J. Bot. **68:** 1139-1154.

Meisel, L. and Lam, E. (1996). The conserved ELK-homeodomain of KNOTTED-1 contains two regions that signal nuclear localisation. Plant Mol. Biol. **30:** 1-14.

Modrusan, Z. et al., (1994). Homeotic transformation of ovules into carpel-like structures in Arabidopsis. Plant Cell **6:** 333-349.

Muller, K. J., Romano, N., Gerstner, O., Garcia-Maroto, F., Pozzi, C., Salamini, F. and Rohde W. (1995). The barley Hooded mutation caused by a duplication in a homeobox gene intron. Nature **374:** 727-730.

Murray, N. E. (1982). Phage lambda and molecular cloning. In Lambda II. Hendrix, R. W., Roberts, J. W., Stahl, F. W. and Weissberg R. A. Eds. Cold Spring Habor laboratory Press New York. 395-442.

Nacken, W. K. F., Piotrowiak, R., Saedler, H. and Sommer, H. (1991). The transposable element *Tam1* from *Antirrhinum majus* shows structural homology to maize transposon *EN/Spm* and has no sequence specificity of insertion. Mol. Gen. Genet. **28:** 201-208.

Neuhaus, G., Bowler, C., Kern, R. and Chua N-H. (1993). Calcium/calmodulin-dependent and -independent phytochrome signal transduction pathways. Cell **73:** 937-52

Otting, G., Qian, Y. Q., Billeter, M., Muller, M., Affolter, M., Gehring, W. J. and Wuthrich, K. (1990). Protein-DNA contacts in the structure of a homeodomain-DNA complex determined by nuclear magnetic resonance spectroscopy in solution. EMBO J **9:** 3085-92

Pabo, C. O. and Sauer, R. T. (1984). Protein-DNA recognition. Ann. Rev. Biochem. **53:** 293-321.

Perbal, M. C., Haughn, G., Saedler, H. and Schwarz-Sommer, Z. (1996). Non-cell-autonomous function of *Antirrhinum* floral homeotic proteins *DEFICIENS* and *GLOBOSA* is exerted by their polar cell-to-cell trafficking. Development **122:** 3433-3441.

Poethig, R. S. (1984a). Cellular parameters of leaf morphogenesis in maize and tobacco. In Contemporary Problems in Plant Anatomy. Eds R. A. White and W. C. Dickinson. Academic Press, New York. 235-259.

Poethig, R. S. (1984b). Patterns and problems in angiosperm leaf morphogenesis. In Pattern Formation: A Primer in Development Biology. Eds G. M. Malacinski and S. V. Bryant Macmillan, New York: 413-432

Poethig, R. S. (1987). Clonal analysis of cell lineage patterns plant development. Am. J. Bot. **74(4):** 581-594.

Poethig, R. S. (1989). Genetic mosaics and cell lineage analysis in plants. Trends Genet. **5:** 273-277.

Poethig, R. S. (1990). Phase change and the regulation of shoot morphogenesis in plants. Science **250:** 923-930.

Poethig, R. S. and Sussex, I. M. (1985a). The development and growth dynamics of the tobacco leaf. Planta **165:** 158-169.

Poethig, R. S. and Sussex, I. M. (1985b). The cellular parameters of leaf development in tobacco: a clonal analysis. Planta **165:** 170-184

Poethig, R. S. and Szymkowick, E. J. (1995). Clonal analysis of leaf development in maize. Maydica 1995 **40:** 67-76.

Pooviah, B. W. and Reddy, A. S. N. (1993). Calcium and signal trasduction in plant. Critical Reviews in Plant Sciences **12:** 185:211.

Ptashne, M. and Gann, A. A. F. (1990). Activators and target. Nature **346:** 329-331.

Qian, Y. Q., Billeter, M., Otting, G., Muller, M., Gehring, W. J. and Wuthrich, K. (1989). The structure of Antennapedia homeodomain determined by NMR spectroscopy in solution: comparison with prokaryotic repressors. Cell **59:** 573-580.

Ray, A., Robinson-Beers, K., Ray, S., Baker, S. C., Lang, J. D., Preuss, D., Milligan, S. B. and Gasser, C. S. (1994). *Arabidopsis* floral homeotic gene *BELL* (*BEL1*) controls ovule development through negative regulation of *AGAMOUS* gene (*AG*). Proc. Natl. Acad. Sci. USA **91:** 5761-5.

Reiser, L., Modrusan, Z., Margossian, L., Samach, A., Ohad, N., Haughn, G. W. and Fischer, R. L. (1995). The BELL1 gene encodes a homeodomain protein involved in pattern formation in the Arabidopsis ovule primordium. Cell **83:** 735-742.

Rembur, J. and Nougarede, A. (1977). Duration of cell cycles in the shoot apex of *Chrysanthem segetum* L. Z. Pflanzenphys. **81:** 173-179.

Rerie, W., Feldmann K. A. and Marks M. D. (1994). The *GLABRA2* gene encodes a homeodomain protein required for normal trichome development in *Arabidopsis*. Gen. Dev. 8: 1388-1399.

Ruberti, I., Sessa, G., Luchetti, S. and Morelli G. (1991). A novel class of plant proteins containing a homeodomain with a closely linked leucine zipper motif. EMBO J. **7:** 1787-1791.

Rushlow, C., Frasch, M., Doyle, H. and Levine, M. (1987). Maternal regulation of *zerknullt*: a homoeobox gene controlling differentiation of dorsal tissues in *Drosophila*. Nature **330:** 583-6.

Russell, S-H. and Evert, R. F. (1985). Leaf vasculature in *Zea mays* L. Plant **164:** 448-458.

Sachs, T. (1981). The control of the patterned differentiation of vascular tissues. Adv. Bot. Res. **9:** 152-255.

Sachs, T. (1991). Cell polarity and tissue patterning in plants. Development Supp. **1:** 83-93.

Sakai, W. S. (1973). Simple method for differential staining of paraffin embedded plant material using toluidine blue O. Stain Techonl. **48:** 247-249.

Salisbury, F. B. and Ross, C. W. (1992). Plant Physiology and Plant Cells. In Plant Physiology. 14th ed. Wadsworth Publishing Company, Belmont, California.

Sambrook, J., Fritsch, E. F. and Maniatis, T. (1989). Molecular Cloning: A Laboratory Manual 2nd ed. Cold Spring Habor Laboratory Press, NY.

Satina, S., Blakeslee, A. F. and Avery, A. G. (1940). Demonstration of the three germ layers in the shoot apex of Datura by means of induced polyploid in periclinal chimeras. Am. J. Bot **27:** 895-905.

Scanlon, M. J., Schneeberger, R. G. and Freeling, M. (1996). The maize mutant narrow sheath fails to establish leaf margin identity in a meristematic domain. Development **122:** 1683-91

Schindler, U., Beckmann, H. and Cashmore, A. R. (1993). HAT3.1, a novel *Arabidopsis* homeodomain protein containing a conserved cysteine-rich region. Plant J. **4:** 137-150.

Schneeberger, R. G., Becraft, P. W., Hake, S. and Freeling, M. (1995). Ectopic expression of the knox homeobox gene *rough sheath1* alters cell fate in the maize leaf. Genes Dev **9:** 2292-304

Schwabe, W. W. (1971). Chemical modification of phyllotaxis and its implication. In Control Mechanisms of Growth and Differentiation. Eds. D. D. Davies and M. Ball. Academic Press. UK. 403-440.

Schwarz-Sommer, Z., Hue, I., Huijser, P., Flor, P. J., Hansen, R., Tetens, F., Lonnig, W. E., Saedler, H. and Sommer, H. (1992). Characterisation of the *Antirrhinum* floral homeotic MADS-box gene *deficiens*: evidence for DNA binding and autoregulation of its persistent expression throughout flower development. EMBO J. **11:** 251-63

Scott, M. P. and Weiner, A. J. (1984). Structural relationships among genes that control development: sequence homology between the *Antennapedia*, *Ultrabithorax*, and *fushi tarazu* loci of *Drosophila*. Proc. Natl. Acad. Sci. USA **81:** 4115-4119.

Scott, M. P., Tamkun, J. W. and Hartzell. G. W. III (1989). The structure and function of the homeodomain. Biochim. Biophys. Acta. **989:** 25-48.

Sharman, B. C. (1942). Deveopmental anatomy of the shoot of *Zea mays* L. Ann. Bot. **6:** 245-284.

Shepherd, J. C. W., McGinnis W., Carrasco A. E., DeRobertis E. M. and Gehring, W. J. (1984). Fly and frog homeodomains show homologies with yeast mating type regulatory proteins. Nature **310:** 70-71.

Sheridan, W. F. and Thorstenson, Y. R. (1986). Developmental profiles of three embryo-lethal maize mutants lacking leaf primordia: *ptd**-1130, *cp**-1418, and *bno**-747. Dev. Genet. **7:** 35-49.

Sinha, N. and Hake, S. (1990). Mutant characters of knotted maize leaves are determined in the innermost tissue layers. Dev. Biol. **141:** 203-10

Sinha, N. R., Williams, R. E. and Hake, S. (1993). Overexpression of the maize homeo-box gene, *KNOTTED-1*, causes a switch from determinate to indeterminate cell fates. Genes Dev. **7:** 787-95

Sinott, E. W. (1958). The genetic basis of organic form. Ann. New York Acad. Sci. **71:** 1223-1233.

Smith, L. G. and Hake, S. (1992). The initiation and determination of leaves. Plant Cell **4:** 1017-1027.

Smith, L. G. and Hake, S. (1993). Molecular genetic approaches to leaf development: Knotted and beyond. Can. J. Bot. **72:** 619-625.

Smith, L. G., Greene, B., Veit, B. and Hake, S. (1992). A dominant mutation in the maize homeobox gene, *Knotted-1*, causes its ectopic expression in leaf cells with altered fates. Development **116:** 21-30

Smith, L. G., Hake, S. and Sylvester, A. W. (1996). The *tangled-1* mutation alters cell division orientations throughout maize leaf development without altering leaf shape. Development **122:** 481-9

Soderman, E., Mattsson, J. and Engstrom, P. (1996). The *Arabidopsis* homeobox gene ATHB-7 is induced by water deficit and by abscisic acid. Plant J **10:** 375-381.

Sommer, H., Beltran, J. P., Huijser, P., Pape, H., Lonnig, W. E. Saedler, H. and Schwarz-Sommer, Z. (1990). *Deficiens*, a homeotic gene involved in the control of flower morphogenesis in *Antirrhinum majus*: the protein shows homology to transcription factors. EMBO J. **9:** 605-13

Sommer, H., Bonas, U. and Saedler, H. (1988). Transposon-induced alterations in the promoter region affect transcription of the chalcone synthase gene of *Antirrhinum majus*. Mol Gen Genet **211:** 49-55.

Sommer, H., Carpenter, R., Harrison B. J. and Saedler, H. (1985). The transposable element *Tam3* of *Antirrhinum majus* generates a novel type of sequence alteration upon excision. Mol. Gen. Genet. **199:** 225-231.

Souer, E., van Houwelingen, A., Kloos, D., Mol, J. and Koes, R. (1996). The *No Apical Meristem* gene of petunia is required for pattern formation in embryos and flowers and is expressed at the meristem and primordia boundaries. Cell 85: 159-170.

Steeves, T. A. (1963). Morphogenetic studies on *Osmunda cinnamomea* L.: The shoot apex. J. Indian Bot Soc. **42A:** 225-236.

Steeves, T. A. and Sussex, I. M. (1957). Studies on development of excised leaves in sterile culture. Am. J. Bot. **44:** 665-673.

Steeves, T. A. and Sussex, I. M. (1989). Patterns in Plant Development. 2nd Ed. Cambridge University Press., UK.

Struhl, G., Struhl, K. and Macdonald, P. M. (1989). The gradient morphogen *bicoid* is a concentration-dependent transcriptional activator. Cell **57:** 1259-73.

Stubbe, H. (1966). Genetik und Zytologie von *Antirrhinum* L. sect. *Antirrhinum*. Jena: Gustav Fischer.

Sylvester, A. W., Cande, W. Z. and Freeling, M. (1990). Division and differentiation during normal and *liguleless-1* maize leaf development. Development **22:** 985-1000.

Tamaoki, M., Tsugawa, H., Minami, E., Kayano, T., Yamamoto N., Kano-Murakami, Y. and Matsouka M. (1995). Alternative RNA products from a rice homeobox gene. Plant J. **7(6):** 927-938.

Tornero, P., Conejero, V. and Vera, P. (1996). Phloem-specific expression of a plant homeobox gene during secondary phases of vascular development. Plant J. **9(5):** 639-648.

Treisman, J., Gonczy, P., Vashishtha, M., Harris, E. and Desplan C. (1989). A single amino acid can determine the DNA binding specificity of Homeodomain proteins. Cell **59:** 553-562.

Trobner, W., Ramirez, L., Motte, P., Huijser, P., Lonnig, W. E., Saedler, H., Sommer, H. and Schwarz-Sommer, S. (1992). *globosa*: a homeotic gene which interacts with deficiens in the control of *Antirrhinum* floral organogenesis. EMBO J. **11:** 4693-4704.

Tsuge, T., Tsukaya, H. and Uchimiya, H. (1996). Two independent and polarised processes of cell elongation regulate leaf blade expansion in *Arabidopsis thaliana* (L.) Heynh. Development **122:** 1589-1600.

Upadhyaya, K. C., Sommer, H., Krebbers E. and Saedler H. (1985). The paramutagenic line *niv-44* has 5kb insert, *Tam2*, in the chalcone synthase gene of *Antirrhinum majus*. Mol. Gen. Genet. **199:** 201-207.

Veit, B., Vollbrecht, E., Mathern, J. and Hake, S. (1990). A tandem duplication causes the *Kn1-O* allele of *Knotted*, a dominant morphological mutant of maize. Genetics **125:** 623-31

Vollbrecht, E., Veit, B., Sinha, N. and Hake, S. (1991). The developmental *Knotted-1* is a member of a maize homeobox gene family. Nature **350**: 2241-243.

Waiter, R. and Hudson, A. (1995). *phantastica*: a gene required for dorsoventrality of leaves in Antirrhinum majus. Development **121:** 2143-2154.

Wardlaw, C. W. (1946). Experimental and analytical studies of pteridophytes. VII. Stelar morphology: The effect of defoliation on the stele of *Osmunda* and *Todea*. Ann. Bot. **10:** 97-107.

Weigel, D. and Meyerowitz, E. M. (1994). The ABCs of floral homeotic genes. Cell **78:** 203-209.

Wolpert, L. (1996). One hundred years of positional information. Trend Genet. **2:** 359-364.

Young, B. S. (1954). The effect of leaf primordia on differentiation in the stem. New Phytol. **53:** 445-460.

Young, J. P. W. (1983). Pea leaf morphogenesis: a simple model. Ann. Bot. **52:** 311-316.

Zambrisky *et al.*, (1997). In press.

Zecchi, S. (1989). La Metamorfosi delle Piante. 2nd Ed., U. Uganda, Parma, IT.